การหาผลเฉลยดีอาร์เอ็มของสมการคลื่นเชิงเส้นสองมิติ

นายเสน่ห์ รุจิวรรณ

วิทยานิพนธ์นี้เป็นส่วนหนึ่งของการศึกษาตามหลักสูตรปริญญาวิทยาศาสตรมหาบัณฑิต
สาขาวิชาวิทยาการคณนา ภาควิชาคณิตศาสตร์
คณะวิทยาศาสตร์ จุฬาลงกรณ์มหาวิทยาลัย
ปีการศึกษา 2542
ISBN 974-333-909-4

DRM SOLUTIONS TO TWO-DIMENSIONAL LINEAR WAVE EQUATIONS

Mr. Sanae Rujivan

A Thesis Submitted in Partial Fulfillment of the Requirements
for the Degree of Master of Science in Computational Science
Department of Mathematics
Faculty of Science
Chulalongkorn University
Academic Year 1999
ISBN 974-333-909-4

Thesis Title DRM SOLUTIONS TO TWO-DIMENSIONAL LINEAR WAVE EQUATIONS

By Mr. Sanae Rujivan
Department Mathematics
Thesis Advisor Assist. Prof. Dr. Pornchai Satravaha

Accepted by the Faculty of Science, Chulalongkorn University in Partial Fulfillment of the Requirements for the Master's Degree.

.... Dean of Faculty of Science
(Assoc. Prof. Dr. Wanchai Phothiphichitr)

THESIS COMMITTEE

.... Chairperson
(Assoc. Prof. Dr. Wanida Hemakul)

.... Thesis Advisor
(Assist. Prof. Dr. Pornchai Satravaha)

.... Member
(Assist. Prof. Dr. Jack Asavanant)

เสน่ห์ รุจิวรรณ : การหาผลเฉลยดีอาร์เอ็มของสมการคลื่นเชิงเส้นสองมิติ (DRM SOLUTIONS TO TWO-DIMENSIONAL LINEAR WAVE EQUATIONS) อาจารย์ที่ปรึกษา : ผศ. ดร. พรชัย สาตรวาหา ; 88 หน้า ISBN 974-333-909-4

ในวิทยานิพนธ์นี้ วิธีเชิงตัวเลขสองวิธีที่เรียกว่า เอฟดีดีอาร์เอ็ม และ แอลทีดีอาร์เอ็ม ได้ถูกพัฒนาขึ้นเพื่อแก้สมการคลื่นเชิงเส้นใน $\mathbf{R}^2$ โดยทั้งสองวิธีที่ได้นำเสนอนี้มีพื้นฐานจากวิธีดีอาร์เอ็มซึ่งเป็นวิธีที่มีประสิทธิภาพสำหรับการแก้สมการปัวซอง ตามวิธีเอฟดีดีอาร์เอ็มนั้น สมการคลื่นเชิงเส้นถูกแปลงเป็นสมการปัวซองในปริภูมิเวลาโดยใช้บางเทคนิคของวิธีผลต่างสืบเนื่อง ในอีกทางหนึ่ง วิธีแอลทีดีอาร์เอ็มใช้การแปลงลาปลาซแปลงสมการคลื่นเชิงเส้นไปเป็นสมการปัวซองในปริภูมิลาปลาซ ซึ่งหลังจากการแปลงสมการคลื่นเชิงเส้นแล้ว จึงใช้เทคนิคดีอาร์เอ็มเพื่อแก้สมการที่ได้ถูกแปลงมา ด้วยวิธีข้างต้นนี้ทำให้ได้ boundary-only integral equations และ มิติของปัญหาลดลงไปสอง เนื่องจากวิธีเอฟดีดีอาร์เอ็มใช้บางเทคนิคของวิธีผลต่างสืบเนื่อง ดังนั้นผลเฉลย ณ เวลาเฉพาะใดๆจึงได้จากการคำนวณตามลำดับขั้นของเวลา ในขณะที่วิธีแอลทีดีอาร์เอ็มต้องการผลการแปลงผกผันเชิงตัวเลขของการแปลงลาปลาซเพื่อแปลงผลเฉลยที่ได้ในปริภูมิลาปลาซกลับมาสู่ผลเฉลยในปริภูมิเวลา และสำหรับการวิจัยนี้ได้เลือกผลการแปลงผกผันเชิงตัวเลขของการแปลงลาปลาซที่เรียกว่า “ขั้นตอนวิธีของสตีเฟส” ผลเฉลยเชิงตัวเลขที่ได้จากวิธีเอฟดีดีอาร์เอ็มและวิธีแอลทีดีอาร์เอ็มสำหรับหลายตัวอย่างที่ได้นำมาทดสอบถูกแสดงไว้ภายในงานวิจัยนี้ จะเห็นได้ว่าวิธีแอลทีดีอาร์เอ็มมีประสิทธิภาพสูงกว่าวิธีเอฟดีดีอาร์เอ็มเมื่อต้องการผลเฉลย ณ เวลามากๆ

ภาควิชา คณิตศาสตร์ ลายมือชื่อนิสิต เสน่ห์ รุจิวรรณ

สาขาวิชา วิทยาการคณนา ลายมือชื่ออาจารย์ที่ปรึกษา ....

ปีการศึกษา 2542 ลายมือชื่ออาจารย์ที่ปรึกษาร่วม ....

SANAE RUJIVAN : DRM SOLUTIONS TO TWO-DIMENSIONAL LINEAR WAVE EQUATIONS. THESIS ADVISOR: ASSIST. PROF. PORNCHAI SATRAVAHA, Ph.D. 88 pp. ISBN 974-333-909-4

In this thesis, two numerical methods called the Finite Difference Dual Reciprocity Method (FDDRM) and the Laplace Transform Dual Reciprocity Method (LTDRM) are developed for solving Linear Wave Equations (LWEs) in $\mathbf{R}^2$. Both proposed methods are based on the Dual Reciprocity Method (DRM) which is the efficient method for solving Poisson equations. According to FDDRM, an LWE is transformed into the Poisson equation in the time space using some finite difference techniques. On the other hand, LTDRM uses the Laplace transform to transform an LWE into the Poisson equation in the Laplace space. After transformation, the DRM technique is then used to solve the transformed equation. With these methods, boundary-only integral equations can be derived and the dimension of the problem is reduced by two. Since FDDRM uses some finite difference techniques, a solution at any specific time can be attained with a step-by-step calculation in time, while LTDRM needs a numerical inversion of the Laplace transform to convert a solution obtained in the Laplace space into a solution in the time space. In this research, a numerical Laplace transform inversion called " Stehfest's algorithm" is chosen. The numerical solutions obtained from FDDRM and LTDRM for several test examples are presented herein. It will be seen that LTDRM is more efficient than FDDRM when a solution at a large time is required.

ภาควิชา คณิตศาสตร์ ลายมือชื่อนิสิต เสน่ห์ รุจิวรรณ

สาขาวิชา วิทยาการคณนา ลายมือชื่ออาจารย์ที่ปรึกษา ....

ปีการศึกษา 2542 ลายมือชื่ออาจารย์ที่ปรึกษาร่วม ....

Acknowledgements

I am greatly indebted to my supervisor, Assistant Professor Dr. Pornchai Satravaha, for his suggestions, untiring helps and guidance in the creation of this thesis. Without him my thesis would have never been accomplished.

Furthermore, I would like to thank all of the lecturers for their previous valuable lectures. Finally, I would like to express my sincere gratitude to my parents, for love, hearty encouragement and unselfish sacrifice during my study.

I truly believe that all people whom I have not personally mentioned here are aware of my deep appreciation.

Contents

Chapter 1

Introduction

The Linear Wave Equation (LWE) is one type of partial differential equations (PDEs) which is expressed as

$$\nabla^2 u(\bar{x},t) - \frac{1}{c^2}\frac{\partial^2 u}{\partial t^2}(\bar{x},t) = b\left(\bar{x},t,u,\frac{\partial u}{\partial t},\frac{\partial u}{\partial x},\frac{\partial u}{\partial y}\right), \quad \bar{x}\in\Omega,\ t>0, \qquad \textbf{(1.1.1)}$$

with

$$b\left(\bar{x},t,u,\frac{\partial u}{\partial t},\frac{\partial u}{\partial x},\frac{\partial u}{\partial y}\right) = z(\bar{x},t) + \beta_1 u + \beta_2\frac{\partial u}{\partial t} + \beta_3\frac{\partial u}{\partial x} + \beta_4\frac{\partial u}{\partial y}, \qquad \textbf{(1.1.2)}$$

where $u(\bar{x},t)$ is the unknown function of spatial point $\bar{x}=(x,y)$ in a bounded domain Ω with an enclosing boundary $\Gamma = \partial\Omega$ in $\mathbf{R}^2$ at time t, ∇^2 is the two-dimensional Laplacian operator, a non-zero constant c represents the velocity of wave propagation, b is a function which describes the distribution of the source intensity and its time dependence at each point in the domain Ω, z is a known function, and $\beta_i, i=1, 2, 3, 4$ are constants. If $b\equiv 0$, Equation **(1.1.1)** is called Homogeneous Linear Wave Equation (HLWE) and it is called Inhomogeneous Linear Wave Equation (ILWE) when b is not a zero function.

LWEs play a significant role in engineering and applied science. There are many problems that occur in engineering practice and applied science such as vibrations of a membrane problems, propagation of acoustic waves problems, propagation of electromagnetic waves problems, etc., can be modeled by this type of equations in formulations. Efficiently and accurately solving LWEs are a usual task faced by scientists and engineers.

Generally, the interpretation of the unknown function u depends upon the problem under consideration, which may be the displacement of a membrane from its equilibrium position in the vibrations of a membrane problem, a velocity potential in the propagation of acoustic waves or in electromagnetic waves problem.

Consider an LWE as in Equation **(1.1.1)**. By the theory for linear partial differential equations, we know that an LWE is well-posed if it equips with two types of conditions. The fist type is initial conditions, also known as Cauchy conditions, which are values of the unknown function u and its fist time-derivative at the initial point , i.e.,

$$u(\bar{x},t_0) = u_0(\bar{x}), \qquad \bar{x} \in \Omega \tag{1.1.3}$$

and

$$\frac{\partial u}{\partial t}(\bar{x},t_0) = v_0(\bar{x}), \quad \bar{x} \in \Omega . \tag{1.1.4}$$

Without loss of generality, we shall let $t_0 = 0$.

The second type is boundary conditions which fall into the following three categories:

- Dirichlet conditions (also known as boundary conditions of the first kind or essential boundary conditions) are the values of the unknown function u prescribed at each point on the boundary Γ_1 as

$$u(\bar{x},t) = \bar{u}(\bar{x},t), \quad \bar{x} \in \Gamma_1, t > 0, \tag{1.1.5}$$

- Neumann conditions (also known as boundary conditions of the second kind or natural boundary conditions) are the values of the normal derivatives of the unknown function u prescribed at each point on the boundary Γ_2 as

$$\frac{\partial u}{\partial n}(\bar{x},t) = \bar{q}(\bar{x},t), \quad \bar{x} \in \Gamma_2, t > 0, \tag{1.1.6}$$

- Robin conditions (also known as boundary conditions of the third kind or mixed boundary conditions) are the values of a linear combination of the unknown function u and its normal derivative prescribed at each point on the boundary Γ_3 as

$$u(\bar{x},t) + \lambda \frac{\partial u}{\partial n}(\bar{x},t) = \bar{r}(\bar{x},t), \quad \bar{x} \in \Gamma_3, t > 0, \tag{1.1.7}$$

where $\Gamma_i, i = 1,2,3$ are complementary segments of Γ, n is the unit outward normal vector on the boundary Γ, λ is a non-zero constant, and $\bar{u}$, $\bar{q}$, $\bar{r}$ are known functions.

Usually in the vibrations of a membrane problem, the edges of a membrane are fixed. Thus the only boundary condition imposed is the Dirichlet boundary condition and it reads $u \equiv 0$ on the boundary for all t. However, sometimes the boundary (or part of it) is left "free" meaning that it can move in the vertical direction and there is no external transverse force acting on it. This is equivalent to the boundary condition $\frac{\partial u}{\partial n} \equiv 0$. Moreover, an intermediate case is also possible; the boundary may be elastically supported and capable of producing a transverse force proportional to the displacement. This situation is equivalent to the boundary condition $\frac{\partial u}{\partial n} + \lambda u \equiv 0$ on the boundary for all t.

Since problems modeled by LWEs are very important problems in science and engineering, many scientists and engineers try to find the solutions for these problems. There are many analytical methods to solve LWEs. For instance, the method of separation of variables, the method of fundamental solution, and weight residual method are all well known. Unfortunately, these methods often work with only some HLWEs on a regular domain. Therefore numerical approaches such as Finite Difference Method (FDM), Lapalce Transform Method, Boundary Element Method (BEM), Dual Reciprocity Method (DRM), which are described in Sections 1.1 – 1.4, are resorted to. As for this research, two numerical approaches called Finite Difference Dual Reciprocity Method (FDDRM) and Laplace Transform Dual Reciprocity Method (LTDRM), are employed to solve LWEs.

1.1 Finite Difference Method (FDM)

The development of high-speed digital and personal computer has made it possible to effectively use different numerical techniques for solving boundary and initial value problems involving partial differential equations. Among different methods available, the Finite Difference Method (FDM) is widely used. It has a straightforward structure which is derived from truncated Taylor's series, also known as Taylor's formula. However, there are difficulties with the implementation of the FDM for problems with complex geometrical shapes, and with some types of boundary conditions.

Nevertheless, FDM is still a well-established technique for the analysis of transient problems and in computational fluid dynamics.

In this research, we shall only apply FDM with the time derivative terms in an LWE by using the central difference formula as

$$\frac{\partial^2 u}{\partial t^2}(\bar{x},t_i) = \frac{u(\bar{x},t_{i+1}) - 2u(\bar{x},t_i) + u(\bar{x},t_{i-1})}{\Delta t^2} + O(\Delta t^2) \qquad \textbf{(1.1.8)}$$

and the forward difference formula as

$$\frac{\partial u}{\partial t}(\bar{x},t_i) = \frac{u(\bar{x},t_{i+1}) - u(\bar{x},t_i)}{\Delta t} + O(\Delta t), \qquad \textbf{(1.1.9)}$$

where $t_i = i\Delta t$ with a truncation error of $O(\Delta t^2)$ and $O(\Delta t)$, respectively. With this method, an LWE become the Poisson equation for each particular time t_i and there are many methods to solve it.

1.2 Laplace Transform Method

The technique of integral transforms is a powerful tool for the solution of linear partial differential equations. As for this research, the Laplace transform technique is employed for solving LWEs by using the formula

$$U(\bar{x},p) = L\{u(\bar{x},t)\} = \int_0^\infty u(\bar{x},t)e^{-pt}\,dt, \qquad \textbf{(1.1.10)}$$

where p is the Laplace parameter. Furthermore, some basic properties of the Laplace transform are used such as

$$L\left\{\frac{\partial^2 u}{\partial t^2}(\bar{x},t)\right\} = p^2U(\bar{x},p) - pu_0(\bar{x}) - v_0(\bar{x}), \qquad \textbf{(1.1.11)}$$

and

$$L\left\{\frac{\partial u}{\partial t}(\bar{x},t)\right\} = pU(\bar{x},p) - u_0(\bar{x}). \qquad \textbf{(1.1.12)}$$

The main attraction of this method is the removal of the time variable so that the hyperbolic equation (or the LWE) is transformed to an elliptic one which can then be solved more easily in the transformed space with BEM, FEM or DRM.

1.3 Boundary Element Method (BEM)

Boundary Element Method (BEM) is one of the most important development in numerical mathematics occurred in this century for solving partial differential equations (PDEs). This technique has been developed, within only a few decades, into a widely used and richly varies computational approach for various scientific and technological fields. There is a counting rapid expansion in a number of users, range of applications for this method which covers the areas of solid mechanics, fluid mechanics, coupled systems, chemical reactions, neutron flux, plasmas, acoustics, electric and magnetic fields, and many other related specialized fields.

In this technique, the PDE is converted to an equivalent integral equation whose discretized form yields the solution. For linear problem, the dimensionality is reduced because only boundary integrals need to be discretized that differs from "domain type" methods such as FDM or FEM. Besides, the computer implementation of the BEM is simpler than domain type methods. Hence the technique has been widely used in the solution of the Laplace equation, Helmholtz equation in domains of irregular geometry and non-uniform boundary conditions.

The efficiency demonstrated in early applications of the BEM for steady problems (time independent problems) [1, 2] has encouraged its further user in other fields of science and engineering. However, applications of the BEM for linear wave problems still remain to be done. The first work of solving this problem can be traced to Rizzo and Cruse [3, 4] who solved the linear wave problem in the Lapace transform domain and used a numerical algorithm due to Papoulis [5] to obtain time domain solutions. Unfortunately, numerical results were accurate only for early times. As an extension of Cruse's work, Manolis et al. [6] compared Papoulis' and Durbin's algorithms for the inversion of the Laplace transform. They found that Durbin's algorithm was more time consuming than Papoulis' but its accuracy was very high even for late times. Later, this method is called the Laplace Transform Boundary Element Method (LTBEM).

However, the disadvantage of LTBEM which is in common with the time-domain BEM is due to the domain integration of inhomogeneous terms in BEM analysis. Such a disadvantage can be overcome by the use of a domain-integration-free method, the Dual Reciprocity Method (DRM).

1.4 Dual Reciprocity Method (DRM)

In the literature, there have been several techniques such as Galerkin Vector Method [7], Fourier Expansion Technique [8], Dual Reciprocity Method [9], Multiple Reciprocity Method [10, 11], Particular Integral Approach [12], and Atkinson's Method [13], among others, proposed to deal with domain integrals that arise in the BEM analysis. However, the best method so far is the so-called Dual Reciprocity Method (DRM), proposed by Nardini and Brebbia [9], with which one is able to convert domain integral in the BEM analysis into equivalent boundary integrals by using a set of localized particular solutions and the reciprocity theorem twice. Thus, a "purely" boundary-only integral formulation is obtained. The DRM was further extended by many authors, e.g., Nardini and Brebbia [14], Partridge and Brebbia [15], and Partridge and Wrobel [16], and its applications to a wide variety of problems (especially, Poisson type problems) can be found in [17]. As for this research, the method is used along with FDM and Laplace transform method to solve LWEs.

1.5 The Current Research Projects

It can be obviously seen from the above literature review that there are two ways to transform an LWE into a Poisson equation before using DRM to find approximate solutions. The first way is FDM. With this method, the transformed equation is solved for each particular time (depending on time-step). The method that combines FDM and DRM proposed herein will be called the Finite Difference Dual Reciprocity Method (FDDRM). Another way is to use Laplace transform. After the transformed equation is solved in Laplace space, the numerical inversion of the Laplace transform is employed to yield approximate solutions in the original domain. This method is called the Laplace Transform Dual Reciprocity Method (LTDRM).

This thesis is organized into five chapters, with the background of the research outlined in Chapter 1.

In Chapter 2, FDDRM formulations for Linear Wave Problems (LWPs) are presented, begin with formulations for Homogeneous Linear Wave Problems (HLWPs) and followed by Inhomogeneous Linear Wave Problems (ILWPs).

In Chapter 3, both HLWPs and ILWPs are solved by using the LTDRM approach. Moreover, the numerical inversion of the Laplace transform known as "Stehfest's algorithm" with its applications are described.

In Chapter 4, several examples of LWPs, which illustrate the efficiency and the accuracy of the FDDRM and LTDRM, are provided. Furthermore, a comparison of these two formulations for solving LWPs is also made.

The major findings in these research projects are summarized in Chapter 5.

Chapter 2

FDDRM formulations for LWPs

The Finite Difference Method (FDM) is a simple approach which can be applied directly to the governing ordinary or partial differential equations. The derivatives of the unknown parameters are approximated by means of algebraic expression in terms of the differences between the numerical values of the parameters at close points. The problem domain is usually represented in terms of a grid of nodes, and the difference equations result in a system of algebraic equations in terms of the values of the parameters at the specified nodes.

In this research, FDM and DRM are applied to solve LWEs. Since LWEs contain temporal derivative terms of the unknown function u, we can not use DRM with LWEs directly. However, at a particular time, we can approximate temporal derivatives by using FDM after which the LWE is transformed into a Poisson equation. We can now apply the DRM technique to this transformed equation and the solution is obtained for each particular time. This method is called Finite Difference Dual Reciprocity Method (FDDRM) since it combines some finite difference techniques and the DRM technique.

In this chapter, the FDDRM is developed for the solution of Linear Wave Problems (LWPs) including Homogeneous Linear Wave Problems (HLWPs) and Inhomogeneous Linear Wave Problems (ILWPs).

2.1 FDDRM formulations for HLWPs

Let Ω be a bounded set in $\mathbf{R}^2$ with an enclosing boundary $\Gamma = \partial\Omega$. We consider solving the HLWP which is governed by

$$\nabla^2 u(\bar{x},t) - \frac{1}{c^2}\frac{\partial^2 u}{\partial t^2}(\bar{x},t) = 0, \quad \bar{x} \in \Omega,\, t > 0, \qquad \textbf{(2.1.1)}$$

with two initial conditions;

$$u(\bar{x},0) = u_0(\bar{x}), \quad \bar{x} \in \Omega, \tag{2.1.2}$$

$$\frac{\partial u}{\partial t}(\bar{x},0) = v_0(\bar{x}), \quad \bar{x} \in \Omega, \tag{2.1.3}$$

and three types of boundary conditions;

the Dirichlet condition,

$$u(\bar{x},t) = \bar{u}(\bar{x},t), \quad \bar{x} \in \Gamma_1, t > 0, \tag{2.1.4}$$

the Neumann condition,

$$\frac{\partial u}{\partial n}(\bar{x},t) = \bar{q}(\bar{x},t), \quad \bar{x} \in \Gamma_2, t > 0, \tag{2.1.5}$$

the Robin condition,

$$u(\bar{x},t) + \lambda\frac{\partial u}{\partial n}(\bar{x},t) = \bar{r}(\bar{x},t), \quad \bar{x} \in \Gamma_3, t > 0, \tag{2.1.6}$$

where $\{\Gamma_i, i = 1,2,3\}$ is a set of complementary segments of Γ, λ is a non-zero constant, ∇^2 is the two-dimensional Laplacian operator, $\bar{x} = (x, y)$, and $\bar{u}$, $\bar{q}$, $\bar{r}$ are known functions. We are seeking for an approximate solution of this problem when c is a non-zero constant interpreting as the velocity of wave propagation.

Let $t_i = i\Delta t$, $i = 1, 2, ..., m$ with $t_0 = 0$. By fixing $t = t_i$, Equation **(2.1.1)** at the particular time t_i is in the form

$$\nabla^2 u(\bar{x},t_i) = \frac{1}{c^2}\frac{\partial^2 u}{\partial t^2}(\bar{x},t_i), \quad \bar{x} \in \Omega. \tag{2.1.7}$$

Applying the centered finite difference approximation with RHS of Equation **(2.1.7)**, i.e.,

$$\frac{\partial^2 u}{\partial t^2}(\bar{x},t_i) = \frac{u(\bar{x},t_{i+1}) - 2u(\bar{x},t_i) + u(\bar{x},t_{i-1})}{\Delta t^2} + O(\Delta t^2), \tag{2.1.8}$$

Equation **(2.1.7)** then becomes the Poisson equation, after dropping the error term,

$$\nabla^2 u(\bar{x},t_i) = \frac{1}{c^2}\left(\frac{u(\bar{x},t_{i+1}) - 2u(\bar{x},t_i) + u(\bar{x},t_{i-1})}{\Delta t^2}\right). \tag{2.1.9}$$

BEM technique can now be applied. Multiplying Equation **(2.1.9)** with a weighting function u^* and integrating both sides of this equation over the considered domain Ω gives

$$\int_{\Omega} \nabla^2 u(\bar{x},t_i)\, u^*(\bar{x})\, d\Omega = \frac{1}{(c\Delta t)^2} \int_{\Omega} \big(u(\bar{x},t_{i+1}) - 2u(\bar{x},t_i) + u(\bar{x},t_{i-1}) \big)\, u^*(\bar{x})\, d\Omega . \quad \textbf{(2.1.10)}$$

Applying Green-Guass theorem with LHS of the above equation leads to the integral formulation

$$\int_{\Omega} u(\bar{x},t_i) \nabla^2 u^*(\bar{x})\, d\Omega + \int_{\Gamma} \big(u(\bar{x},t_i) q^*(\bar{x}) - q(\bar{x},t_i) u^*(\bar{x}) \big) d\Gamma$$
$$= \frac{1}{(c\Delta t)^2} \int_{\Omega} \big(u(\bar{x},t_{i+1}) - 2u(\bar{x},t_i) + u(\bar{x},t_{i-1}) \big)\, u^*(\bar{x})\, d\Omega, \quad \textbf{(2.1.11)}$$

where $q(\bar{x},t_i) = \frac{\partial u}{\partial n}(\bar{x},t_i)$, $q^*(\bar{x}) = \frac{\partial u^*}{\partial n}(\bar{x})$, and n is the unit outward vector normal to Γ.

It should be noted that the above equation contains two domain integrals (one each on the LHS and RHS). Examination of the domain integral on the LHS suggests that the weighting function u^* which is the fundamental solution of the Laplace equation should be chosen and u^* is given by

$$u^*(\bar{x}) = \frac{1}{2\pi} \ln|\bar{x} - \bar{\varsigma}|, \quad \textbf{(2.1.12)}$$

where $\bar{\varsigma}$ is a " source point" in the domain Ω. With this choice of u^*, the domain integral on the LHS of the Equation **(2.1.11)** reduces to a free term and Equation **(2.1.11)** becomes

$$c_{\bar{\varsigma}} u(\bar{\varsigma},t_i) - \int_{\Gamma} q(\bar{x},t_i) u^*(\bar{x})\, d\Gamma + \int_{\Gamma} u(\bar{x},t_i) q^*(\bar{x})\, d\Gamma$$
$$= \frac{1}{(c\Delta t)^2} \int_{\Omega} \big(u(\bar{x},t_{i+1}) - 2u(\bar{x},t_i) + u(\bar{x},t_{i-1}) \big)\, u^*(\bar{x})\, d\Omega. \quad \textbf{(2.1.13)}$$

The value of $c_{\bar{\varsigma}}$ in this equation depends upon the location of the source point $\bar{\varsigma}$. It can be shown [18] that

$$c_{\bar{\varsigma}} = \begin{cases} \dfrac{\theta(\bar{\varsigma})}{2\pi} & if \quad \bar{\varsigma} \in \Gamma \\ 1 & if \quad \bar{\varsigma} \in \Omega - \Gamma \end{cases}, \quad \textbf{(2.1.14)}$$

where $\theta(\bar{\varsigma})$ denotes the internal angle of the boundary at $\bar{\varsigma}$. It should be noticed that the domain integral on the RHS of Equation **(2.1.13)** still remains and this integral is very difficult to be evaluated because it contains the unknown function u.

The motivation behind DRM is to avoid evaluating such integral by transforming it into an equivalent boundary integral. This is achieved by expanding the RHS of Equation **(2.1.9)** in terms of Radial Basis Functions (RBFs) at some chosen N boundary collocation points and L internal collocation points of the domain Ω. Thus the RHS of Equation **(2.1.9)** can be approximated by a finite sum of interpolation functions $f_j, j = 1, 2, ..., N+L$ and expressed as

$$\frac{1}{c^2}\left(\frac{u(\bar{x},t_{i+1}) - 2u(\bar{x},t_i) + u(\bar{x},t_{i-1})}{\Delta t^2}\right) = \sum_{j=1}^{N+L} \alpha_j^i f_j(\bar{x}),\ \bar{x} \in \Omega, \qquad \textbf{(2.1.15)}$$

where α_j^i, $j = 1, 2, ..., N+L$ are coefficients to be determined by collocation method with $N+L$ collocation points at time t_i. After replacing Equation **(2.1.15)** into Equation **(2.1.13)**, one obtains

$$c_{\bar{\varsigma}}u(\bar{\varsigma},t_i) - \int_\Gamma q(\bar{x},t_i)u^*(\bar{x})d\Gamma + \int_\Gamma u(\bar{x},t_i)q^*(\bar{x})d\Gamma = \sum_{j=1}^{N+L} \alpha_j^i \int_\Omega f_j(\bar{x})u^*(\bar{x})d\Omega. \ \textbf{(2.1.16)}$$

The essential feature of DRM is to express f_j as a Laplacian of another function $\hat{u}_j$. Thus $\hat{u}_j$ is chosen as the solution of

$$\nabla^2 \hat{u}_j(\bar{x}) = f_j(\bar{x}),\ \ \bar{x} \in \Omega. \qquad \textbf{(2.1.17)}$$

Replacing f_j in Equation **(2.1.16)** by $\nabla^2 \hat{u}_j$ and applying the Green-Guass theorem once again, Equation **(2.1.16)** reduces to a boundary-only integral equation

$$c_{\bar{\varsigma}}u(\bar{\varsigma},t_i) - \int_\Gamma q(\bar{x},t_i)u^*(\bar{x})d\Gamma + \int_\Gamma u(\bar{x},t_i)q^*(\bar{x})d\Gamma$$
$$= \sum_{j=1}^{N+L}\left(\alpha_j^i\left(c_{\bar{\varsigma}}\hat{u}_j(\bar{\varsigma}) - \int_\Gamma \hat{q}_j(\bar{x})u^*(\bar{x})d\Gamma + \int_\Gamma \hat{u}_j(\bar{x})q^*(\bar{x})d\Gamma\right)\right)$$

(2.1.18)

where $\hat{q}_j(\bar{x}) = \dfrac{\partial \hat{u}_j}{\partial n}(\bar{x})$ is the normal derivative of $\hat{u}_j$.

As for the interpolation functions f_j, Partridge and Berbbia [15] showed that the RBF of the form $f_j = 1 + r_j$ gives the best results. Here $r_j = |\bar{x} - \bar{x}_j|$ is the distance from the collocation point j, $\bar{x}_j$, to a filed point $\bar{x}$. Hence for this research, we only took the simplest form $f_j = 1 + r_j$ in all of our numerical experiments so far completed.

We now consider all boundary integral terms in Equation **(2.1.18)**. We divide Γ into N complementary segments Γ^1, Γ^2, ..., Γ^N so that $\int_{\Gamma} u(\bar{x},t_i)\, q^*(\bar{x})\, d\Gamma$, for example, becomes

$$\int_{\Gamma} u(\bar{x},t_i) q^*(\bar{x}) d\Gamma = \int_{\Gamma^1} u(\bar{x},t_i) q^*(\bar{x}) d\Gamma + \int_{\Gamma^2} u(\bar{x},t_i) q^*(\bar{x}) d\Gamma + \ldots + \int_{\Gamma^N} u(\bar{x},t_i) q^*(\bar{x}) d\Gamma. \quad \textbf{(2.1.19)}$$

Next, we approximate $\int_{\Gamma^k} u(\bar{x},t_i) q^*(\bar{x}) d\Gamma$ for $k = 1, 2, ..., N$ with corresponding constant element . Then boundary point $\bar{x}_k$ is selected to be a middle point of the element k, and we approximate $u(\bar{x},t_i)$ on Γ^k for all $k = 1, 2, ..., N$ by using the value of u at point $\bar{x}_k$, that is

$$u(\bar{x},t_i) = u(\bar{x}_k,t_i), \qquad \bar{x} \in \Gamma^k. \quad \textbf{(2.1.20)}$$

Hence Equation **(2.1.19)** now becomes

$$\int_{\Gamma} u(\bar{x},t_i) q^*(\bar{x}) d\Gamma = \sum_{k=1}^{N} u(\bar{x}_k,t_i) \int_{\Gamma^k} q^*(\bar{x}) d\Gamma. \quad \textbf{(2.1.21)}$$

We approximate $q(\bar{x},t_i)$, $\hat{u}_j(\bar{x})$, and $\hat{q}_j(\bar{x})$ on Γ^k for all $k = 1, 2, ..., N$ in the same fashion as $u(\bar{x},t_i)$, i.e.,

$$q(\bar{x},t_i) = q(\bar{x}_k,t_i), \qquad \bar{x} \in \Gamma^k, \quad \textbf{(2.1.22)}$$

$$\hat{u}_j(\bar{x}) = \hat{u}_j(\bar{x}_k), \qquad \bar{x} \in \Gamma^k, \quad \textbf{(2.1.23)}$$

$$\hat{q}_j(\bar{x}) = \hat{q}_j(\bar{x}_k), \qquad \bar{x} \in \Gamma^k, \quad \textbf{(2.1.24)}$$

where $\bar{x}_k$ is the k's boundary collocation point on Γ^k. Now, we can write Equation **(2.1.18)** in the form

$$c_{\bar{\varsigma}} u_{\bar{\varsigma}}(t_i) + \sum_{k=1}^{N} u_k(t_i) h_{\bar{\varsigma}k} - \sum_{k=1}^{N} q_k(t_i) g_{\bar{\varsigma}k} = \sum_{j=1}^{N+L} \left(\alpha_j^i \left(c_{\bar{\varsigma}} \hat{u}_j(\bar{\varsigma}) + \sum_{k=1}^{N} \hat{u}_j(\bar{x}_k) h_{\bar{\varsigma}k} - \sum_{k=1}^{N} \hat{q}_j(\bar{x}_k) g_{\bar{\varsigma}k} \right) \right) \quad \textbf{(2.1.25)}$$

where $u_{\bar{\varsigma}}(t_i) = u(\bar{\varsigma},t_i)$, $u_k(t_i) = u(\bar{x}_k,t_i)$, and $q_k(t_i) = q(\bar{x}_k,t_i)$ with

$$h_{\bar{\varsigma}k} = -\int_{\Gamma^k} q^*(\bar{x},\bar{\varsigma})\,d\Gamma, \tag{2.1.26}$$

$$g_{\bar{\varsigma}k} = -\int_{\Gamma^k} u^*(\bar{x},\bar{\varsigma})\,d\Gamma. \tag{2.1.27}$$

Applying Equation **(2.1.25)** to all collocation points, i.e., $\bar{\varsigma} = \bar{x}_l, l = 1,2,...,N+L,$ we then obtain the linear system of order $(N+L)$ as

$$c_l u_l(t_i) + \sum_{k=1}^{N} u_k(t_i)h_{lk} - \sum_{k=1}^{N} q_k(t_i)g_{lk} = \sum_{j=1}^{N+L}\left(\alpha_j^i\left(c_l\hat{u}_j(\bar{x}_l) + \sum_{k=1}^{N}\hat{u}_j(\bar{x}_k)h_{lk} - \sum_{k=1}^{N}\hat{q}_j(\bar{x}_k)g_{lk}\right)\right), \tag{2.1.28}$$

which can be written in a matrix form as

$$\mathbf{Hu_i} - \mathbf{Gq_i} = (\mathbf{H\hat{U}} - \mathbf{G\hat{Q}})\boldsymbol{\alpha}^{\mathbf{i}}, \tag{2.1.29}$$

where **H** and **G** are matrices with their elements being h_{lk} and g_{lk} respectively and the coefficients c_l have been incorporated into the principle diagonal elements of the matrix **H** on both sides of the above equation. $\mathbf{\hat{U}}$ and $\mathbf{\hat{Q}}$ in the above equation are matrices with the *j*th column being vectors $\mathbf{\hat{u}_j}$ and $\mathbf{\hat{q}_j}$, respectively. $\mathbf{u_i}$, $\mathbf{q_i}$, and $\boldsymbol{\alpha}^{\mathbf{i}}$ are vectors with their elements being $u_l(t_i)$, $q_l(t_i)$, and α_j^i, respectively.

Now we return to Equation **(2.1.15)**. We apply Equation **(2.1.15)** to all collocation points in order to obtain the resulting matrix

$$\frac{1}{(c\Delta t)^2}\left(\mathbf{u_{i+1}} - 2\mathbf{u_i} + \mathbf{u_{i-1}}\right) = \mathbf{F}\boldsymbol{\alpha}^{\mathbf{i}}, \tag{2.1.30}$$

and thus get

$$\boldsymbol{\alpha}^{\mathbf{i}} = \mathbf{F}^{-1}\frac{1}{(c\Delta t)^2}\left(\mathbf{u_{i+1}} - 2\mathbf{u_i} + \mathbf{u_{i-1}}\right), \tag{2.1.31}$$

where **F** is the matrix with its elements being $f_j(\bar{x}_l)$. A remark should be made that $\mathbf{F}^{-1}$ always exists for the interpolation chosen in this research [15]. After substituting Equation **(2.1.31)** into Equation **(2.1.29)**, we obtain a system of simultaneous equations in matrix form as

$$\mathbf{Hu_i} - \mathbf{Gq_i} = \omega\mathrm{S}\left(\mathbf{u_{i+1}} - 2\mathbf{u_i} + \mathbf{u_{i-1}}\right), \tag{2.1.32}$$

where

$$\omega = 1/(c\Delta t)^2 \tag{2.1.33}$$

and

$$\mathbf{S} = \left(\mathbf{H}\hat{\mathbf{U}} - \mathbf{G}\hat{\mathbf{Q}}\right)\mathbf{F}^{-1}. \qquad (2.1.34)$$

Then after rearranging terms in Equation **(2.1.32)**, a final $(N+L)\times(N+L)$ linear system of equations at the particular time t_i is obtained as

$$\omega\mathbf{S}\mathbf{u}_{i+1} + \mathbf{G}\mathbf{q}_i = \left(\mathbf{H} + 2\omega\mathbf{S}\right)\mathbf{u}_i - \omega\mathbf{S}\mathbf{u}_{i-1}, \qquad (2.1.35)$$

for $i = 1, 2, ..., m$ where initial conditions $\mathbf{u}_{-1}$ and $\mathbf{u}_0$ are given as follows

$$\mathbf{u}_{-1} = \left[\, u_0(\bar{x}_l) - \Delta t\, v_0(\bar{x}_l) \,\right], \qquad (2.1.36)$$

$$\mathbf{u}_0 = \left[\, u_0(\bar{x}_l) \,\right] \quad \text{for } l = 1, 2, ..., N+L. \qquad (2.1.37)$$

Upon imposing the appropriate boundary conditions, the linear system at the particular time t_i can be readily solved.

2.2 FDDRM formulations for ILWPs

In this section, we will seek for an approximate solution to a problem governed by an ILWE of the form

$$\nabla^2 u(\bar{x},t) - \frac{1}{c^2}\frac{\partial^2 u}{\partial t^2}(\bar{x},t) = b\left(\bar{x},t,u,\frac{\partial u}{\partial t},\frac{\partial u}{\partial x},\frac{\partial u}{\partial y}\right), \qquad \bar{x}\in\Omega,\ t>0, \qquad (2.2.1)$$

where a function b is in the form

$$b\left(\bar{x},t,u,\frac{\partial u}{\partial t},\frac{\partial u}{\partial x},\frac{\partial u}{\partial y}\right) = z(\bar{x},t) + \beta_1 u + \beta_2\frac{\partial u}{\partial t} + \beta_3\frac{\partial u}{\partial x} + \beta_4\frac{\partial u}{\partial y}, \qquad (2.2.2)$$

when z is a known function and $\beta_i, i = 1, 2, 3, 4$ are constants. The initial conditions and the boundary conditions for this equation are stated the same as for the case of an HLWE in the previous section (Equations **(2.1.2) - (2.1.6)**). Since the form of b in Equation **(2.2.2)** is complicated and it is not convenient for FDDRM formulation, it is necessary to separate this problem into four cases as described below.

2.2.1 The $b = z + \beta_1 u$ case

For this case, the governing equation at a particular time t_i is

$$\nabla^2 u(\bar{x},t_i) = \frac{1}{c^2}\frac{\partial^2 u}{\partial t^2}(\bar{x},t_i) + z(\bar{x},t_i) + \beta_1 u(\bar{x},t_i), \qquad \bar{x}\in\Omega. \qquad (2.2.3)$$

Following FDDRM formulation as described in the previous section, we arrive at Equation **(2.1.9)**. The same procedure used to get Equation **(2.1.30)** then gives for this case

$$\omega(\mathbf{u}_{i+1} - 2\mathbf{u}_i + \mathbf{u}_{i-1}) + \mathbf{z}_i + \beta_1\mathbf{u}_i = \mathbf{F}\boldsymbol{\alpha}^i \quad \textbf{(2.2.4)}$$

and

$$\boldsymbol{\alpha}^i = \mathbf{F}^{-1}\left(\omega(\mathbf{u}_{i+1} - 2\mathbf{u}_i + \mathbf{u}_{i-1}) + \mathbf{z}_i + \beta_1\mathbf{u}_{i\text{-}1}\right). \quad \textbf{(2.2.5)}$$

Substituting the above equation into Equation **(2.1.29)** gives the formulation for this case as

$$\omega\mathbf{S}\mathbf{u}_{i+1} + \mathbf{G}\mathbf{q}_i = (\mathbf{H} + (2\omega - \beta_1)\mathbf{S})\mathbf{u}_i - \omega\mathbf{S}\mathbf{u}_{i-1} - \mathbf{S}\mathbf{z}_i, \quad \textbf{(2.2.6)}$$

for $i = 1, 2, ..., m$.

2.2.2 The $b = z + \beta_2 \frac{\partial u}{\partial t}$ case

At a particular time t_i, we approximate the fist time derivative term by using forward finite difference formula as

$$\frac{\partial u}{\partial t}(\bar{x}, t_i) = \frac{u(\bar{x}, t_{i+1}) - u(\bar{x}, t_i)}{\Delta t} + O(\Delta t). \quad \textbf{(2.2.7)}$$

Then vector $\boldsymbol{\alpha}^i$ can be found as

$$\boldsymbol{\alpha}^i = \mathbf{F}^{-1}\left(\omega(\mathbf{u}_{i+1} - 2\mathbf{u}_i + \mathbf{u}_{i-1}) + \mathbf{z}_i + \frac{\beta_2}{\Delta t}\mathbf{u}_{i+1} - \frac{\beta_2}{\Delta t}\mathbf{u}_i\right). \quad \textbf{(2.2.8)}$$

Replacing $\boldsymbol{\alpha}^i$ in Equation **(2.1.29)** and rearranging terms give the formulation for this case as

$$\left(\omega + \frac{\beta_2}{\Delta t}\right)\mathbf{S}\mathbf{u}_{i+1} + \mathbf{G}\mathbf{q}_i = \left(\mathbf{H} + \left(2\omega + \frac{\beta_2}{\Delta t}\right)\mathbf{S}\right)\mathbf{u}_i - \omega\mathbf{S}\mathbf{u}_{i-1} - \mathbf{S}\mathbf{z}_i, \quad \textbf{(2.2.9)}$$

for $i = 1, 2, ..., m$.

2.2.3 The $b = z + \beta_3 \frac{\partial u}{\partial x}$ or $b = z + \beta_4 \frac{\partial u}{\partial y}$ case

For $t = t_i$, we have

$$\nabla^2 u(\bar{x},t_i) = \frac{1}{c^2}\frac{\partial^2 u}{\partial t^2}(\bar{x},t_i) + z(\bar{x},t_i) + \beta_3 \frac{\partial u}{\partial x}(\bar{x},t_i), \quad \bar{x} \in \Omega. \qquad \textbf{(2.2.10)}$$

After applying FDM and DRM technique with this equation, we get Equation **(2.1.29)** and

$$\boldsymbol{\alpha}^{\mathbf{i}} = \mathbf{F}^{-1}\left(\omega\left(\mathbf{u}_{\mathbf{i+1}} - 2\mathbf{u}_{\mathbf{i}} + \mathbf{u}_{\mathbf{i-1}}\right) + \mathbf{z}_{\mathbf{i}} + \beta_3 \frac{\partial \mathbf{u}_{\mathbf{i}}}{\partial \mathbf{x}} \right), \qquad \textbf{(2.2.11)}$$

where $\frac{\partial \mathbf{u}_{\mathbf{i}}}{\partial \mathbf{x}}$ is a vector with its elements being $\frac{\partial u}{\partial x}(\bar{x}_l,t_i)$.

Now, $\frac{\partial u}{\partial x}(\bar{x}_l,t_i)$ are new unknowns and we have to rid them off by associating them with the old unknowns $u(\bar{x}_l,t_i)$. To do this we approximate the unknown function u at the particular time t_i as

$$u_i(\bar{x}) = \sum_{j=1}^{N+L} \gamma_j^i f_j(\bar{x}), \qquad \bar{x} \in \Omega, \qquad \textbf{(2.2.12)}$$

where $\gamma_j^i, j = 1, 2, ..., N+L$ are constants different from α_j^i's. We can write this equation in matrix form as

$$\mathbf{u}_{\mathbf{i}} = \mathbf{F}\boldsymbol{\gamma}^{\mathbf{i}} \qquad \textbf{(2.2.13)}$$

and inverting it gives

$$\boldsymbol{\gamma}^{\mathbf{i}} = \mathbf{F}^{-1}\mathbf{u}_{\mathbf{i}}. \qquad \textbf{(2.2.14)}$$

From Equation **(2.2.13)** and the above equation, we have

$$\frac{\partial \mathbf{u}_{\mathbf{i}}}{\partial \mathbf{x}} = \frac{\partial \mathbf{F}}{\partial \mathbf{x}}\boldsymbol{\gamma}^{\mathbf{i}} = \frac{\partial \mathbf{F}}{\partial \mathbf{x}}\mathbf{F}^{-1}\mathbf{u}_{\mathbf{i}} \qquad \textbf{(2.2.15)}$$

and then applying Equation **(2.2.15)** to Equation **(2.2.11)** gives

$$\boldsymbol{\alpha}^{\mathbf{i}} = \mathbf{F}^{-1}\left(\omega\left(\mathbf{u}_{\mathbf{i+1}} - 2\mathbf{u}_{\mathbf{i}} + \mathbf{u}_{\mathbf{i-1}}\right) + \mathbf{z}_{\mathbf{i}} + \beta_3 \frac{\partial \mathbf{F}}{\partial \mathbf{x}} \mathbf{F}^{-1}\mathbf{u}_{\mathbf{i}} \right). \qquad \textbf{(2.2.16)}$$

Plugging $\boldsymbol{\alpha}^{\mathbf{i}}$ into Equation **(2.1.29)** gives the complete formulation for this case as

$$\omega\mathbf{S}\mathbf{u}_{\mathbf{i+1}} + \mathbf{G}\mathbf{q}_{\mathbf{i}} = \left(\mathbf{H} + 2\omega\mathbf{S} - \beta_3\mathbf{R}_{\mathbf{x}}\right)\mathbf{u}_{\mathbf{i}} - \omega\mathbf{S}\mathbf{u}_{\mathbf{i-1}} - \mathbf{S}\mathbf{z}_{\mathbf{i}}, \qquad \textbf{(2.2.17)}$$

where

$$\mathbf{R}_{\mathbf{x}} = \mathbf{S}\frac{\partial \mathbf{F}}{\partial \mathbf{x}}\mathbf{F}^{-1}. \qquad \textbf{(2.2.18)}$$

In the case $b = z + \beta_4 \frac{\partial u}{\partial y}$, we replace $\mathbf{R_x}$ in Equation **(2.2.17)** with

$$\mathbf{R_y} = \mathbf{S}\frac{\partial \mathbf{F}}{\partial \mathbf{y}}\mathbf{F}^{-1} \tag{2.2.19}$$

and the formulation becomes

$$\omega \mathbf{S}\mathbf{u}_{i+1} + \mathbf{G}\mathbf{q}_i = \left(\mathbf{H} + 2\omega\mathbf{S} - \beta_4 \mathbf{R_y}\right)\mathbf{u}_i - \omega\mathbf{S}\mathbf{u}_{i-1} - \mathbf{S}\mathbf{z}_i, \tag{2.2.20}$$

2.2.4 The general case

Let us now consider the general case

$$b = z + \beta_1 u + \beta_2 \frac{\partial u}{\partial t} + \beta_3 \frac{\partial u}{\partial x} + \beta_4 \frac{\partial u}{\partial y}.$$

By using results from all previous cases, we immediately obtain the formulation for the general case

$$\kappa_1 \mathbf{S}\mathbf{u}_i + \mathbf{G}\mathbf{q}_i = \left(\mathbf{H} + \kappa_2\mathbf{S} - \beta_3 \mathbf{R_x} - \beta_4 \mathbf{R_y}\right)\mathbf{u}_i - \omega\mathbf{S}\mathbf{u}_{i-1} - \mathbf{S}\mathbf{z}_i, \tag{2.2.21}$$

for $i = 1, 2, \ldots, m$, where

$$\kappa_1 = \omega + \frac{\beta_2}{\Delta t} \tag{2.2.22}$$

and

$$\kappa_2 = 2\omega - \beta_1 + \frac{\beta_2}{\Delta t}. \tag{2.2.23}$$

Now, FDDRM formulations for LWPs are completed. The efficiency and accuracy of the FDDRM will be demonstrated and discussed in Chapter 4. Although the computer implementation of the FDDRM is not complicated and easy to apply with LWPs, this method may be time consuming if the number of time-steps (m) in the problem is too large. Therefore the LTDRM is formulated for the solutions of LWPs in the next chapter.

Chapter 3

LTDRM formulations for LWPs

The Laplace transform method is one of a classical method for solving problems governed by ordinary differential equations (ODEs) or partial differential equations (PDEs), especially transient problems such as heat or wave problems which include at least one time derivative term.

For this research, a numerical method, with Laplace Transform (LT) and Dual Reciprocity Method (DRM) combined into the so-called Laplace Transform Dual Reciprocity Method (LTDRM), is employed to solve LWPs. The basic idea of LTDRM for solving LWPs is to firstly adopt the Laplace transform to convert a time dependent hyperbolic differential system into a time independent elliptical boundary value problem in the Laplace space. Secondly, the standard DRM is adopted to solve the problem in the Laplace space. With this method, the domain integral in BEM analysis is transformed into equivalent boundary integrals. Finally, a numerical inversion of the Laplace transform called "Stehfest's algorithm" is utilized to retrieve the solution in the time domain.

This chapter is divided into three sections. In the first and the second sections, the LTDRM is formulated for the solutions of HLWPs and ILWPs, respectively. In the last section, Stehfest's algorithm is reviewed and its applications to these problems are also discussed.

3.1 LTDRM formulations for HLWPs

Consider an HLWE to be solved on a bounded domain Ω in $\mathbf{R}^2$ with an enclosing boundary $\Gamma = \partial\Omega$, i.e.,

$$\nabla^2 u(\bar{x},t) - \frac{1}{c^2}\frac{\partial^2 u}{\partial t^2}(\bar{x},t) = 0, \qquad \bar{x} \in \Omega,\ t > 0, \qquad \textbf{(3.1.1)}$$

where $c \neq 0$ represents velocity of wave propagation. Also consider the following mixed boundary conditions imposed on the boundary Γ,

the Dirichlet condition,

$$u(\bar{x},t) = \bar{u}(\bar{x},t), \qquad \bar{x} \in \Gamma_1, t > 0, \tag{3.1.2}$$

the Neumann condition,

$$\frac{\partial u}{\partial n}(\bar{x},t) = \bar{q}(\bar{x},t), \qquad \bar{x} \in \Gamma_2, t > 0, \tag{3.1.3}$$

the Robin condition,

$$u(\bar{x},t) + \lambda \frac{\partial u}{\partial n}(\bar{x},t) = \bar{r}(\bar{x},t), \qquad \bar{x} \in \Gamma_3, t > 0, \tag{3.1.4}$$

where $\{\Gamma_i, i = 1,2,3\}$ is a set of complementary segments of Γ, λ is a non-zero constant, and $\bar{u}$, $\bar{q}$, $\bar{r}$ are known functions. In addition to these boundary conditions, two initial conditions are prescribed,

$$u(\bar{x},0) = u_0(\bar{x}), \quad \bar{x} \in \Omega, \tag{3.1.5}$$

$$\frac{\partial u}{\partial t}(\bar{x},0) = v_0(\bar{x}), \quad \bar{x} \in \Omega. \tag{3.1.6}$$

In order to make use of the Laplace transform with respect to *t*, we must have the following assumptions.

1. The Laplace transform of the unknown function u exists by

$$L\{u(\bar{x},t)\} = U(\bar{x},p) = \int_0^\infty u(\bar{x},t)e^{-pt}\,dt, \tag{3.1.7}$$

   where p is the Laplace parameter.

2. The Laplace transform of the normal derivative of u exists and

$$L\left\{\frac{\partial u}{\partial n}(\bar{x},t)\right\} = \frac{\partial}{\partial n} L\{u(\bar{x},t)\} = \frac{\partial U}{\partial n}(\bar{x},p). \tag{3.1.8}$$

3. The Laplace transform of $\nabla^2 u$ exists and

$$L\{\nabla^2 u(\bar{x},t)\} = \nabla^2 L\{u(\bar{x},t)\} = \nabla^2 U(\bar{x},p). \tag{3.1.9}$$

4. The Laplace transform of $\bar{u}$, $\bar{q}$, and $\bar{r}$ exist and

$$L\{\bar{u}(\bar{x},t)\} = \bar{U}(\bar{x},p), \tag{3.1.10}$$

$$L\{\bar{q}(\bar{x},t)\} = \bar{Q}(\bar{x},p), \tag{3.1.11}$$

$$L\{\bar{r}(\bar{x},t)\} = \bar{R}(\bar{x},p). \tag{3.1.12}$$

First of all, we take the Laplace transform with respect to t of Equations **(3.1.1)** - **(3.1.4)** and use the above assumptions with the following property of the Laplace transform

$$L\left\{\frac{\partial^2 u}{\partial t^2}(\bar{x},t)\right\} = p^2 U(\bar{x},p) - p u_0(\bar{x}) - v_0(\bar{x}), \tag{3.1.13}$$

then the time dependent hyperbolic differential system is transformed into a time independent boundary value problem in the Laplace space as

$$\nabla^2 U(\bar{x},p) = \frac{1}{c^2}\left(p^2 U(\bar{x},p) - p u_0(\bar{x}) - v_0(\bar{x}) \right), \tag{3.1.14}$$

with three boundary conditions;

$$U(\bar{x},p) = \bar{U}(\bar{x},p) \quad \text{on } \Gamma_1 \tag{3.1.15}$$

$$\frac{\partial U}{\partial n}(\bar{x},p) = \bar{Q}(\bar{x},p) \quad \text{on } \Gamma_2 \tag{3.1.16}$$

$$\frac{\partial U}{\partial n}(\bar{x},p) + \lambda U(\bar{x},p) = \bar{R}(\bar{x},p) \quad \text{on } \Gamma_3 . \tag{3.1.17}$$

Note that Equation **(3.1.14)** is a Poisson equation and solving it with the traditional BEM leads to an integral equation with a domain integral containing initial conditions. Therefore, the most powerful and elegant approach so far in converting domain integrals into equivalent boundary integrals being DRM is employed and its application to the current formulation in the Laplace space is described as follows. The RHS of Equation **(3.1.14)** is approximated by a finite sum of interpolation functions $f_j, j = 1, 2, ..., N+L$ as

$$\frac{1}{c^2}\left(p^2 U(\bar{x},p) - p u_0(\bar{x}) - v_0(\bar{x})\right) = \sum_{j=1}^{N+L} \alpha_j f_j(\bar{x}), \tag{3.1.18}$$

where $\alpha_j, j = 1, 2, ..., N+L$ are the coefficients to be determined by the collocation method with N boundary collocation points and L internal collocation points.

After applying Equation **(3.1.18)** to all collocation points, the matrix form of this equation is obtained as

$$\boldsymbol{\alpha} = \frac{1}{c^2}\mathbf{F}^{-1}\left(p^2 \mathbf{U} - p\mathbf{U}_0 - \mathbf{V}_0\right), \tag{3.1.19}$$

where $\boldsymbol{\alpha}, \mathbf{U}, \mathbf{U}_0$, and $\mathbf{V}_0$ are vectors with their elements being α_j, $U(\bar{x}_j, p)$, $u_0(\bar{x}_j)$, and $v_0(\bar{x}_j)$, respectively. Replacing Equation **(3.1.18)** into Equation **(3.1.14)**, we have

$$\nabla^2 U(\bar{x}, p) = \sum_{j=1}^{N+L} \alpha_j f_j(\bar{x}). \tag{3.1.20}$$

Following the DRM procedure as described in the previous chapter, we obtain the value of unknown function U at a source point $\bar{\varsigma}$ in a domain Ω as

$$c_{\bar{\varsigma}} U_{\bar{\varsigma}}(p) + \sum_{k=1}^{N} U_k(p) h_{\bar{\varsigma}k} - \sum_{k=1}^{N} Q_k(p) g_{\bar{\varsigma}k} = \sum_{j=1}^{N+L} \left(\alpha_j \left(c_{\bar{\varsigma}} \hat{u}_{\bar{\varsigma}j} + \sum_{k=1}^{N} \hat{u}_{jk} h_{\bar{\varsigma}k} - \sum_{k=1}^{N} \hat{q}_{jk} g_{\bar{\varsigma}k} \right) \right) \tag{3.1.21}$$

where $U_k(p) = U(\bar{x}_k, p)$ and $Q_k(p) = \frac{\partial U}{\partial n}(\bar{x}_k, p)$. Applying Equation **(3.1.21)** to all collocation points gives the linear system of order $(N+L)$ as

$$c_l U_l(p) + \sum_{k=1}^{N} U_k(p) h_{lk} - \sum_{k=1}^{N} Q_k(p) g_{lk} = \sum_{j=1}^{N+L} \left(\alpha_j \left(c_{\bar{\varsigma}} \hat{u}_{lj} + \sum_{k=1}^{N} \hat{u}_{jk} h_{lk} - \sum_{k=1}^{N} \hat{q}_{jk} g_{lk} \right) \right), \tag{3.1.22}$$

$l = 1, 2, \dots, N+L$ which can be written in a matrix form as

$$\mathbf{HU} - \mathbf{GQ} = \left(\mathbf{H\hat{U}} - \mathbf{G\hat{Q}} \right) \boldsymbol{\alpha}, \tag{3.1.23}$$

where $\mathbf{Q}$ is a vector with its elements being $Q_k(p)$. Substituting $\boldsymbol{\alpha}$ from Equation **(3.1.19)** into Equation **(3.1.23)** gives

$$\mathbf{HU} - \mathbf{GQ} = \frac{1}{c^2} \mathbf{S} \left(p^2 \mathbf{U} - p \mathbf{U}_0 - \mathbf{V}_0 \right). \tag{3.1.24}$$

Rearranging terms in the above equation leads to the LTDRM formulation for HLWPs in the Laplace space as

$$\left(\mathbf{H} - \frac{p^2}{c^2} \mathbf{S} \right) \mathbf{U} - \mathbf{GQ} = -\frac{p}{c^2} \mathbf{S} \mathbf{U}_0 - \frac{1}{c^2} \mathbf{S} \mathbf{V}_0. \tag{3.1.25}$$

After applying the boundary conditions, Equation **(3.1.25)** can be solved by using a standard Guassian elimination to find values of $(N+L)$ unknowns.

It should be noted that after these $(N+L)$ unknowns are found, we can find $U_{\bar{\varsigma}}(p_\nu)$ for all $\bar{\varsigma}$ in the domain Ω in the Laplace space by using Equation **(3.1.21)**. Finally, in order to obtain the solution for $u(\bar{\varsigma}, t)$ in the time domain, the numerical inversion of Laplace transform is needed. In this research, Stehfest's algorithm is employed after which $u(\bar{\varsigma},t)$ is obtained as

$$u(\bar{\varsigma},t)=\frac{\ln 2}{t}\sum_{\nu=1}^{N_p} W_\nu\, U_{\bar{\varsigma}}(p_\nu), \qquad \textbf{(3.1.26)}$$

for all $\bar{\varsigma}\in\Omega$ and $t>0$, where N_p, W_ν, and p_ν are described in Section 3.3.

3.2 LTDRM formulations for ILWPs

In this section, the LTDRM is formulated for the solutions of ILWPs. Let us consider

$$\nabla^2 u(\bar{x},t)-\frac{1}{c^2}\frac{\partial^2 u}{\partial t^2}(\bar{x},t)=b\left(\bar{x},t,u,\frac{\partial u}{\partial t},\frac{\partial u}{\partial x},\frac{\partial u}{\partial y}\right),\quad \bar{x}\in\Omega,\ t>0, \qquad \textbf{(3.2.1)}$$

where a function b is in the form

$$b\left(\bar{x},t,u,\frac{\partial u}{\partial t},\frac{\partial u}{\partial x},\frac{\partial u}{\partial y}\right)=z(\bar{x},t)+\beta_1 u+\beta_2\frac{\partial u}{\partial t}+\beta_3\frac{\partial u}{\partial x}+\beta_4\frac{\partial u}{\partial y}, \qquad \textbf{(3.2.2)}$$

when z is a known function and $\beta_i, i=1,2,3,4$ are constants. The initial conditions and the boundary conditions for this equation are as stated previously, i.e., Equations **(3.1.2)** - **(3.1.6)**. Similar to Section 2.2, these problems are separated into four cases as explained below.

3.2.1 The $b=z+\beta_1 u$ case

Let

$$Z(\bar{x},p)=L\{z(\bar{x},t)\}, \qquad \textbf{(3.2.3)}$$

then in the Laplace space, we obtain the Poisson equation

$$\nabla^2 U(\bar{x},p)=\frac{1}{c^2}\left(p^2U(\bar{x},p)-pu_0(\bar{x})-v_0(\bar{x})\right)+\beta_1 U(\bar{x},p)+Z(\bar{x},p). \qquad \textbf{(3.2.4)}$$

Similar to the previous section, approximating the RHS of the above equation with the interpolation functions $f_j, j=1,2,\ldots,N+L$ gives $\boldsymbol{\alpha}$ as

$$\boldsymbol{\alpha} = \mathbf{F}^{-1}\left(\frac{1}{c^2}\left(p^2\mathbf{U} - p\mathbf{U_0} - \mathbf{V_0}\right) + \beta_1\mathbf{U} + \mathbf{Z}\right), \qquad \textbf{(3.2.5)}$$

where $\mathbf{Z}$ is a vector with its elements being $Z(\bar{x}_k, p)$. Replacing $\boldsymbol{\alpha}$ into Equation **(3.1.23)** and rearranging terms lead to the formulation for this case

$$\left(\mathbf{H} - \left(\frac{p^2}{c^2} + \beta_1\right)\mathbf{S}\right)\mathbf{U} - \mathbf{GQ} = -\frac{p}{c^2}\mathbf{SU_0} - \frac{1}{c^2}\mathbf{SV_0} + \mathbf{SZ}. \qquad \textbf{(3.2.6)}$$

3.2.2 The $b = z + \beta_2 \dfrac{\partial u}{\partial t}$ case

By using the property of the Laplace transform, we get that

$$L\left\{\beta_2 \frac{\partial u}{\partial t}(\bar{x}, t)\right\} = \beta_2\left(pU(\bar{x}, p) - u_0(\bar{x})\right). \qquad \textbf{(3.2.7)}$$

Therefore in the Laplace space, we have

$$\nabla^2 U(\bar{x}, p) = \left(\frac{p^2}{c^2} + \beta_2 p\right)U(\bar{x}, p) - \left(\frac{p}{c^2} + \beta_2\right)u_0(\bar{x}) - \frac{1}{c^2}v_0(\bar{x}) + Z(\bar{x}, p).$$

(3.2.8)

Then we obtain the vector $\boldsymbol{\alpha}$

$$\boldsymbol{\alpha} = \mathbf{F}^{-1}\left(\left(\frac{p^2}{c^2} + \beta_2 p\right)\mathbf{U} - \left(\frac{p}{c^2} + \beta_2\right)\mathbf{U_0} - \frac{1}{c^2}\mathbf{V_0} + \mathbf{Z}\right). \qquad \textbf{(3.2.9)}$$

Thus the formulation of this case is achieved, i.e.,

$$\left(\mathbf{H} - \left(\frac{p^2}{c^2} + \beta_2 p\right)\mathbf{S}\right)\mathbf{U} - \mathbf{GQ} = -\left(\frac{p}{c^2} + \beta_2\right)\mathbf{SU_0} - \frac{1}{c^2}\mathbf{SV_0} + \mathbf{SZ}.$$

(3.2.10)

3.2.3 The $b = z + \beta_3 \dfrac{\partial u}{\partial x}$ or $b = z + \beta_4 \dfrac{\partial u}{\partial y}$ case

Assume that the Laplace transform of $\dfrac{\partial u}{\partial x}$ exists and

$$L\left\{\beta_3 \frac{\partial u}{\partial x}(\bar{x}, t)\right\} = \beta_3 \frac{\partial U}{\partial x}(\bar{x}, p). \qquad \textbf{(3.2.11)}$$

Then in the Laplace space, we get that

$$\nabla^2 U(\bar{x}, p) = \frac{1}{c^2}\left(p^2 U(\bar{x}, p) - p u_0(\bar{x}) - v_0(\bar{x}) \right) + \beta_3 \frac{\partial U}{\partial x}(\bar{x}, p) + Z(\bar{x}, p).$$

(3.2.12)

By approximating the RHS of Equation **(3.2.12)** with the interpolation functions $f_j, j = 1, 2, ..., N + L,$ one gets $\boldsymbol{\alpha}$ as

$$\boldsymbol{\alpha} = \mathbf{F}^{-1}\left(\frac{1}{c^2}\left(p^2\mathbf{U} - p\mathbf{U}_0 - \mathbf{V}_0\right) + \beta_3 \frac{\partial \mathbf{U}}{\partial \mathbf{x}} + \mathbf{Z}\right), \qquad \textbf{(3.2.13)}$$

where $\frac{\partial \mathbf{U}}{\partial \mathbf{x}}$ is a vector with its elements being $\frac{\partial U}{\partial x}(\bar{x}_j, p)$. Similar to the procedure in Sub-section 2.2.3, we can show that

$$\frac{\partial \mathbf{U}}{\partial \mathbf{x}} = \frac{\partial \mathbf{F}}{\partial \mathbf{x}}\mathbf{F}^{-1}\mathbf{U}. \qquad \textbf{(3.2.14)}$$

Substituting Equation **(3.2.13)** and Equation **(3.2.14)** into Equation **(3.1.23)** makes the complete formulation of this case as

$$\left(\mathbf{H} - \frac{p^2}{c^2}\mathbf{S} - \beta_3 \mathbf{R}_\mathbf{x}\right)\mathbf{U} - \mathbf{GQ} = -\frac{p}{c^2}\mathbf{SU}_0 - \frac{1}{c^2}\mathbf{SV}_0 + \mathbf{SZ}. \qquad \textbf{(3.2.15)}$$

For the case $b = z + \beta_4 \frac{\partial u}{\partial y}$, we immediately obtain its formulation

$$\left(\mathbf{H} - \frac{p^2}{c^2}\mathbf{S} - \beta_4 \mathbf{R}_\mathbf{y}\right)\mathbf{U} - \mathbf{GQ} = -\frac{p}{c^2}\mathbf{SU}_0 - \frac{1}{c^2}\mathbf{SV}_0 + \mathbf{SZ}. \qquad \textbf{(3.2.16)}$$

3.2.4 The general case

By using results from all previous cases, we easily obtain the formulation of the general case as

$$\left(\mathbf{H} - \eta_1\mathbf{S} - \beta_3\mathbf{R}_\mathbf{x} - \beta_4\mathbf{R}_\mathbf{y}\right)\mathbf{U} - \mathbf{GQ} = \eta_2\mathbf{SU}_0 - \frac{1}{c^2}\mathbf{SV}_0 + \mathbf{SZ}, \qquad \textbf{(3.2.17)}$$

where

$$\eta_1 = \frac{p^2}{c^2} + \beta_1 + \beta_2 p, \qquad \textbf{(3.2.18)}$$

and

$$\eta_2 = -\left(\frac{p}{c^2} + \beta_2\right). \qquad \textbf{(3.2.19)}$$

3.3 Stehfest's algorithm

After the solution $U(\bar{x},p)$ in the Laplace space is found numerically, the inverse of the Laplace transform is necessary in order to obtain the solution $u(\bar{x},t)$ in the original physical domain. There are many Laplace inverse transform algorithms available in the literature and one of those is Stehfest's algorithm. Stehfest [19] showed that it gives a good accuracy on a fairly wide range of functions. Furthermore, Moridis and Reddell [20] and Cheng et al. [21] also reported successful utilization of Stehfest's algorithm, which is therefore chosen for our numerical inversion. The Stehfest's algorithm is described as follows.

Let F be the Laplace transform of f. Stehfest [19] showed that for any observation time t, $f(t)$ can be approximated by a linear combination of $F(p_\nu)$, $\nu = 1, 2, \ldots, N_p$ and multiplied by $\dfrac{\ln 2}{t}$ as

$$f(t) \approx \frac{\ln 2}{t} \sum_{\nu=1}^{N_p} W_\nu \, F(p_\nu), \tag{3.3.1}$$

where N_p must be taken as an even number and p_ν, $\nu = 1, 2, \ldots, N_p$ are parameters corresponding to time t as

$$p_\nu = \frac{\ln 2}{t} \, \nu, \tag{3.3.2}$$

and weight W_ν being defined as

$$W_\nu = (-1)^{(\sigma+\nu)} \sum_{k=K}^{M} \frac{k^\sigma \; (2k)!}{(\sigma-k)! \; k! \; (k-1)! \, (\nu-k)! \, (2k-\nu)!} \tag{3.3.3}$$

where $\sigma = \dfrac{N_p}{2}$, $K = [\, 0.5\,(\nu+1)\,]$, and $M = \min\{\sigma, \nu\}$.

After applying Equation **(3.3.1)** with Equation **(3.1.21)** to find an approximate solution at any internal point $\bar{\varsigma}$ at any time t, we then obtain

$$u(\bar{\varsigma},t) = \frac{\ln 2}{t} \sum_{\nu=1}^{N_p} W_\nu \, U_{\bar{\varsigma}}(p_\nu). \tag{3.3.4}$$

It should be noted that in obtaining an approximate solution by LTDRM at any particular time t, no matter how t is small or large, only N_p linear systems of order $(N+L)$ such as Equation **(3.1.25)** are solved. On the contrary, we have to solve m

linear systems of equations when using FDDRM. Since m becomes larger as t increases, FDDRM will be more time consuming than LTDRM when solutions at large times are required. Thus, this is the major advantage of the LTDRM over the FDDRM.

As for the selection of the value of N_p with which the algorithm yields best results, Stehfest [19] suggested that the optimum value of N_p be 10 for single precision variables (8 significant figures) and 18 for double precision variables (16 significant figures). However, our experience showed that no significant difference was noticed when using the algorithm for N_p between 6 and 16. In fact, an accurate solution may even be obtained for N_p as small as 6. Thus the choice for the value of N_p in this research is 6.

Now, although all formulations of the LTDRM for LWPs are formulated, the Laplace transform of boundary conditions and the known function z are not convenient to implement for a computer program if they are too complicated. In 1994, Zhu, S. P., Satravaha, P. and Lu, X. P. [22] solved this problem by approximating them as

$$U(\bar{x},p_\nu)=\bar{U}(\bar{x},p_\nu)\approx L\{\bar{u}(\bar{x},t_i)\}=\frac{\bar{u}(\bar{x},t_i)}{p_\nu} \quad \text{on } \Gamma_1 \qquad \textbf{(3.3.5)}$$

$$\frac{\partial U}{\partial n}(\bar{x},p_\nu)=\bar{Q}(\bar{x},p_\nu)\approx L\{\bar{q}(\bar{x},t_i)\}=\frac{\bar{q}(\bar{x},t_i)}{p_\nu} \quad \text{on } \Gamma_2 \qquad \textbf{(3.3.6)}$$

$$\frac{\partial U}{\partial n}(\bar{x},p_\nu)+\lambda U(\bar{x},p_\nu)=\bar{R}(\bar{x},p_\nu)\approx L\{\bar{r}(\bar{x},t_i)\}=\frac{\bar{r}(\bar{x},t_i)}{p_\nu} \quad \text{on } \Gamma_3, \qquad \textbf{(3.3.7)}$$

where $p_\nu=\frac{\ln 2}{t_i}\nu$, $\nu=1, 2, ..., N_p$, for a particular time t_i. Since $\bar{u}$, $\bar{q}$, and $\bar{r}$ are known exactly in the time domain at time t_i, thus $\bar{U}$, $\bar{Q}$, and $\bar{R}$ are easily evaluated and implemented into the computer program. They used these approximations in LTDRM procedure for solving linear diffusion problems and it gave a good accuracy. However, they did not verify about the Laplace transform of z.

In Appendix A, we already show that Laplace transform of z such as in Equation **(3.2.3)** can also be approximated as

$$Z(\bar{x},p_\nu)\approx L\{z(\bar{x},t_i)\}=\frac{z(\bar{x},t_i)}{p_\nu}, \qquad \textbf{(3.3.8)}$$

where $p_\nu = \frac{\ln 2}{t_i}\,\nu,\ \nu = 1, 2, ..., N_p$, for a particular time t_i. Therefore in this research, these approximations are employed in all computer implementations of the LTDRM. In the next chapter, the efficiency and the accuracy of the LTDRM are demonstrated via several numerical examples.

Chapter 4

Numerical examples and Discussions

From Chapter 1, we know that there are a lot of problems in science and engineering governed by LWEs. Vibrations of a membrane problems are one type of those problems which can be mathematically modeled by two-dimensional linear wave equations. The analytical solutions for some homogeneous problems can often be found by using the method of separation of variables if the boundary of a membrane is rectangular or circular. However, many practical problems are governed by ILWEs which are defined on a membrane with irregular boundary, and analytical solutions are either difficult or impossible to be obtained. Thus in this research, we illustrate the usefulness of both numerical techniques, i.e., FDDRM and LTDRM, developed in Chapter 2 and Chapter 3 for solving these problems.

In this chapter, thirteen numerical examples of vibrations of a membrane problems are chosen to be solved by FDDRM and LTDRM. These examples include various cases of vibrations of a membrane problems. In order to measure the accuracy of numerical solutions obtained by these methods, an average absolute error at time t denoted by $A_{av}(t)$ and an average relative error at time t denoted by $E_{av}(t)$, defined in Appendix B, will be used.

This chapter consists of two sections. In the first section, five problems governed by HLWEs are used to investigate the accuracy and the efficiency of FDDRM and LTDRM for HLWPs. In another section, eight problems which can be modeled by ILWEs are utilized to investigate the accuracy and the efficiency of FDDRM and LTDRM for ILWPs.

4.1 Numerical examples and Discussions for HLWPs

In this section, five examples (Examples 1 - 5) of HLWPs describing vibrations of a membrane are presented and solved by FDDRM and LTDRM. $\Delta t = 0.1$ and $N_p = 6$ are used in FDDRM and LTDRM procedures, respectively. It should be observed that numerical results obtained from these problems are very accurate when $c \leq 10^{-5}$ at small observation times as well as large observation times while they are accurate only at small observation times when $c > 10^{-5}$.

4.1.1 Example 1

The vibrations of a membrane problem without a source term is governed by the HLWE (Equation **(2.1.1)**) with two initial conditions and three types of boundary conditions (Equations **(2.1.2)** – **(2.1.6)**), where $u(\bar{x},t)$ is the displacement of a membrane at a point $\bar{x}$ from its equilibrium position at a time t and c is a non-zero constant depending on the properties of a membrane. If the boundary of a membrane is rectangular such as $\Omega = [0,a]\times[0,b]$ and it is fixed ($u \equiv 0$ on Γ) then the analytical solution is obtained by using the method of separation of variables as

$$u(x,y,t) = \sum_{m=1}^{\infty}\sum_{n=1}^{\infty}\left(A_{mn}\cos(\omega_{mn}t) + B_{mn}\sin(\omega_{mn}t)\right)\sin\left(\frac{m\pi x}{a}\right)\sin\left(\frac{n\pi y}{b}\right), \qquad \textbf{(4.1.1)}$$

where

$$A_{mn} = \frac{4}{ab}\int_0^a\int_0^b u_0(x,y)\sin\left(\frac{m\pi x}{a}\right)\sin\left(\frac{n\pi y}{b}\right)dx\,dy, \qquad \textbf{(4.1.2)}$$

$$B_{mn} = \frac{4}{ab\omega_{mn}}\int_0^a\int_0^b v_0(x,y)\sin\left(\frac{m\pi x}{a}\right)\sin\left(\frac{n\pi y}{b}\right)dx\,dy \qquad \textbf{(4.1.3)}$$

and

$$\omega_{mn} = \pi c\sqrt{\frac{m^2}{a^2}+\frac{n^2}{b^2}}. \qquad \textbf{(4.1.4)}$$

As for this example, we let $a = b = 1$ and two initial conditions are

$$u_0(x,y) = x(1-x)y(1-y) \text{ on } \Omega \tag{4.1.5}$$

and

$$v_0(x,y) = 0 \text{ on } \Omega. \tag{4.1.6}$$

The displacements of all points in the domain Ω at $t=0$ are shown in Figure 4.1.1. In applying the FDDRM and the LTDRM to this problem, the boundary Γ is discretized into 20 equal-size constant elements and 16 internal points in Ω are used as shown in Figure 4.1.2. Average relative errors $E_{av}(t)$ obtained by using FDDRM and LTDRM to solve this problem for $c=10^{-4}$ and 10^{-5} are illustrated in Figures 4.1.3 – 4.1.4. It can be seen that numerical solutions obtained from both methods when $c=10^{-5}$ are more accurate than the ones obtained when $c=10^{-4}$. In fact, our experiments have shown that they are in very good agreement with analytical solutions for small observation times as well as large observation times when $c \le 1\times10^{-5}$. On the other hand, they are often accurate only at small observation times when $c > 1\times10^{-5}$. Figures 4.1.5 – 4.1.10 show displacements of all points in the domain Ω obtained from both methods and analytical solutions at $t=5000$ and 15000 when $c=10^{-5}$. It should be noted that although t is large, numerical solutions are still in good agreement with the analytical solution.

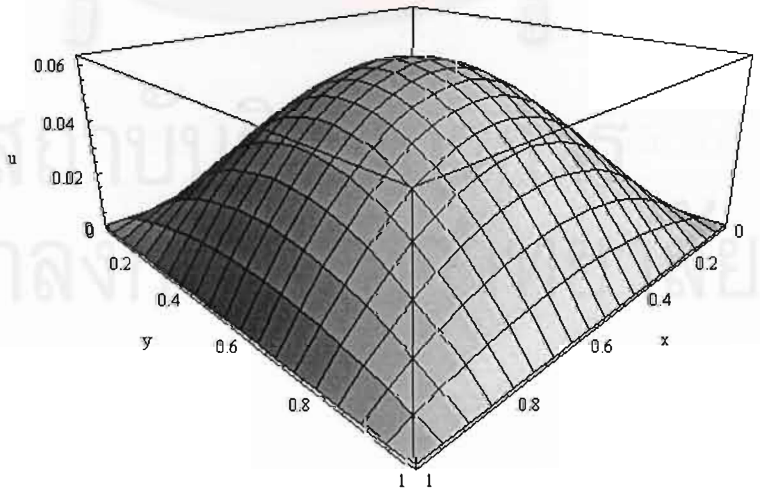

Figure 4.1.1: The displacements of all points in the domain $\Omega = [0,1]\times[0,1]$ at $t=0$.

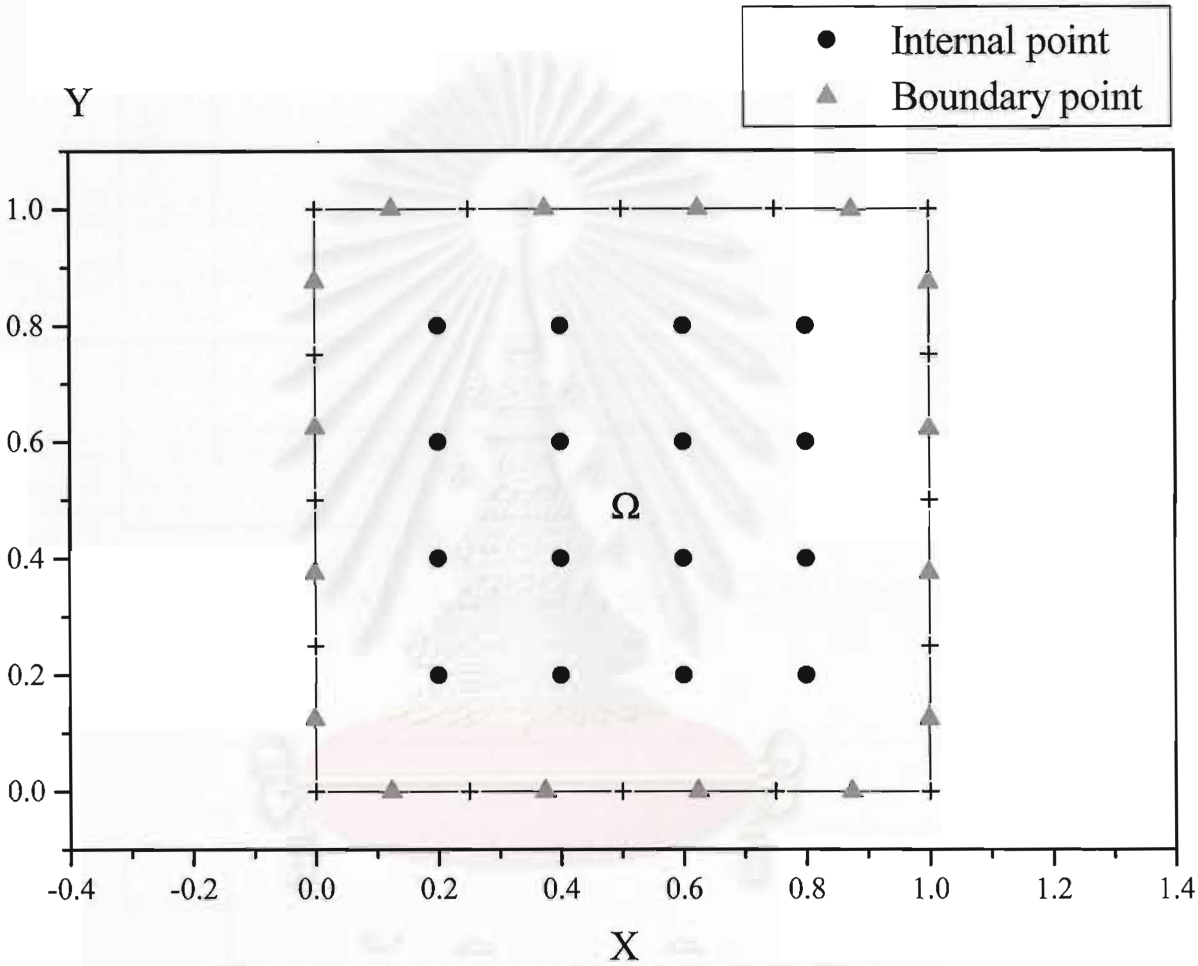

Figure 4.1.2: The domain Ω and all collocation points in Example 1.

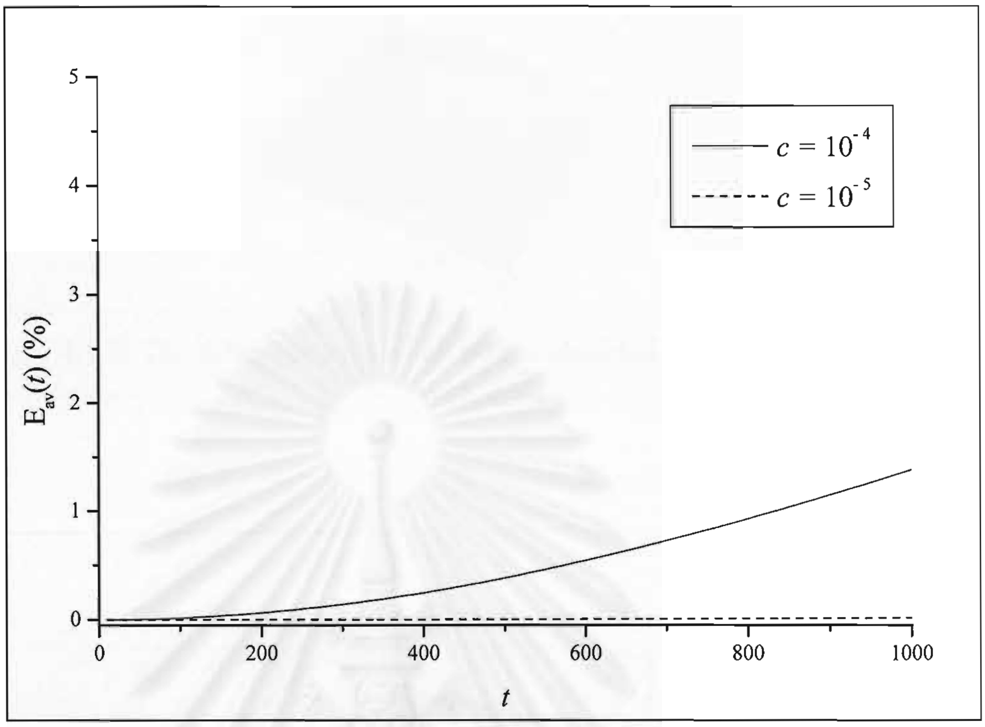

Figure 4.1.3: Average relative errors of the FDDRM.

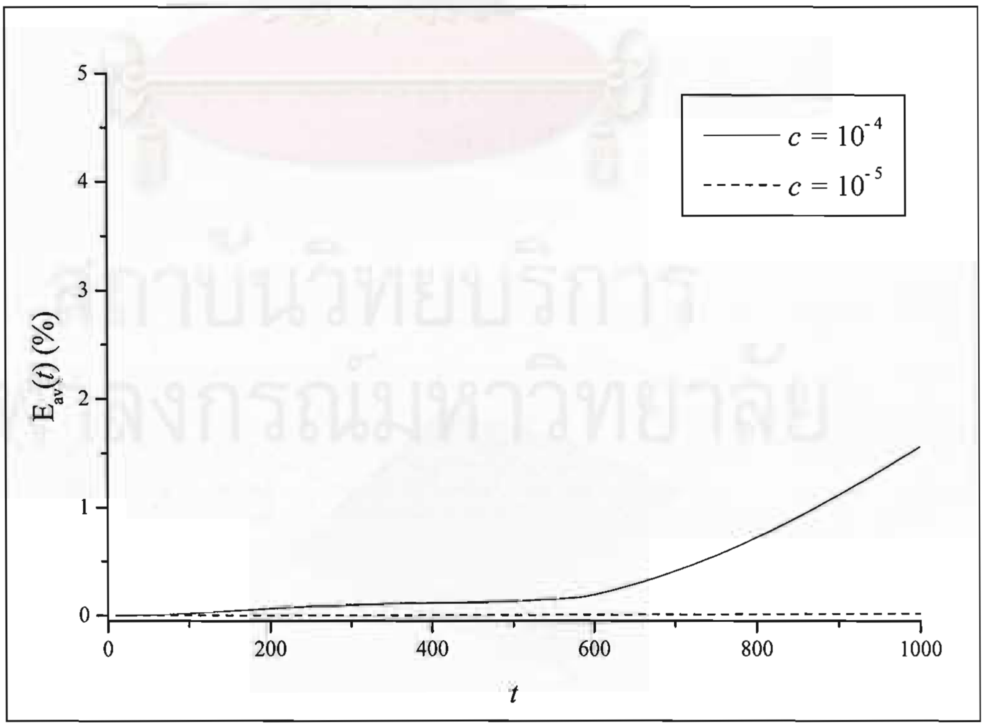

Figure 4.1.4: Average relative errors of the LTDRM.

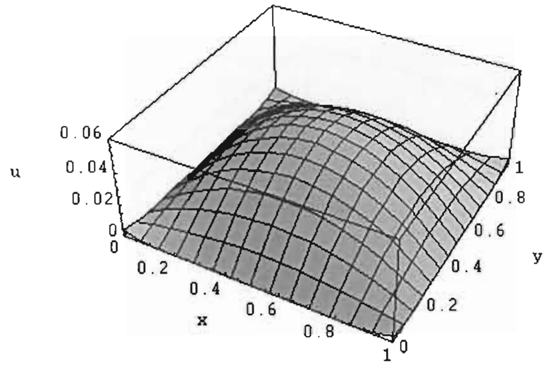

Figure 4.1.5: The displacements of all points obtained from the FDDRM at t = 5000 with $c=10^{-5}$.

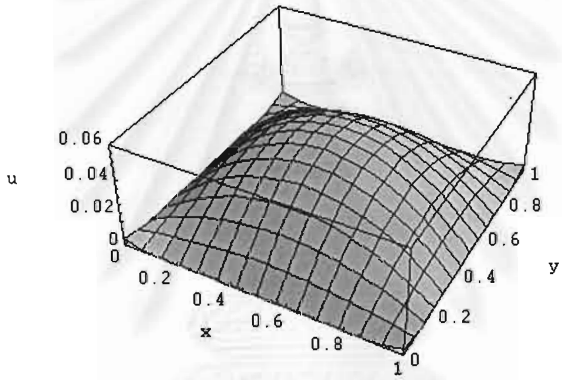

Figure 4.1.6: The displacements of all points obtained from the LTDRM at t = 5000 with $c=10^{-5}$.

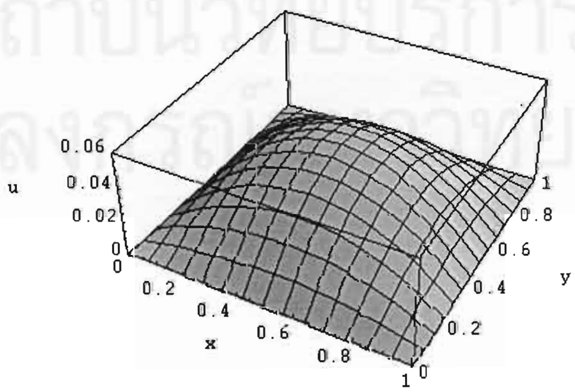

Figure 4.1.7: The displacements of all points obtained from the analytical solution at t = 5000 with $c=10^{-5}$.

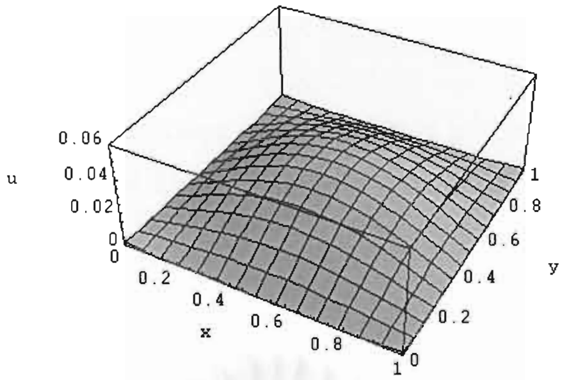

Figure 4.1.8: The displacements of all points obtained from the FDDRM at $t = 15000$ with $c = 10^{-5}$.

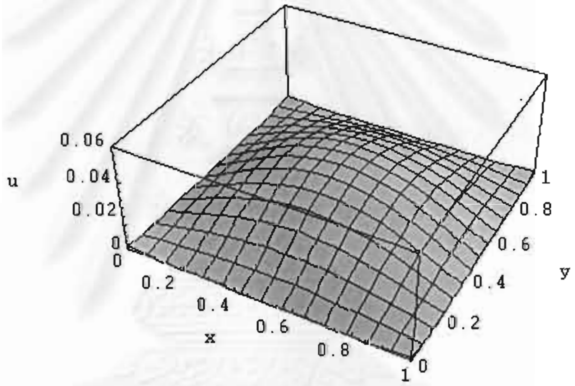

Figure 4.1.9: The displacements of all points obtained from the LTDRM at $t = 15000$ with $c = 10^{-5}$.

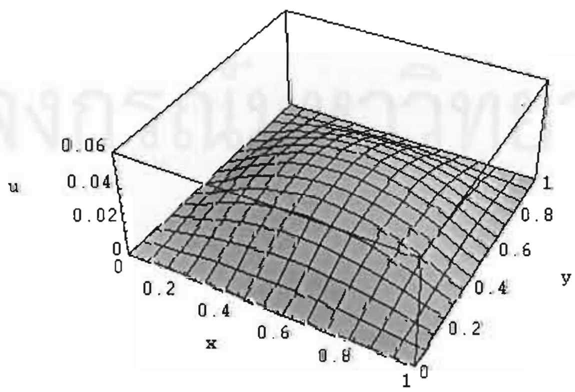

Figure 4.1.10: The displacements of all points obtained from the analytical solution at $t = 15000$ with $c = 10^{-5}$.

4.1.2 Example 2

In this example, the vibrations of a membrane problem without a source term with $\Omega = [0,1]\times[0,1]$ is solved. Unlike Example 1, two initial conditions are changed to

$$u(x,y,0) = 0 \tag{4.1.7}$$

and

$$\frac{\partial u}{\partial t}(x,y,0) = x \tag{4.1.8}$$

and the free boundary condition $\dfrac{\partial u}{\partial n} \equiv 0$ on Γ is imposed. To solve this problem, all collocation points in Example 1 are used in FDDRM and LTDRM procedure. The analytical solution, which is obtained by using the method of separation of variables, is of the form

$$u(x,y,t) = \sum_{m=0}^{\infty}\sum_{n=0}^{\infty} A_{nm}\cos(n\pi x)\cos(m\pi y)h_{nm}(t), \tag{4.1.9}$$

where

$$h_{nm}(t) = \begin{cases} t & , \quad m = 0, n = 0 \\ \sin(\omega_{nm}t) & , \quad \text{otherwise} \end{cases} \tag{4.1.10}$$

and

$$A_{nm}h'_{nm}(0) = \frac{\int_0^1\int_0^1 x\cos(n\pi x)\cos(m\pi y)\,dx\,dy}{\int_0^1\int_0^1 \cos^2(n\pi x)\cos^2(m\pi y)\,dx\,dy}. \tag{4.1.11}$$

Better than the previous example, numerical solutions obtained from both methods are accurate when $c \le 1\times10^{-4}$ as shown in Figures 4.1.11 – 4.1.12. The displacements of a membrane obtained by using FDDRM and LTDRM at $t = 2000$ with $c = 10^{-5}$ are shown in Figures 4.1.13 – 4.1.14 and also shown in Figure 4.1.15 are the displacements of a membrane from the analytical solution.

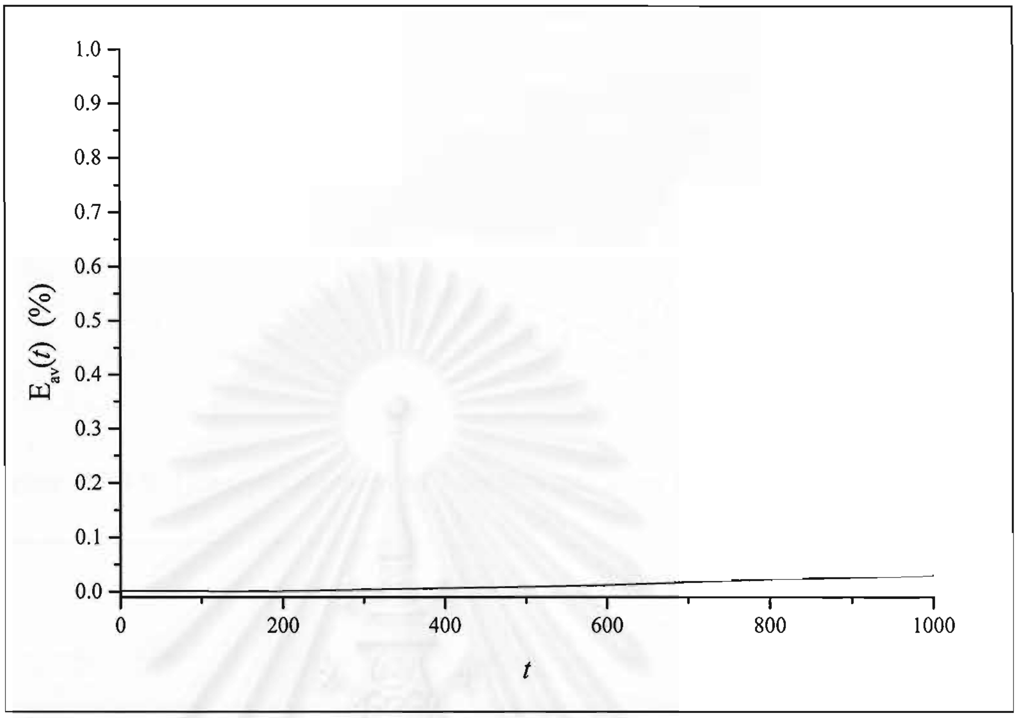

Figure 4.1.11: Average relative errors of the FDDRM with $c = 10^{-4}$.

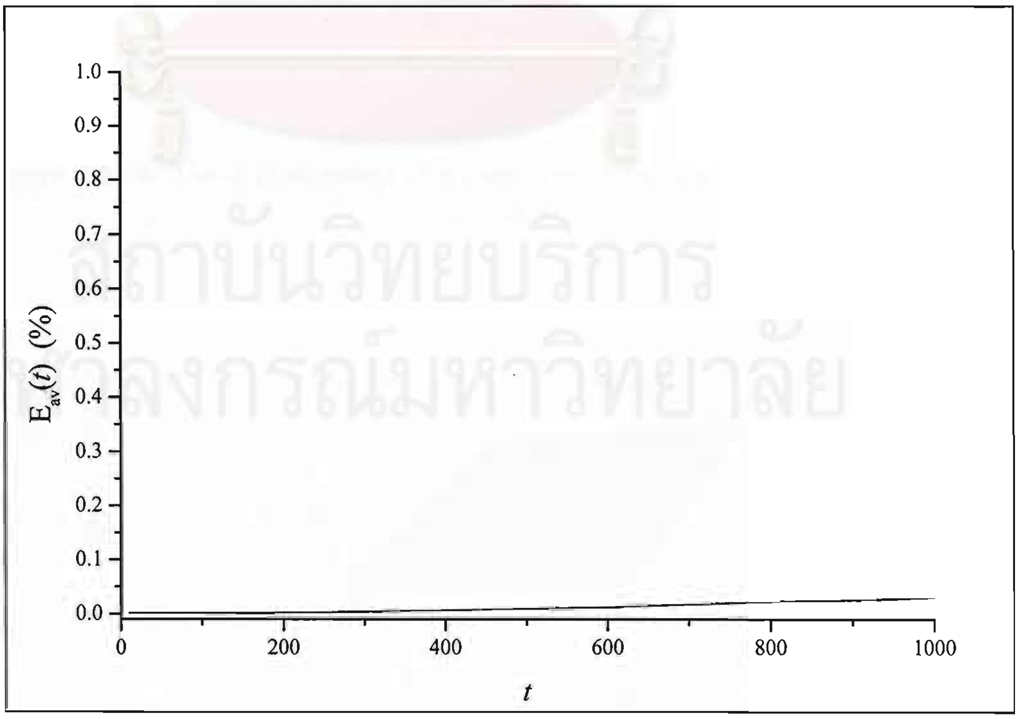

Figure 4.1.12: Average relative errors of the LTDRM with $c = 10^{-4}$.

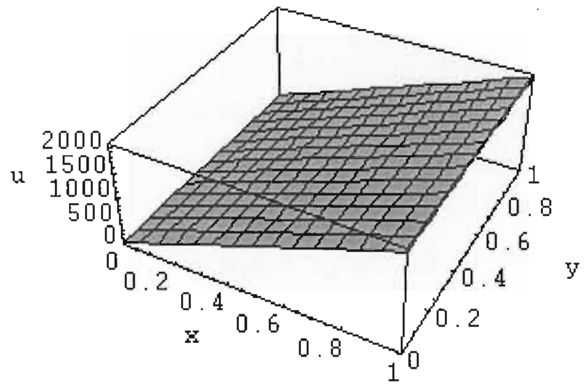

Figure 4.1.13: The displacement of a membrane from the FDDRM with $c = 10^{-5}$ at $t = 2000$.

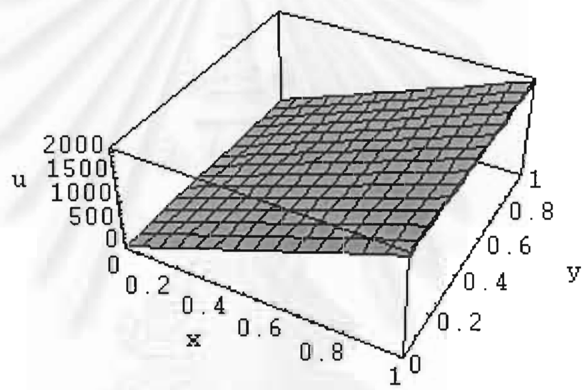

Figure 4.1.14: The displacement of a membrane from the LTDRM with $c = 10^{-5}$ at $t = 2000$.

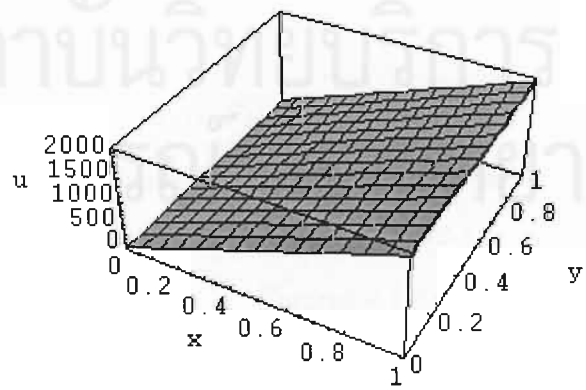

Figure 4.1.15: The displacement of a membrane from the analytical solution with $c = 10^{-5}$ at $t = 2000$.

4.1.3 Example 3

In this example, we investigate vibrations of a circular membrane. The governing equation of this problem is

$$\frac{\partial^2 u}{\partial t^2} = c^2\nabla^2 u - b, \qquad \textbf{(4.1.12)}$$

where $\nabla^2 \equiv \frac{1}{r}\frac{\partial}{\partial r}\left(r\frac{\partial}{\partial r}\right)+\frac{1}{r^2}\frac{\partial^2}{\partial \theta^2}$ is the Laplacian operator in polar coordinates. The domain in this case can be described as $\Omega = \{(r,\theta), \text{where } 0 < r \le r_0 \text{ and} -\pi < \theta < \pi\}$ for some r_0>0, $r = \sqrt{x^2+y^2}$ and $\theta = \tan^{-1}\left(\frac{y}{x}\right)$. If a source term is neglected $(b \equiv 0)$, the boundary of the membrane is fixed ($u \equiv 0$ on Γ), and $\left.\frac{\partial u}{\partial t}\right|_{t=0} \equiv v_0 \equiv 0$

then the analytical solution is expressed as

$$u(r,\theta,t) = \sum_{m=0}^{\infty}\sum_{n=1}^{\infty} J_m(\lambda_{mn} r)\big(A_{mn}\cos(m\theta) + B_{mn}\sin(m\theta)\big)\cos(\lambda_{mn} ct), \qquad \textbf{(4.1.13)}$$

where J_m is the Bessel function of the first kind of order m, $r_0\lambda_{mn}$ is nth root of J_m and

$$A_{mn} = \frac{2}{\pi r_0^2 J_{m+1}^2(\lambda_{mn} r_0)}\int_0^{r_0}\int_{-\pi}^{\pi} r J_m(\lambda_{mn} r)\, u_0(r,\theta)\cos(m\theta)\, d\theta\, dr \qquad \textbf{(4.1.14)}$$

and

$$B_{mn} = \frac{2}{\pi r_0^2 J_{m+1}^2(\lambda_{mn} r_0)}\int_0^{r_0}\int_{-\pi}^{\pi} r J_m(\lambda_{mn} r)\, u_0(r,\theta)\sin(m\theta)\, d\theta\, dr. \qquad \textbf{(4.1.15)}$$

To solve this problem, 56 collocation points as shown in Figure 4.1.16 are chosen with r_0=1 and the initial condition

$$u_0(r,\theta) = (r_0^2 - r^2)\sin(\theta). \qquad \textbf{(4.1.16)}$$

Figure 4.1.17 shows the displacements of a circular membrane at $t = 0$. Average relative errors $E_{av}(t)$ obtained by using FDDRM and LTDRM to solve this problem for $c = 10^{-4}$ and 10^{-5} are illustrated in Figures 4.1.18 – 4.1.19. From these Figures, it should be noticed that average relative errors grow up with time when $c = 10^{-4}$ while they are small (less than 1%) and stable over a long time period when $c = 10^{-5}$. In fact, they are small when $c \le 10^{-5}$.

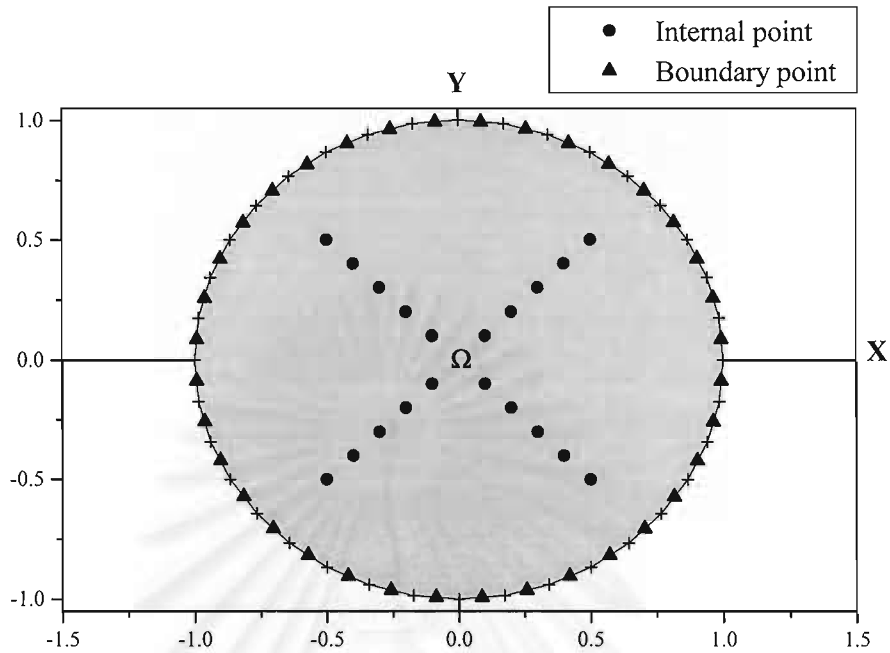

Figure 4.1.16: The domain Ω and 56 collocation points in Example 3.

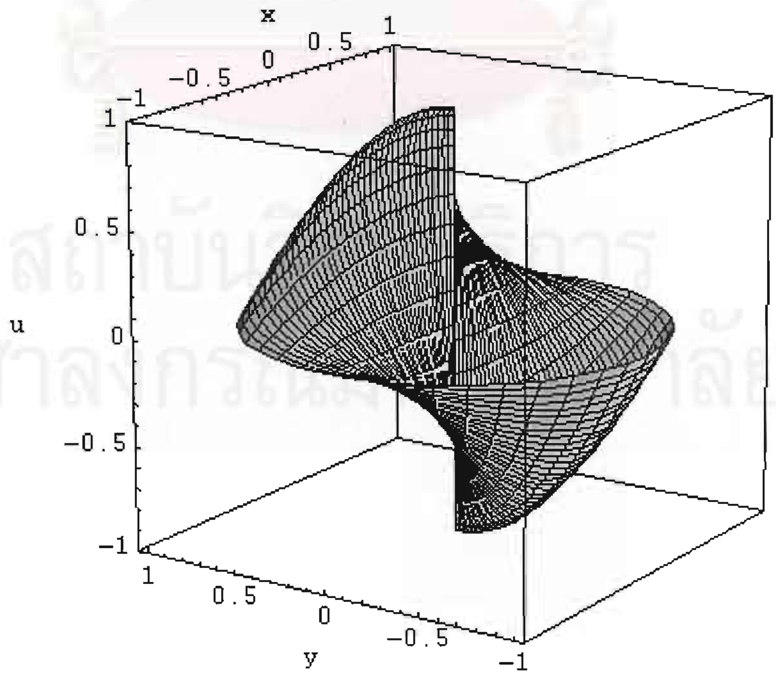

Figure 4.1.17: The displacement of a circular membrane at $t = 0$ in Example 3.

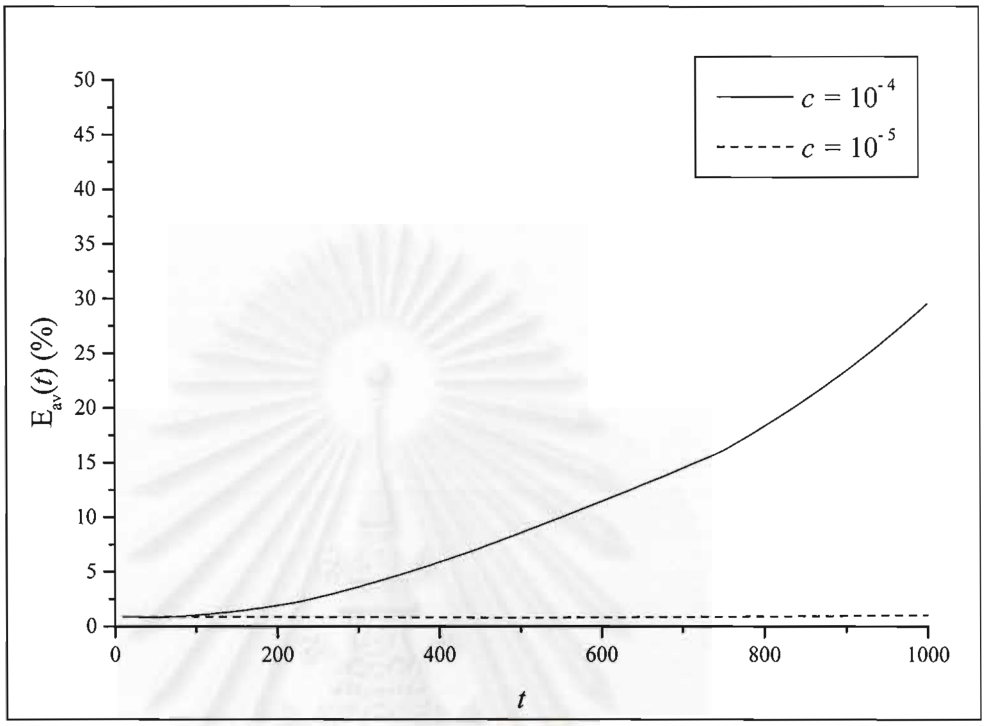

Figure 4.1.18: Average relative errors of the FDDRM.

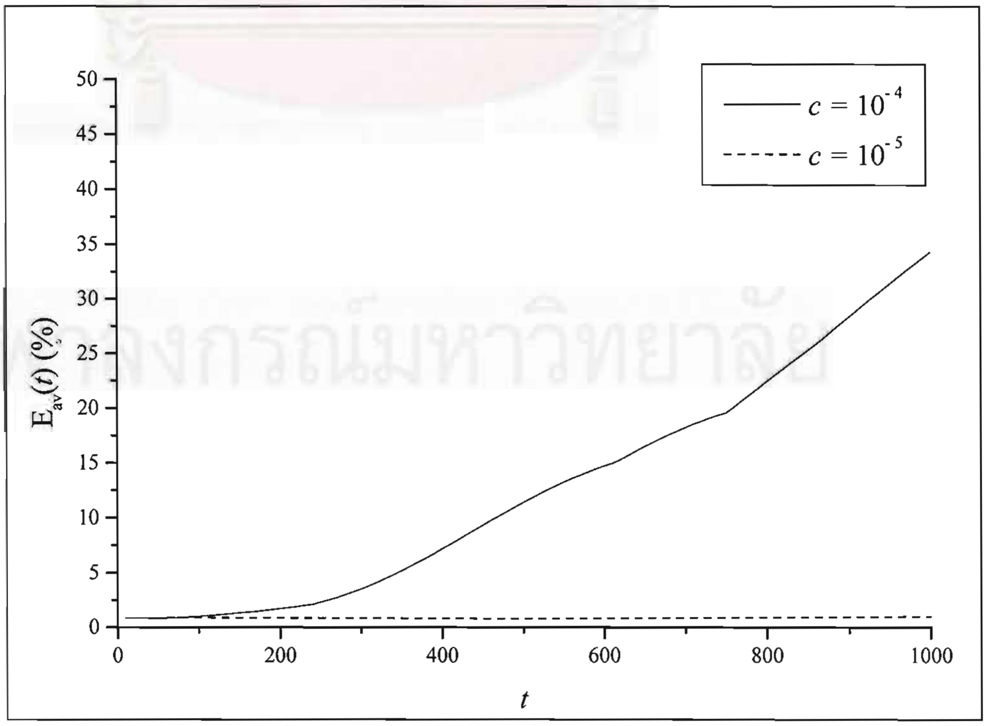

Figure 4.1.19: Average relative errors of the LTDRM.

4.1.4 Example 4

Consider the HLWE (Equation **(2.2.1)**) on a domain Ω as shown in Figure 4.1.20 with Robin condition on Γ_1 and Dirichlet conditions on $\bigcup \Gamma_i, i = 2,3,4,5$.

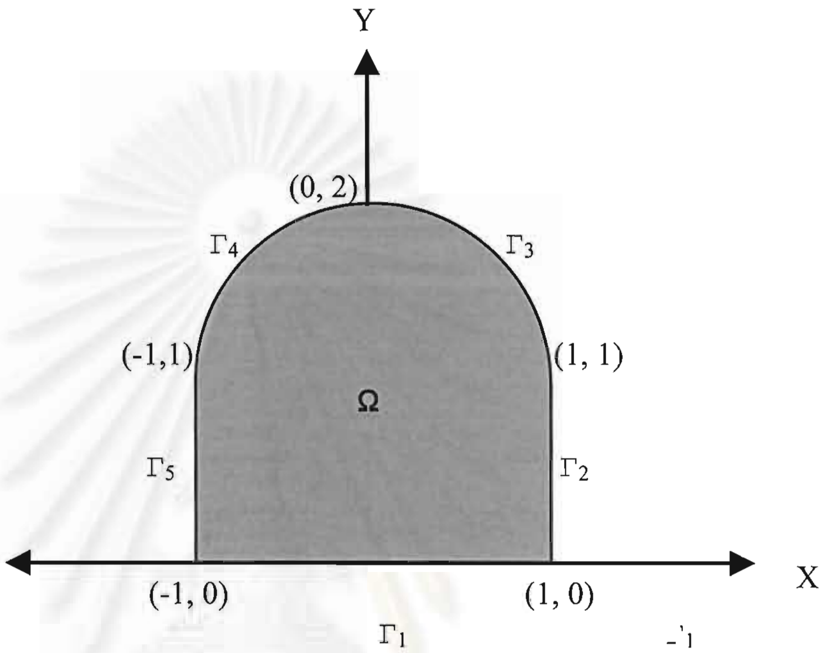

Figure 4.1.20: The domain Ω in Example 4.

39 boundary collocation points and 23 internal collocation points are used in the numerical procedures. Even though this problem includes two types of boundary conditions, numerical solutions obtained from FDDRM and LTDRM when $c \le 1\times10^{-5}$ show a very good agreement (as shown in Figures 4.1.21 – 4.1.22) with the corresponding exact solution, i.e.,

$$u(x,y,t) = e^{x-ct} + e^{y-ct}. \qquad \textbf{(4.1.17)}$$

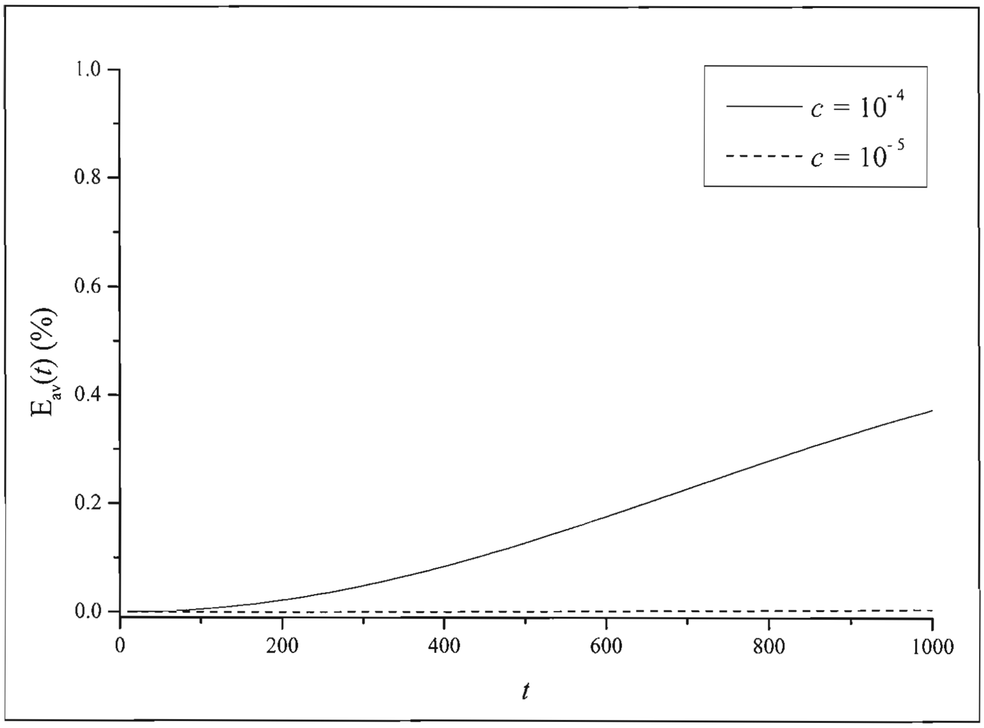

Figure 4.1.21: Average relative errors of the FDDRM.

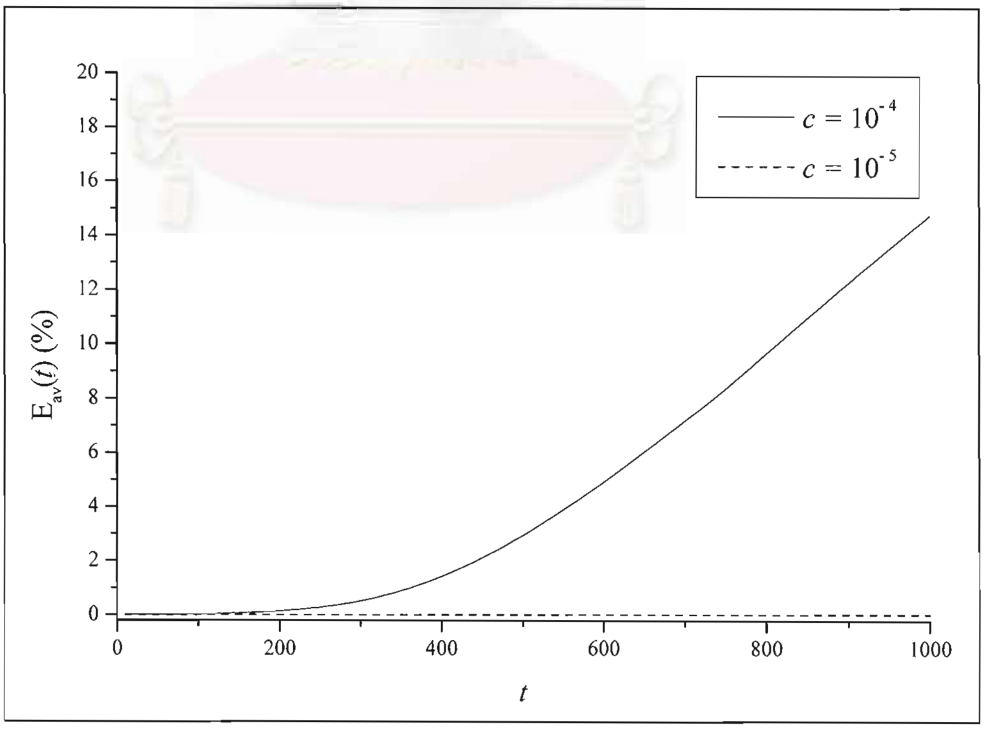

Figure 4.1.22: Average relative errors of the LTDRM.

4.1.5 Example 5

Let

$$u(x,y,t) = \frac{x^2}{2} + \frac{y^2}{2} + t^2, \qquad (x,y) \in \Omega,\ t > 0, \qquad \textbf{(4.1.18)}$$

where $\Omega = \left\{ (x,y) \in \mathbf{R}^2 \,/\, \frac{x^2}{4} + y^2 \le 1 \right\}$ (see Figure 4.1.23). It can be easily verified that u satisfies the HLWE (Equation **(2.1.1)**) with $c = 1$. For testing FDDRM and LTDRM with this problem, 33 collocation points are chosen, and the Dirichlet condition is imposed on Γ. Average relative errors $E_{av}(t)$ from both methods are displayed in Figures 4.1.24 – 4.1.25. From these figures we find that average relative errors are very small for a long time period even though $c = 1$.

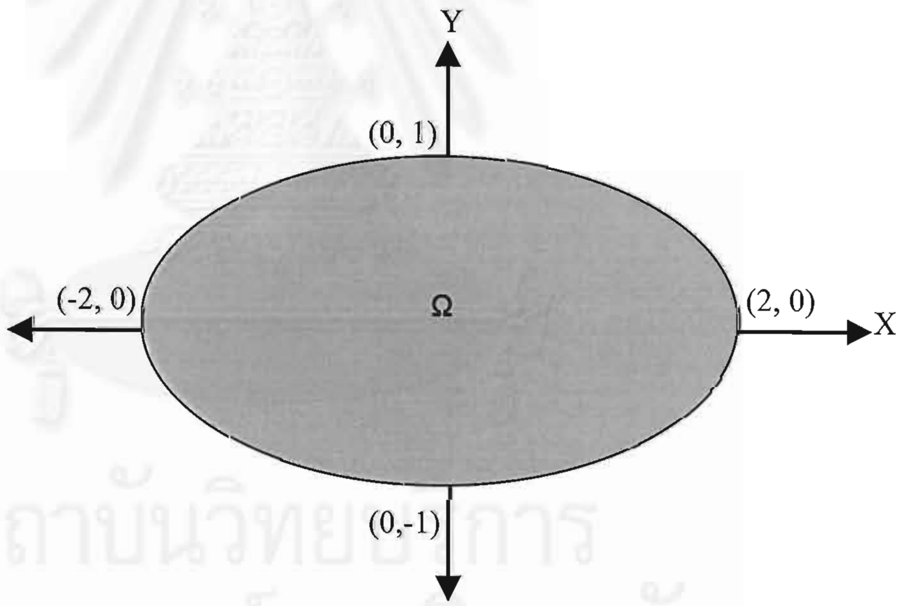

Figure 4.1.23: The domain Ω in Example 5.

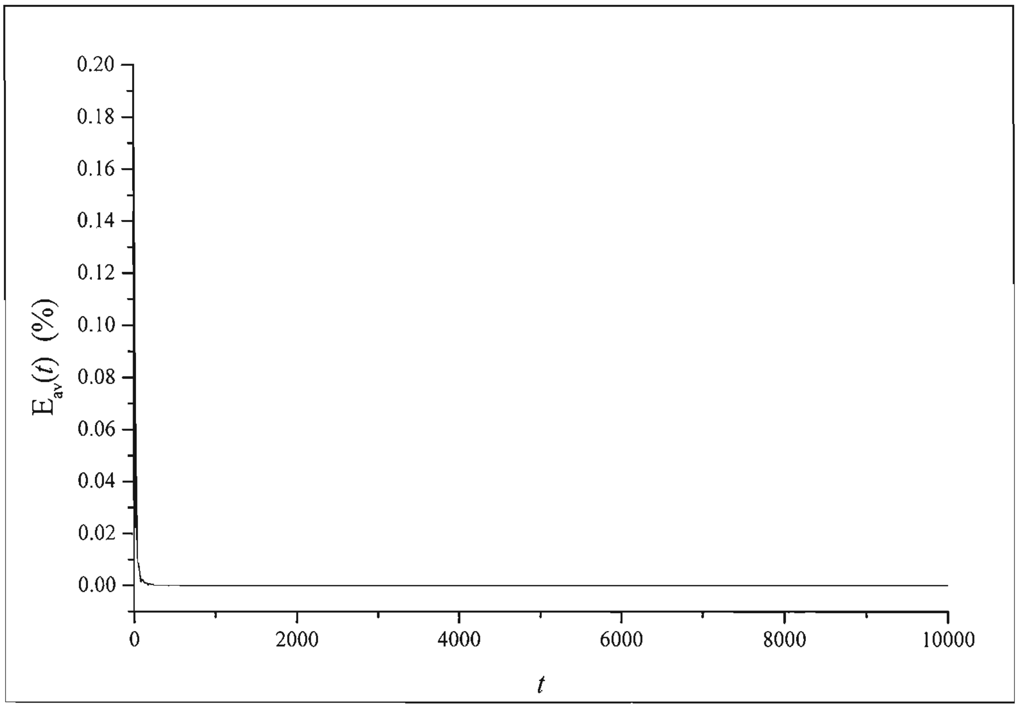

Figure 4.1.24: Average relative errors of the FDDRM with $c = 1$.

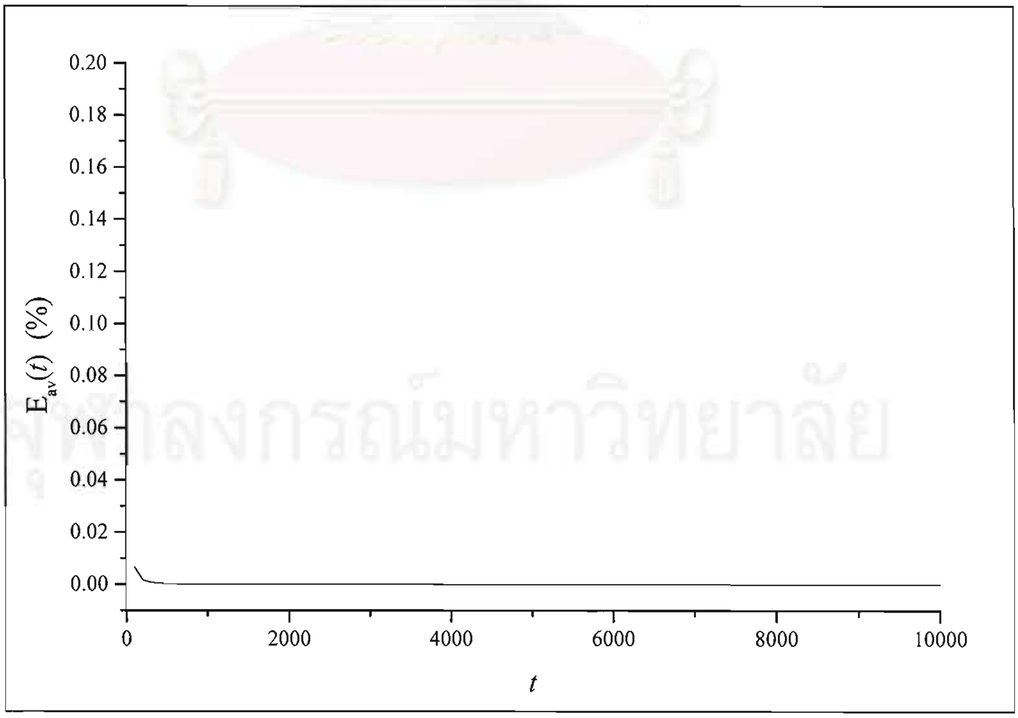

Figure 4.1.25: Average relative errors of the LTDRM with $c = 1$.

4.1.6 Discussions for HLWPs

From five examples presented, FDDRM and LTDRM are applied to solve HLWPs including vibrations of a rectangle membrane (Examples 1 – 2), a circular membrane (Example 3), and an irregular membrane (Examples 4 – 5). These problems have three types of boundary conditions, solutions of which are difficult to be found. From Examples 1 – 4, we find that FDDRM and LTDRM give accurate numerical solutions when $c \leq 1 \times 10^{-5}$. Though the results have been shown for time up to 1000, it can be seen that $E_{av}(t)$ is still small, i.e., less than 1%, for longer period. However, this time period seems to be shorter when c is increased. For example, in Example 1; $E_{av}(t)$ < 1% for $t \in [0, 800]$ when $c = 1 \times 10^{-4}$ and Figures 4.1.26 – 4.1.27 show that $E_{av}(t)$ < 1% for $t \in [0, 0.8]$ when $c = 1 \times 10^{-1}$ and for $t \in [0, 0.1]$ when $c = 1$. On the other hand, in Example 5, although $c = 1$ FDDRM and LTDRM give very high accuracy for very long time ($t \in [0, 10000]$). This is because the exact solution is a polynomial function of degree 2 in variable t.

In comparison between FDDRM and LTDRM for HLWPs, although both methods are found to give accurate results when $c \leq 1 \times 10^{-5}$ and computer implementations are very simple and straightforward, the execution time for LTDRM is less than execution time for FDDRM when the unknown function value at a large observation time needs to be calculated. Therefore LTDRM is more efficient than FDDRM for HLWPs.

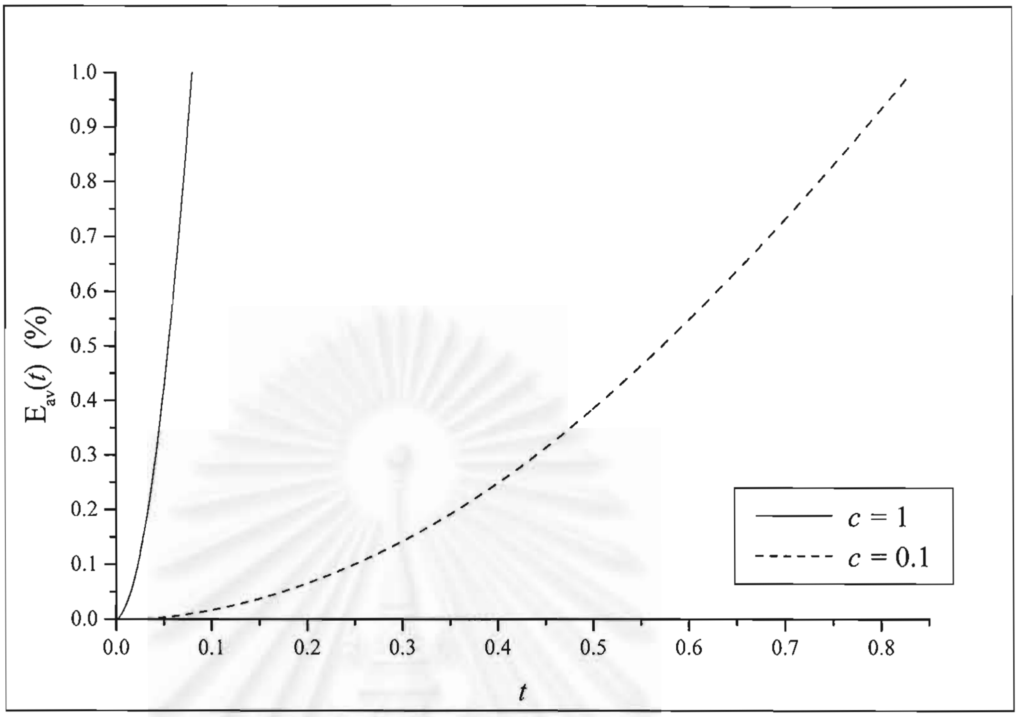

Figure 4.1.26:Average relative errors of the FDDRM in Example 1.

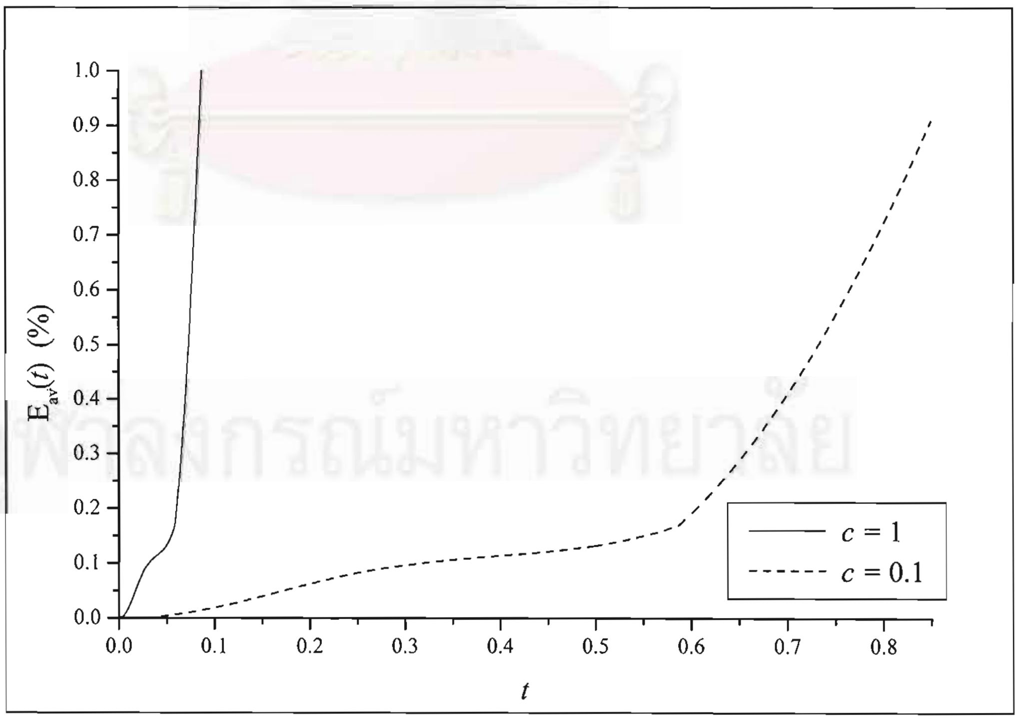

Figure 4.1.27:Average relative errors of the LTDRM in Example 1.

4.2 Numerical examples and Discussions for ILWPs

In this section, eight examples (Examples 6 – 13) of ILWPs describing vibrations of a membrane are presented and solved by FDDRM and LTDRM. Similar to HLWPs, $\Delta t = 0.1$ and $N_p = 6$ are used in FDDRM and LTDRM procedures, respectively. These examples include all cases of a function b which are explained in Chapter 2 and Chapter 3. Numerical results obtained after using these two approaches show that FDDRM and LTDRM give a good accuracy when $c \leq 10^{-5}$ which is similar to HLWPs. However, for $c > 10^{-5}$, numerical results are often accurate only at small observation times. In addition, it should be noted that FDDRM results are often more accurate than LTDRM results.

4.2.1 Example 6

The vibrations of a membrane problem with a source term governed by

$$\nabla^2 u - \frac{1}{c^2}\frac{\partial^2 u}{\partial t^2} = e^{-t}, \qquad \bar{x} \in \Omega, t > 0, \tag{4.2.1}$$

with two initial conditions

$$u(\bar{x},0) = -c^2, \tag{4.2.2}$$

$$\frac{\partial u}{\partial t}(\bar{x},0) = c^2 + c(\sin(x) + \cos(y)), \tag{4.2.3}$$

where the domain Ω is an irregular domain as shown in Figure 4.2.1. This problem has the exact solution u of the form

$$u(x,y,t) = (\sin(x) + \cos(y))\sin(ct) - c^2 e^{-t}. \tag{4.2.4}$$

To solve this problem with the Dirichlet boundary condition prescribed on Γ, we choose 36 collocation points (as shown in Figure 4.2.1) for FDDRM and LTDRM. Average relative errors obtained from these methods for $c = 10^{-5}$ and 10^{-6} are illustrated in Figures 4.2.2 – 4.2.3. Although the domain of this problem is an irregular domain, numerical solutions obtained from FDDRM are very accurate when $c \leq 1\times 10^{-5}$ while numerical solutions obtained from LTDRM are very accurate when $c \leq 10^{-6}$.

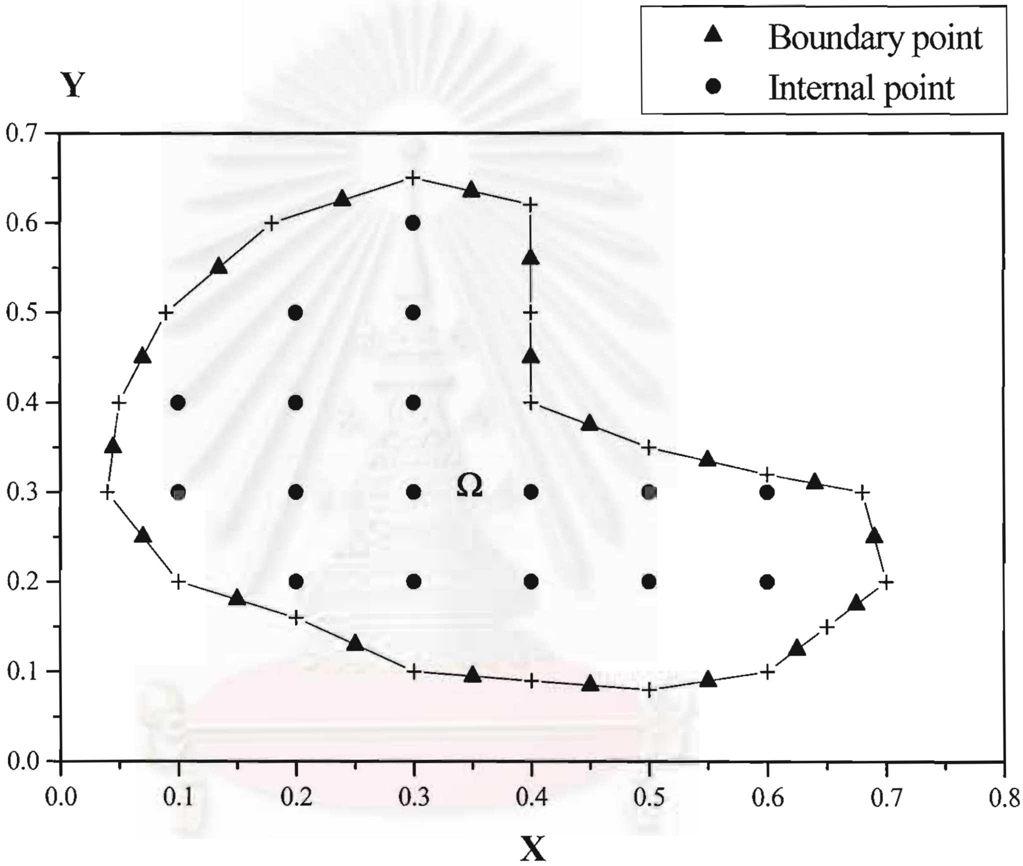

Figure 4.2.1: The domain Ω and all collocation points in Example 6.

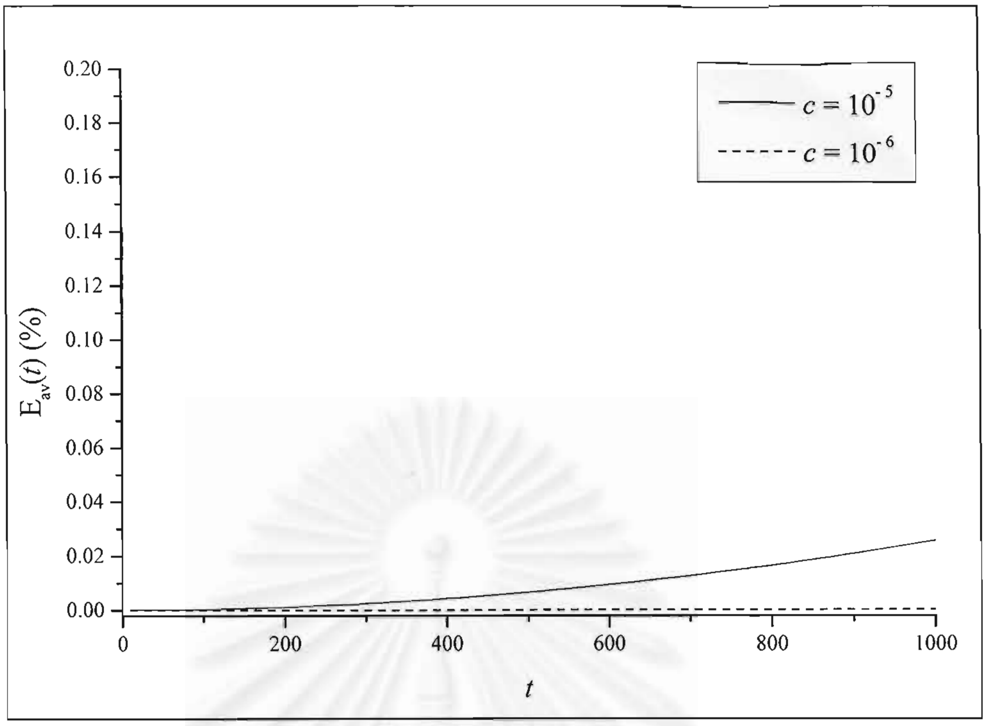

Figure 4.2.2: Average relative errors of the FDDRM.

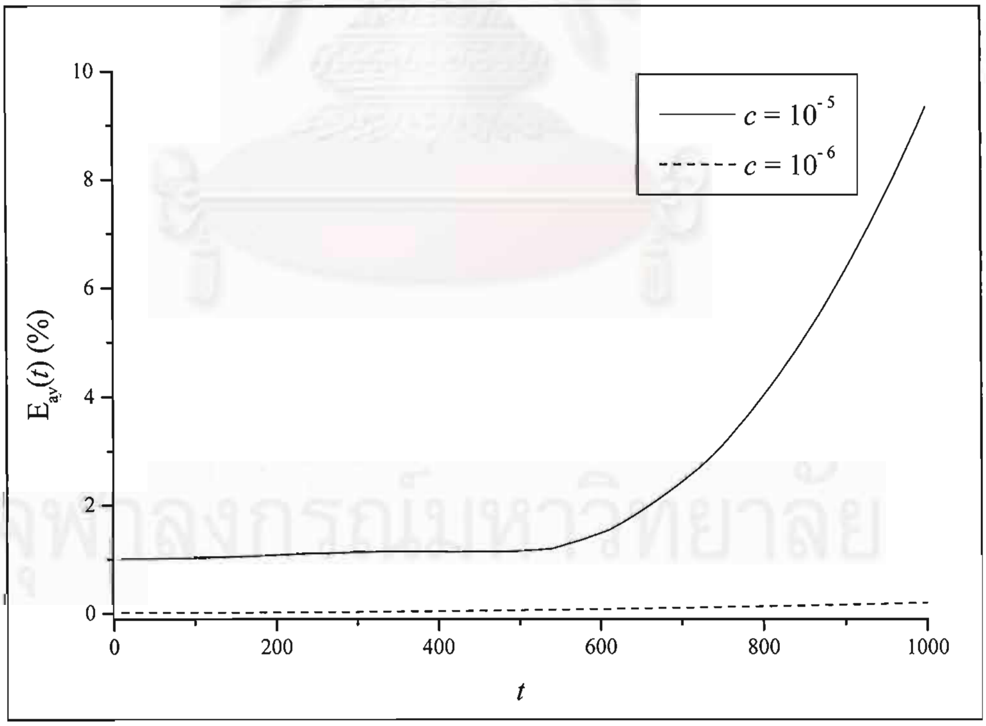

Figure 4.2.3: Average relative errors of the LTDRM.

4.2.2 Example 7

In this example, we seek for numerical solutions of an ILWE of the form

$$\nabla^2 u - \frac{1}{c^2}\frac{\partial^2 u}{\partial t^2} = 2u - \sin(x)\cos(y)e^{-ct} \text{ on } \Omega, \quad \textbf{(4.2.5)}$$

where Ω is a triangular domain as shown in Figure 4.2.4.

Two initial conditions are

$$u(\bar{x},0) = \sin(x)\cos(y), \quad \textbf{(4.2.6)}$$

$$\frac{\partial u}{\partial t}(\bar{x},0) = -c\sin(x)\cos(y). \quad \textbf{(4.2.7)}$$

The Neumann boundary conditions are

$$\frac{\partial u}{\partial n}(\bar{x},t) = \begin{cases} \sin(x)\sin(y)e^{-ct} & \text{on } \Gamma_1 \\ -\cos(x)\cos(y)e^{-ct} & \text{on } \Gamma_3 \end{cases} \quad \textbf{(4.2.8)}$$

and the Dirichlet boundary condition is

$$u(\bar{x},t) = \sin(x)\cos(y)e^{-ct} \text{ on } \Gamma_2. \quad \textbf{(4.2.9)}$$

66 collocation points (as shown in Figure 4.2.4) are chosen to find numerical solutions in FDDRM and LTDRM procedures. Similar to previous examples, average relative errors decrease when c is decreased as illustrated in Figures 4.2.5 – 4.2.6.

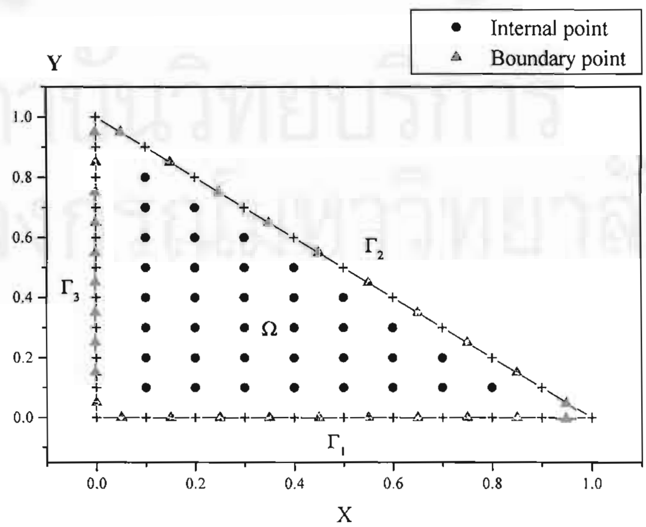

Figure 4.2.4: The domain Ω and all collocation points in Example 7.

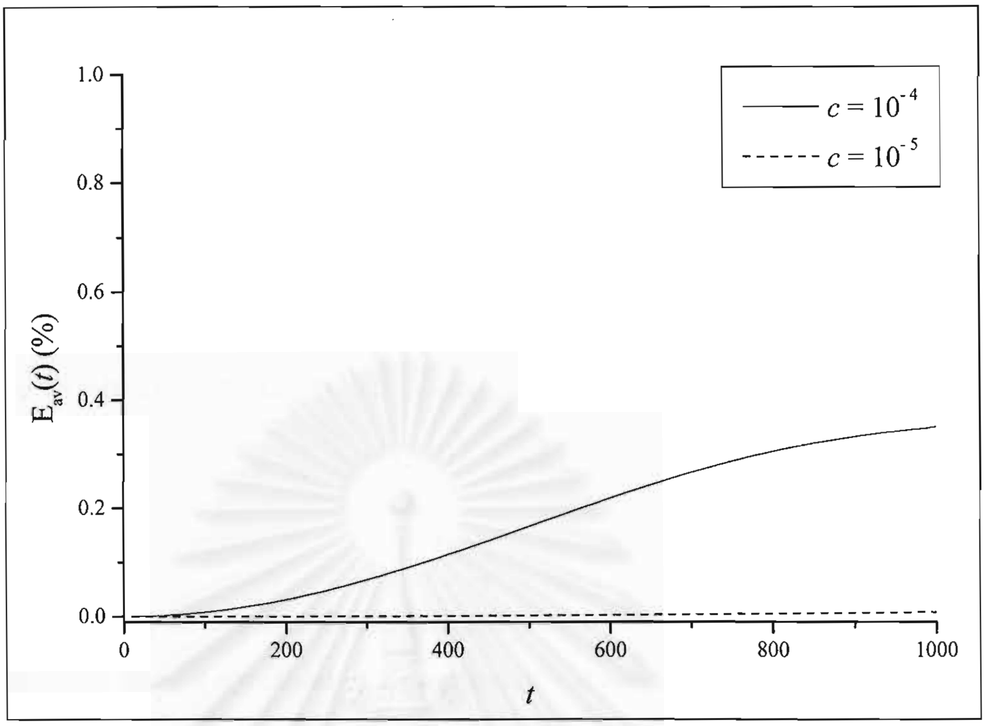

Figure 4.2.5: Average relative errors of the FDDRM.

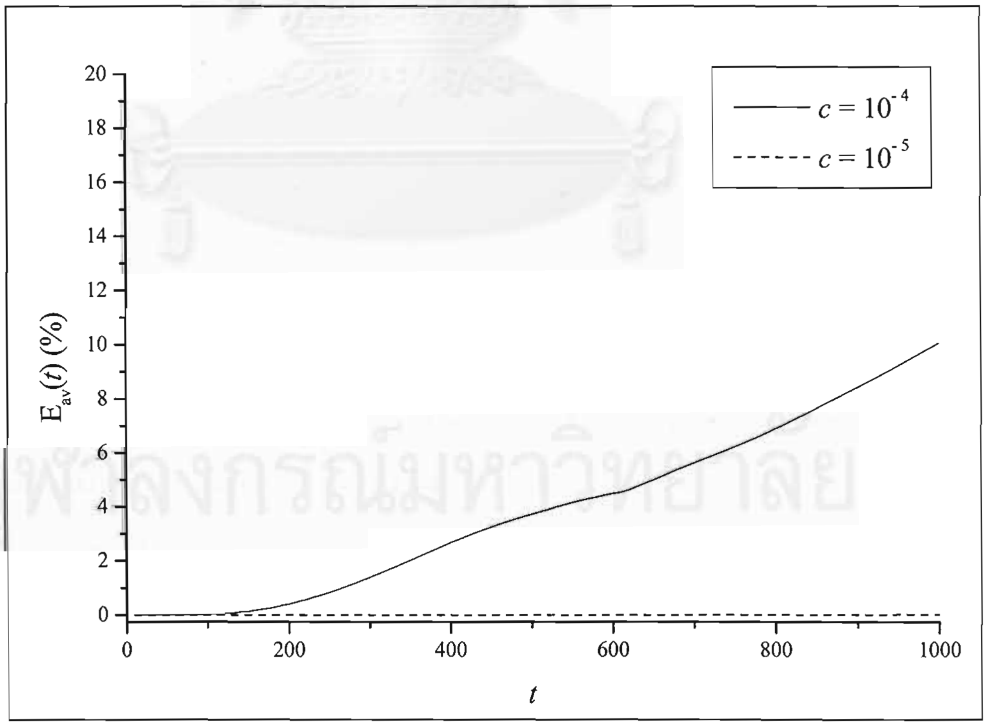

Figure 4.2.6: Average relative errors of the LTDRM.

4.2.3 Example 8

The vibrations of a rectangular membrane problem with a friction term as $k\frac{\partial u}{\partial t}$ is governed by an ILWE of the form

$$c^2 \nabla^2 u - \frac{\partial^2 u}{\partial t^2} = k\frac{\partial u}{\partial t} \qquad \text{on } \Omega, \qquad \textbf{(4.2.10)}$$

where $\Omega = [0,1]\times[0,1]$ and $k > 0$ is a constant, with two initial conditions

$$u(x,y,0) = x(1-x)y(1-y), \qquad \textbf{(4.2.11)}$$

$$\frac{\partial u}{\partial t}(x,y,0) = 0. \qquad \textbf{(4.2.12)}$$

If the boundary of the membrane is fixed ($u \equiv 0$ on Γ) then the analytical solution obtained by using the method of separation of variables is

$$u(x,y,t) = e^{-\frac{k}{2}t}\{\sum_{m=1}^{\infty}\sum_{n=1}^{\infty} A_{nm}\sin(n\pi x)\sin(m\pi y)\cos(l_{nm}t) + \sum_{m=1}^{\infty}\sum_{n=1}^{\infty} B_{nm}\sin(n\pi x)\sin(m\pi y)\sin(l_{nm}t)\} \qquad \textbf{(4.2.13)}$$

where A_{nm}, B_{nm} and l_{nm} are shown in Appendix C. For this example, we choose $k = \frac{c^2}{4}$ and 36 collocation points in the domain Ω (as shown in Figure 4.1.2). In Figures 4.2.7 – 4.2.8, the displacements of a membrane at $t = 1$, 20000, and 50000 with $c = 10^{-5}$ obtained by FDDRM and LTDRM are shown. Average relative errors $E_{av}(t)$ for $c = 10^{-4}$ and 10^{-5} are illustrated in Figures 4.2.9 – 4.2.10. Although the governing equation of this problem (Equation **(4.2.13)**) contains a first time-derivative of the unknown function u, numerical solutions obtained from both methods are still accurate for a long time period when $c \le 1\times10^{-5}$.

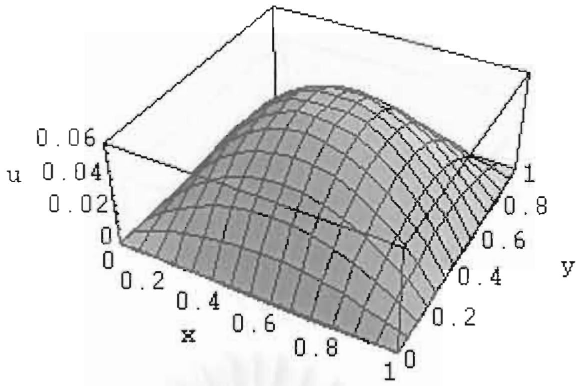

$t = 1.$

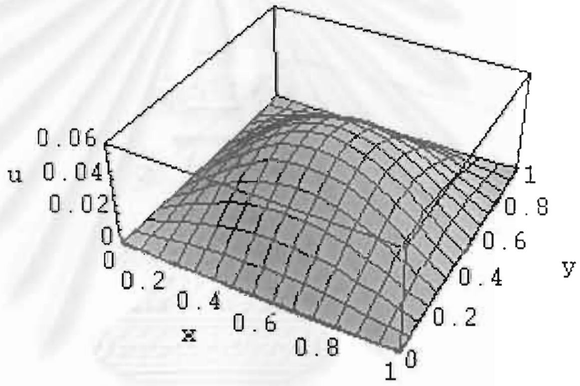

$t = 20000.$

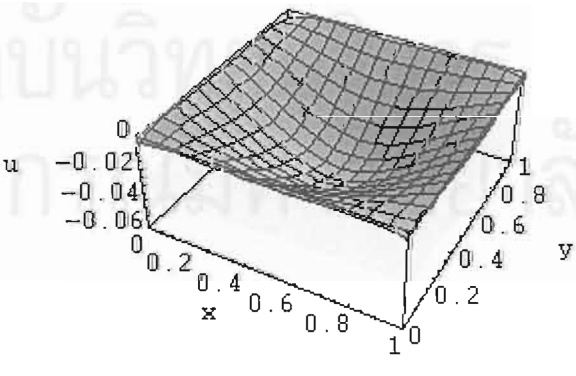

$t = 50000.$

Figure 4.2.7: The displacements of a membrane from the FDDRM with $c = 10^{-5}$.

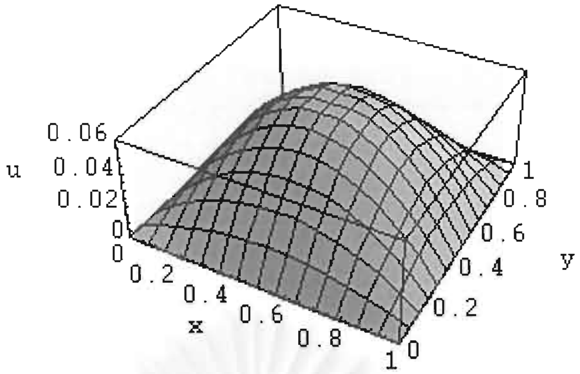

$t = 1.$

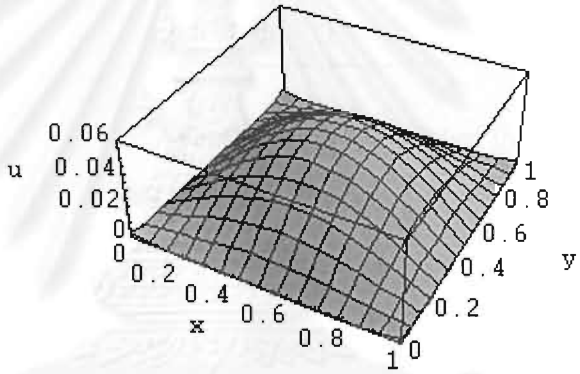

$t = 20000.$

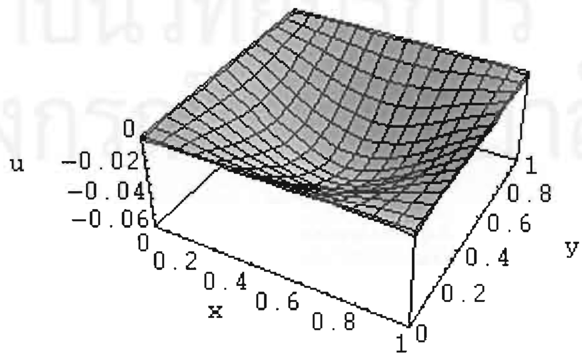

$t = 50000.$

Figure 4.2.8: The displacements of a membrane from the LTDRM with $c = 10^{-5}$.

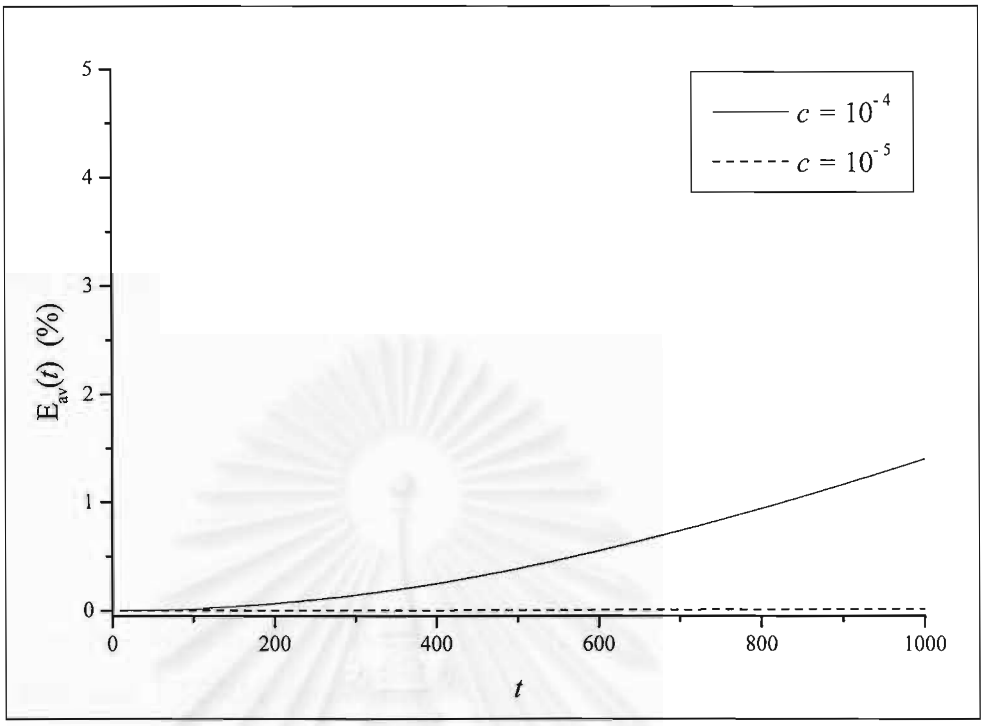

Figure 4.2.9: Average relative errors of the FDDRM.

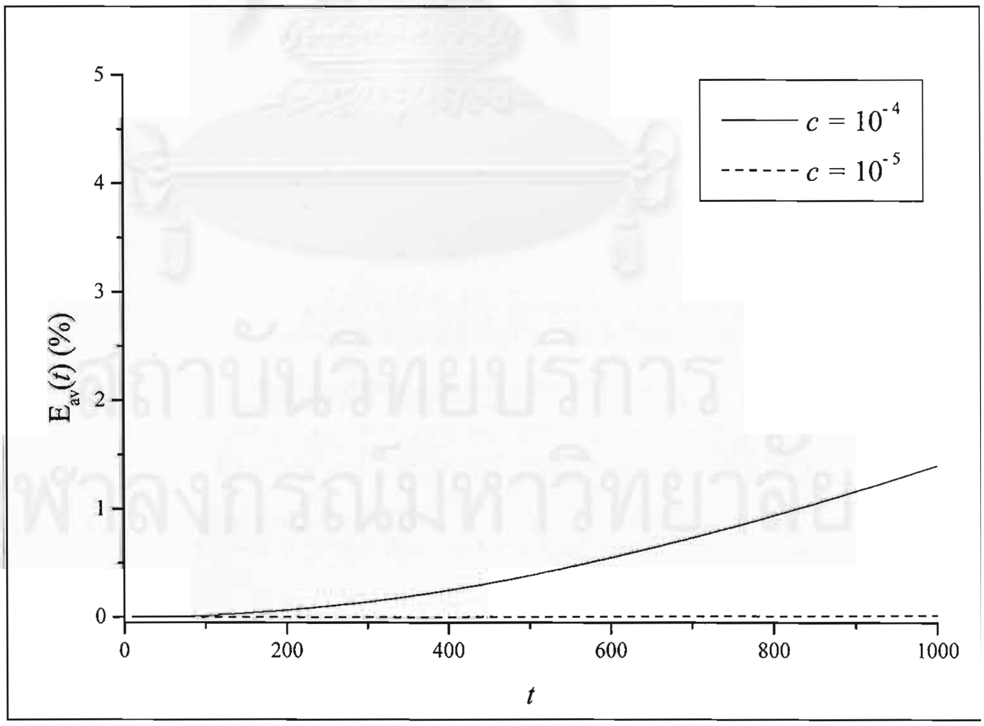

Figure 4.2.10: Average relative errors of the LTDRM.

4.2.4 Example 9

Consider an ILWE

$$\nabla^2 u - \frac{1}{c^2}\frac{\partial^2 u}{\partial t^2} = (-2 + cx^2)\cos(ct) + (2 + cy^2)\sin(ct) + u - \frac{\partial u}{\partial t}, \qquad \textbf{(4.2.14)}$$

defined on a half circular domain Ω (see Figure 4.2.11), with two initial conditions

$$u(\bar{x},0) = y^2, \qquad \textbf{(4.2.15)}$$

$$\frac{\partial u}{\partial t}(\bar{x},0) = cx^2, \qquad \textbf{(4.2.16)}$$

and the Dirichlet boundary condition

$$u(\bar{x},t) = x^2\sin(ct) - y^2\cos(ct) \quad \text{on } \Gamma. \qquad \textbf{(4.2.17)}$$

To solve this problem, 70 collocation points (as shown in Figure 4.2.11) are used in FDDRM and LTDRM procedures. Average relative errors obtained from these methods for $c = 10^{-5}$ and 10^{-6} are illustrated in Figures 4.2.12 – 4.2.13. It can be seen again that $E_{av}(t)$ reduces as c decreases.

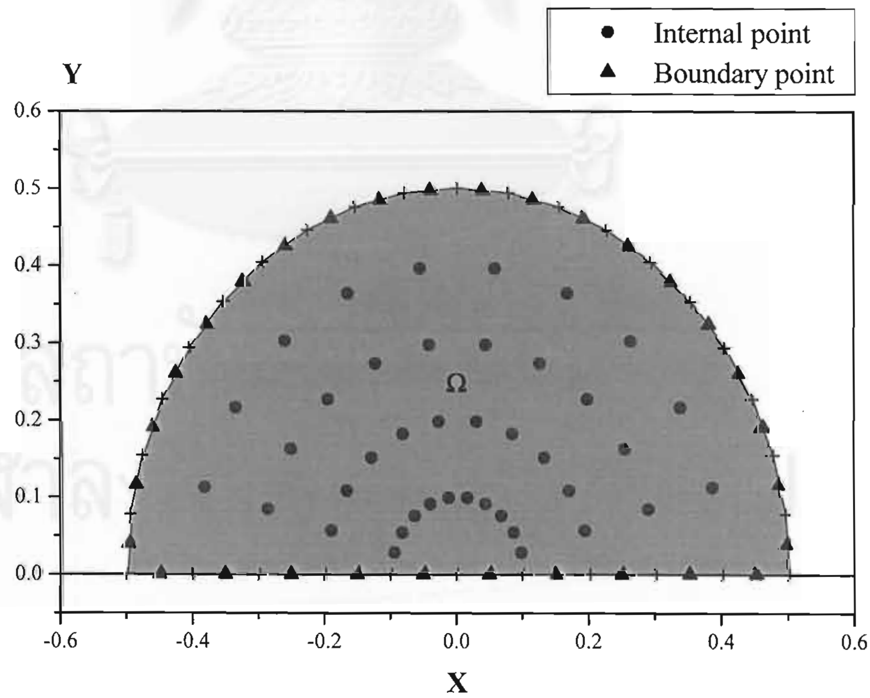

Figure 4.2.11: The domain Ω and all collocation points in Example 9.

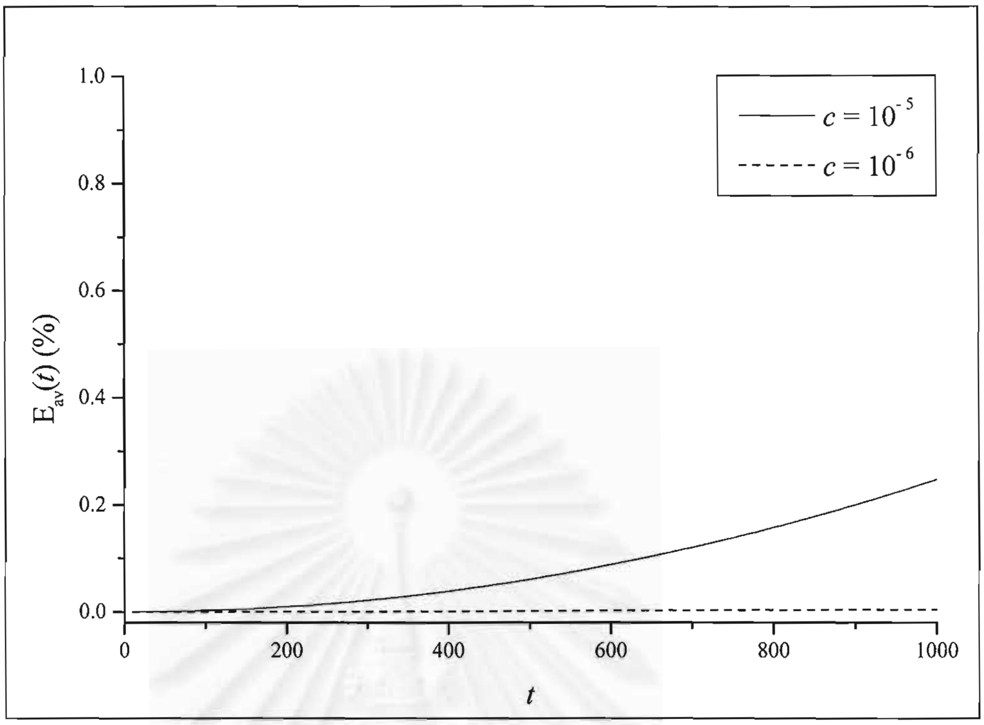

Figure 4.2.12: Average relative errors of the FDDRM.

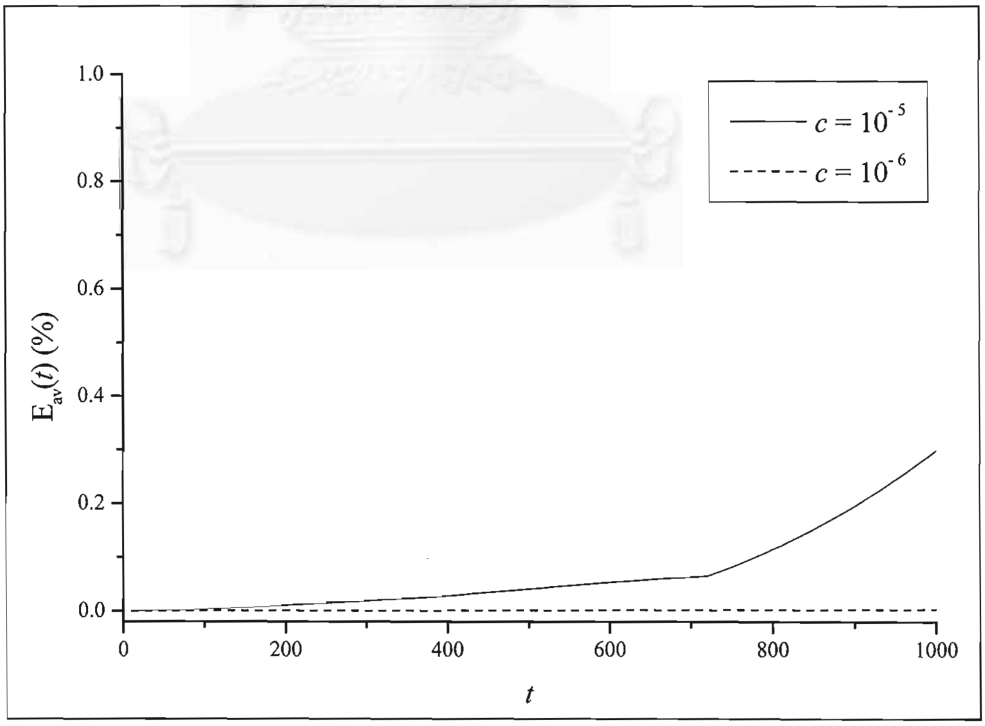

Figure 4.2.13: Average relative errors of the LTDRM.

4.2.5 Example 10

Now, we consider the vibrations of a circular membrane problem with a source term including the unknown function u and its spatial derivative $\frac{\partial u}{\partial y}$ of the form

$$\nabla^2 u - \frac{1}{c^2}\frac{\partial^2 u}{\partial t^2} = z + u - 2\frac{\partial u}{\partial y} \qquad \text{on } \Omega, \tag{4.2.18}$$

where

$$z(x,y,t) = -4\,e^{0.01-x^2-y^2}(-1+x^2-y+y^2)\sin(ct), \tag{4.2.19}$$

with two initial conditions

$$u(\bar{x},0) = 0, \tag{4.2.20}$$

$$\frac{\partial u}{\partial t}(\bar{x},0) = c\left(1-e^{0.01-(x^2+y^2)}\right). \tag{4.2.21}$$

For this problem, $\Omega = \{\ (x,y) \in \mathbf{R}^2 \text{ where } x^2+y^2 \le 0.01\ \}$ as shown in Figure 4.2.14 and the boundary of the membrane is fixed, i.e., $u \equiv 0$ on Γ. Figure 4.2.15 shows the displacements of the circular membrane at $t = 10\pi,\ 200\pi$, and 500π obtained by the analytical solution when $c = 10^{-5}$. After solving this problem by using FDDRM and LTDRM, we find that numerical solutions are accurate when $c \le 1\times10^{-5}$ (as illustrated in Figures 4.2.16 – 4.2.17). The exact solution of this problem is given in Appendix C.

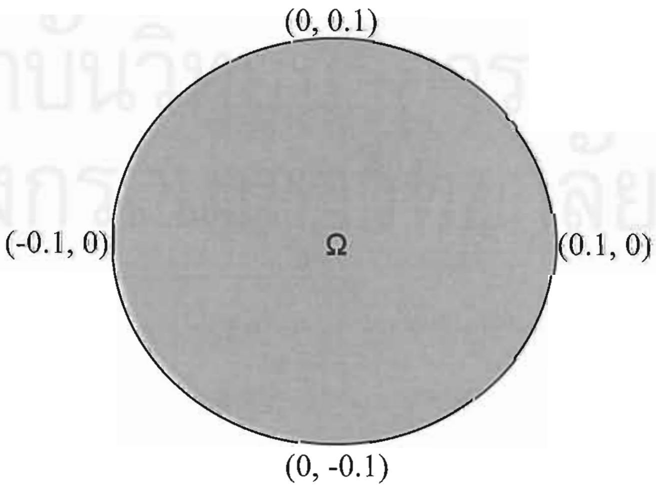

Figure 4.2.14: The domain Ω in Example 10.

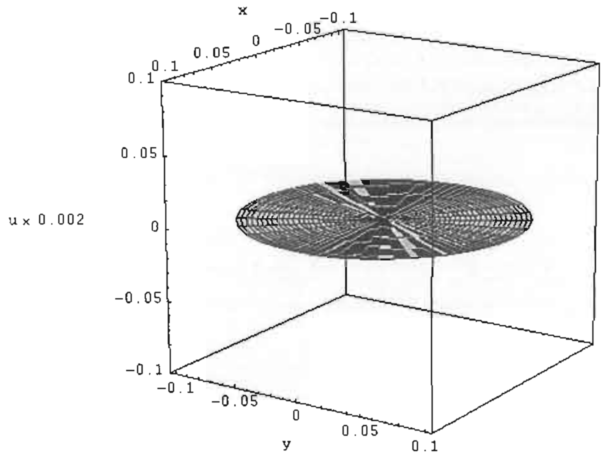

$t = 10\pi.$

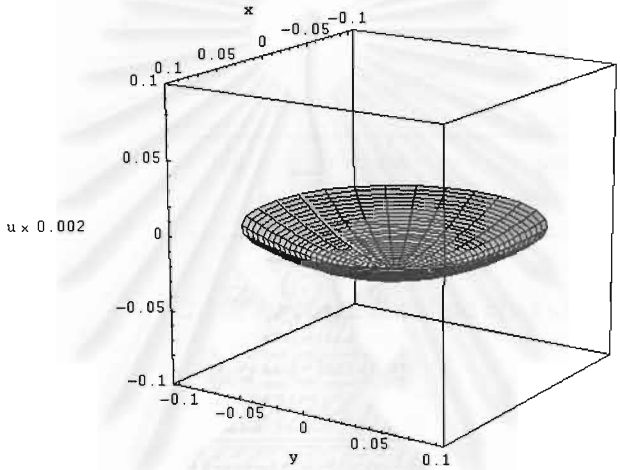

$t = 200\pi.$

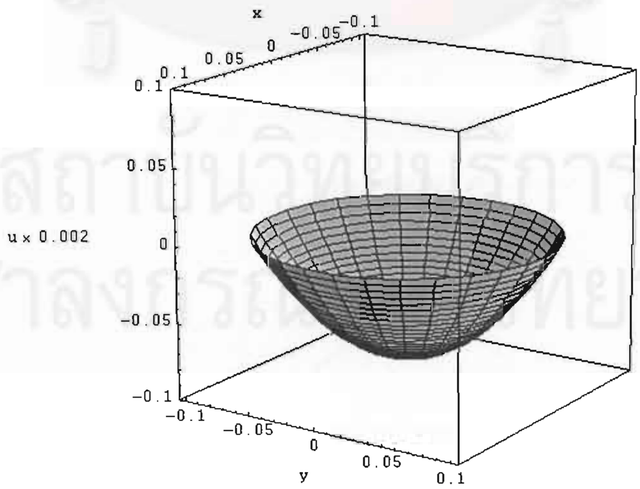

$t = 500\pi.$

Figure 4.2.15: The displacements of a membrane from the exact solution when $c = 10^{-5}$.

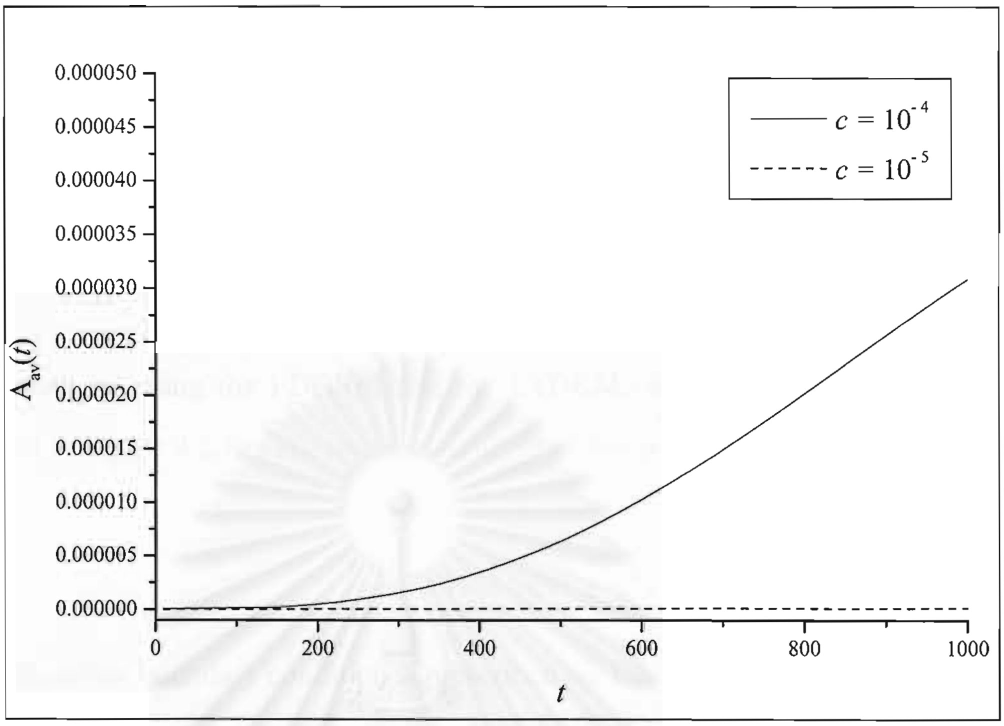

Figure 4.2.16: Average absolute errors of the FDDRM.

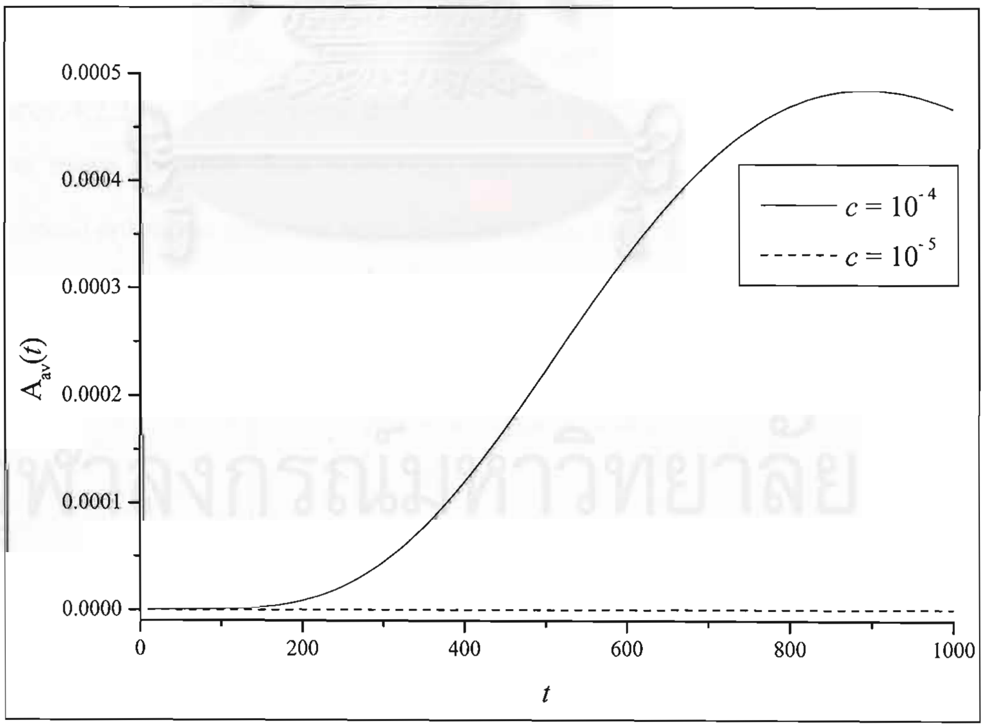

Figure 4.2.17: Average absolute errors of the LTDRM.

4.2.6 Example 11

For this example, the vibrations of a rectangular membrane problem, with a source term including a spatial derivative of the unknown function u as $\frac{\partial u}{\partial x}$, governed by

$$\nabla^2 u - \frac{1}{c^2}\frac{\partial^2 u}{\partial t^2} = \frac{\left(-2x + (x^2+y^2)\ln(x^2+y^2)\right)\sin(ct)}{x^2+y^2} + \frac{\partial u}{\partial x} \quad \text{on } \Omega, \qquad \textbf{(4.2.22)}$$

is solved by using the FDDRM and the LTDRM, where $\Omega = [1,2]\times[1,2]$ which is shown in Figure 4.2.18. The initial conditions of this problem are

$$u(\bar{x},0) = 0, \qquad \textbf{(4.2.23)}$$

$$\frac{\partial u}{\partial t}(\bar{x},0) = c\ln(x^2+y^2). \qquad \textbf{(4.2.24)}$$

The Dirichlet boundary condition is prescribed on Γ as

$$u(\bar{x},t) = \ln(x^2+y^2)\sin(ct). \qquad \textbf{(4.2.25)}$$

36 collocation points (as shown in Figure 4.2.18) are chosen to find the approximate solutions. Average relative errors for $c = 10^{-4}$ and 10^{-5} are illustrated in Figures 4.2.19 – 4.2.20. The displacements of a rectangular membrane at $t = 10$, 10^2, and 10^3 obtained from FDDRM, LTDRM, and the exact solution for $c = 10^{-4}$ (as shown in Figures 4.2.21 – 4.2.29) show that numerical solutions obtained from FDDRM seem to be more accurate than numerical solutions obtained from LTDRM. However, numerical solutions obtained from both methods are very accurate when $c \le 10^{-5}$.

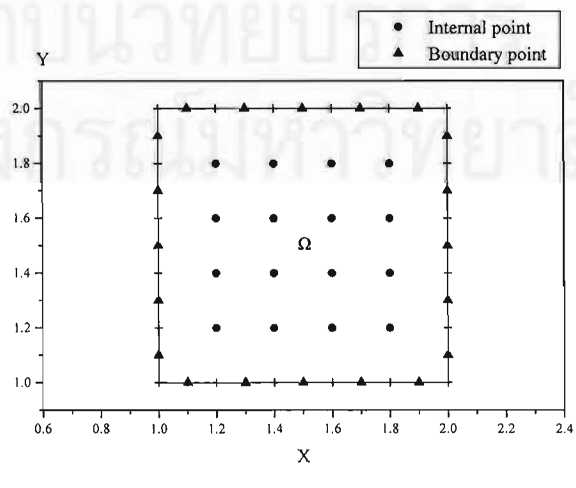

Figure 4.2.18: The domain Ω and all collocation points in Example 11.

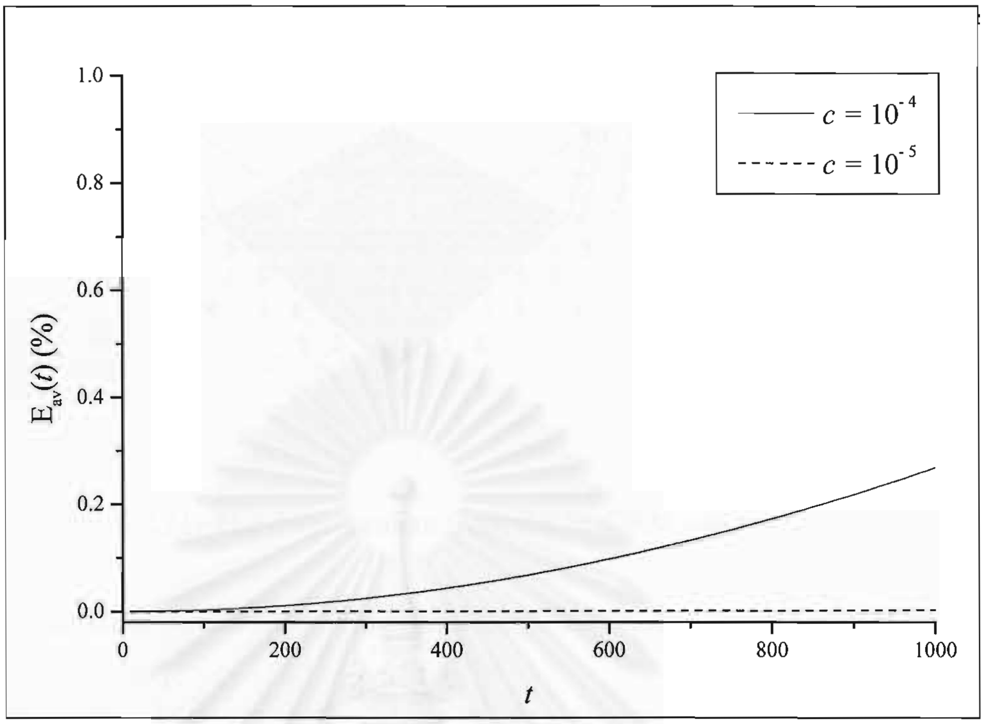

Figure 4.2.19: Average relative errors of the FDDRM.

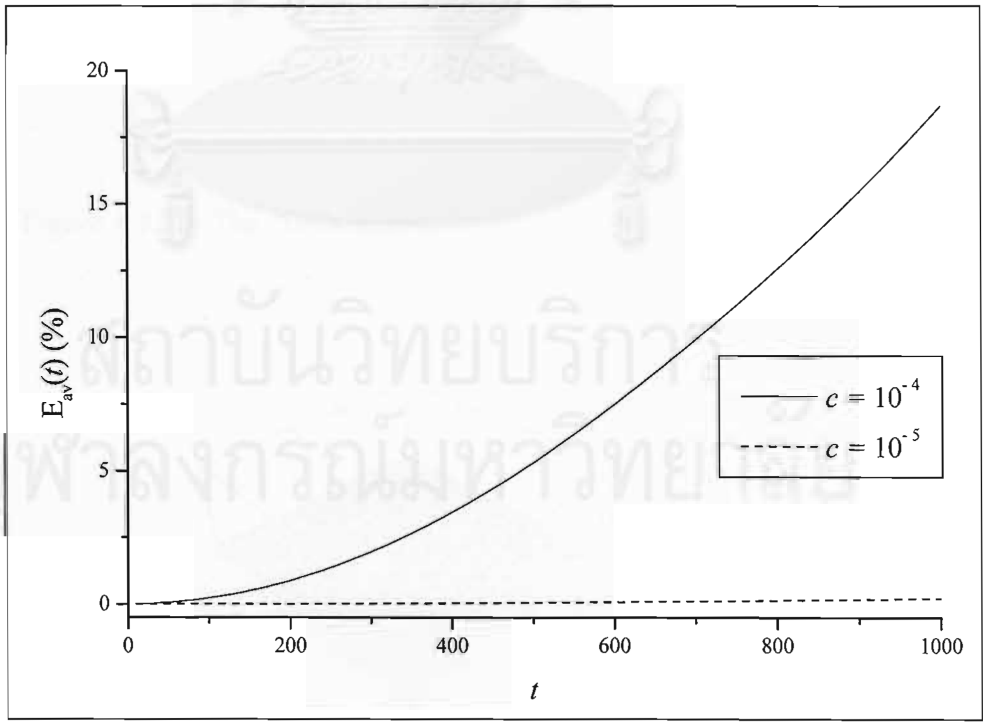

Figure 4.2.20: Average relative errors of the LTDRM.

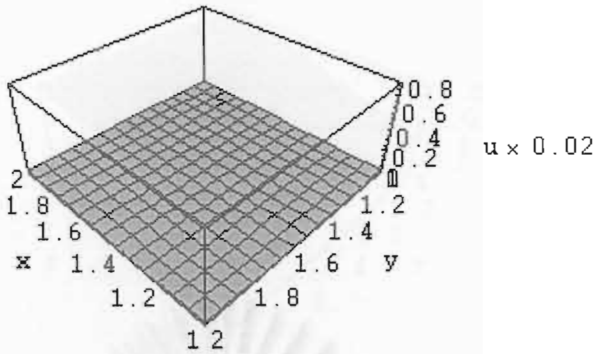

Figure 4.2.21: The displacement from the FDDRM when $c = 10^{-4}$ at $t = 10$.

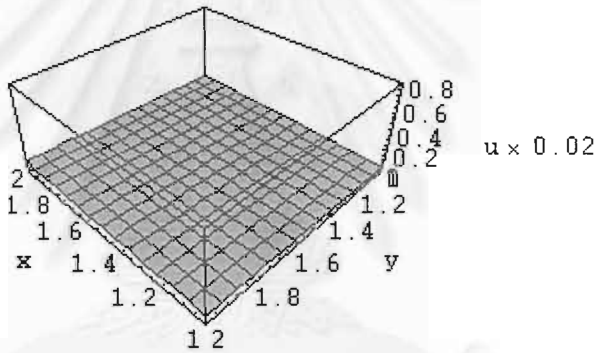

Figure 4.2.22: The displacement from the LTDRM when $c = 10^{-4}$ at $t = 10$.

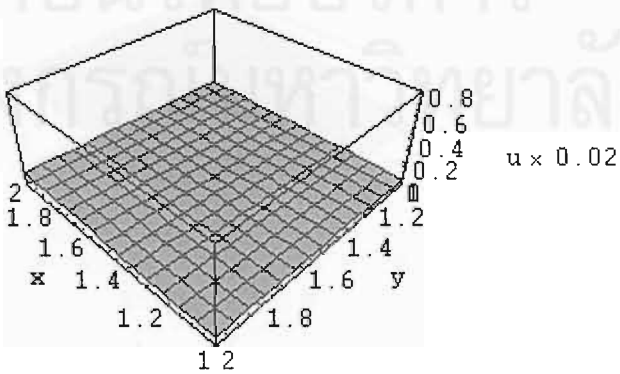

Figure 4.2.23: The displacement from the exact solution when $c = 10^{-4}$ at $t = 10$.

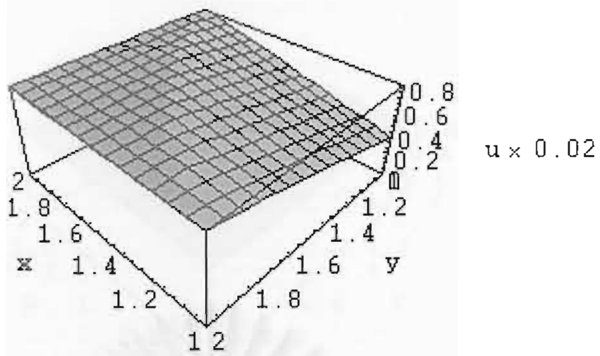

Figure 4.2.24: The displacement from the FDDRM when $c = 10^{-4}$ at $t = 100$.

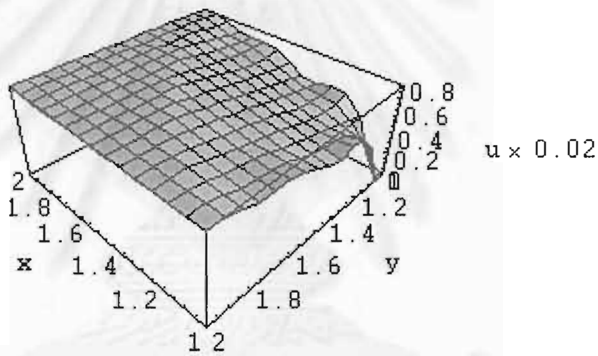

Figure 4.2.25: The displacement from the LTDRM when $c = 10^{-4}$ at $t = 100$.

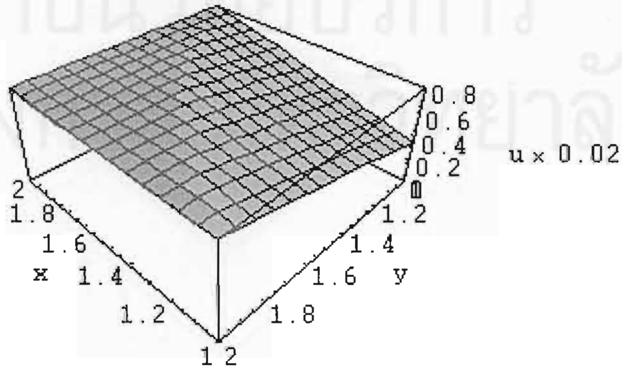

Figure 4.2.26: The displacement from the exact solution when $c = 10^{-4}$ at $t = 100$.

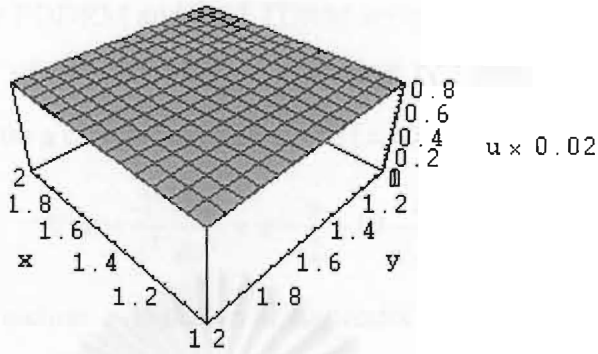

Figure 4.2.27: The displacement from the FDDRM when $c = 10^{-4}$ at $t = 1000$.

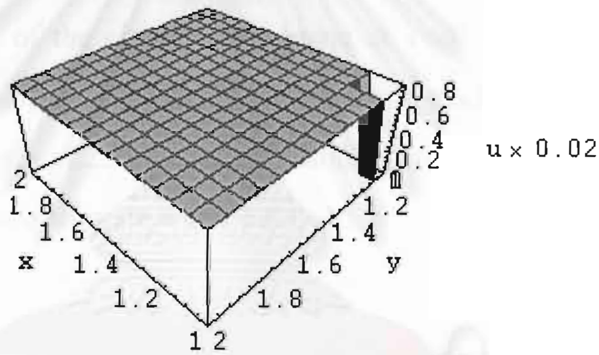

Figure 4.2.28: The displacement from the LTDRM when $c = 10^{-4}$ at $t = 1000$.

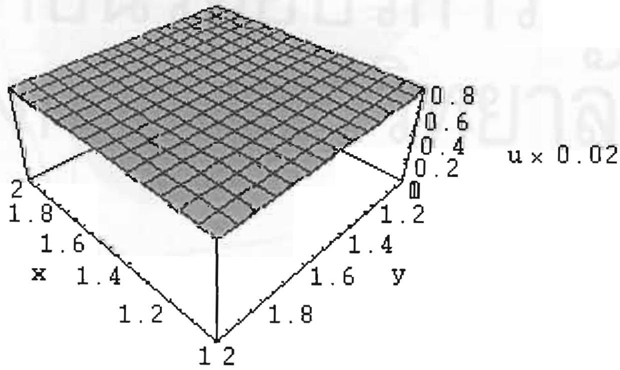

Figure 4.2.29: The displacement from the exact solution when $c = 10^{-4}$ at $t = 1000$.

4.2.7 Example 12

In this example, the FDDRM and the LTDRM are utilized to solve an ILWE in which the source term is of general form as described in Chapter 2 and Chapter 3. The problem is defined on a circular domain $\Omega = \{ (x,y) \in \mathbf{R}^2 \text{ where } x^2 + y^2 \le 1 \}$ as

$$\nabla^2 u - \frac{1}{c^2}\frac{\partial^2 u}{\partial t^2} = z - \frac{u}{2} + 10\frac{\partial u}{\partial t} - 7\frac{\partial u}{\partial x} + 2\frac{\partial u}{\partial y}, \qquad \textbf{(4.2.26)}$$

where the known function z is shown in Appendix C, with two initial conditions

$$u(\bar{x},0) = \sin(x)\sin(y), \qquad \textbf{(4.2.27)}$$

$$\frac{\partial u}{\partial t}(\bar{x},0) = c\sin(x)\sin(y), \qquad \textbf{(4.2.28)}$$

and the Dirichlet boundary condition

$$u(\bar{x},t) = \left(\cos(ct) + \sin(ct)\right)\sin(x)\sin(y). \qquad \textbf{(4.2.29)}$$

The displacements of the circular membrane at $t = 0$ are shown in Figure 4.2.30. Average absolute errors obtained from these methods for $c = 10^{-4}$ and 10^{-5} are illustrated in Figures 4.2.31 – 4.2.32. Similar to previous examples, numerical solutions obtained are accurate when $c \le 1 \times 10^{-5}$.

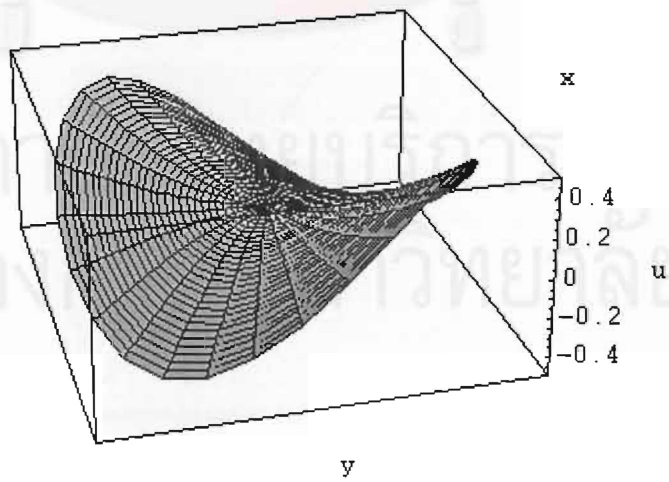

Figure 4.2.230: The displacement of a circular membrane at $t = 0$.

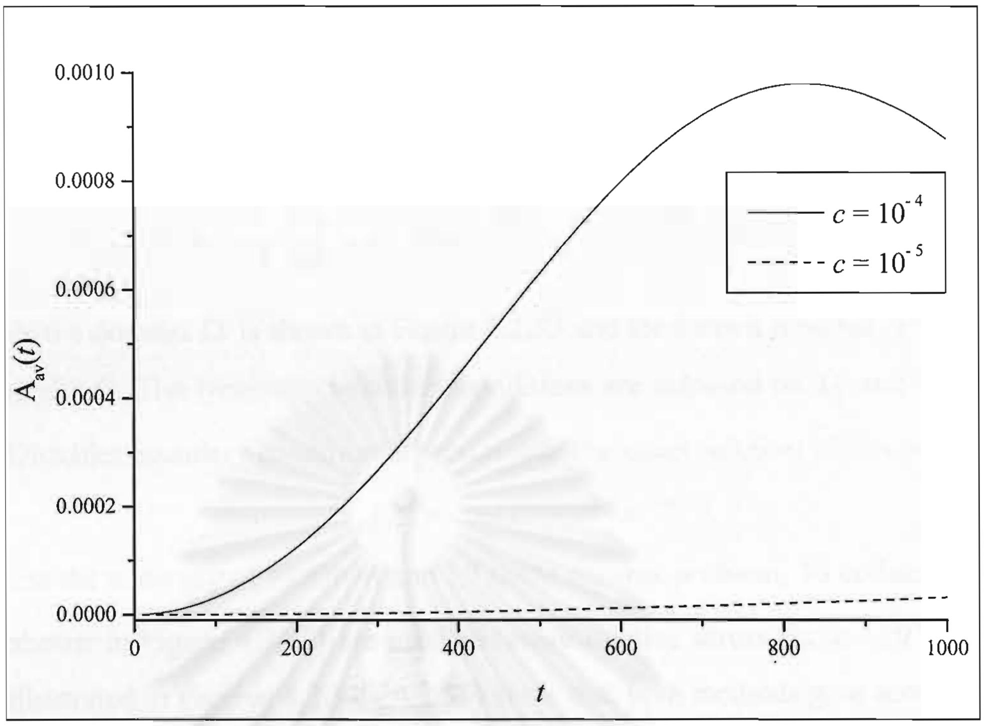

Figure 4.2.31: Average absolute errors of the FDDRM.

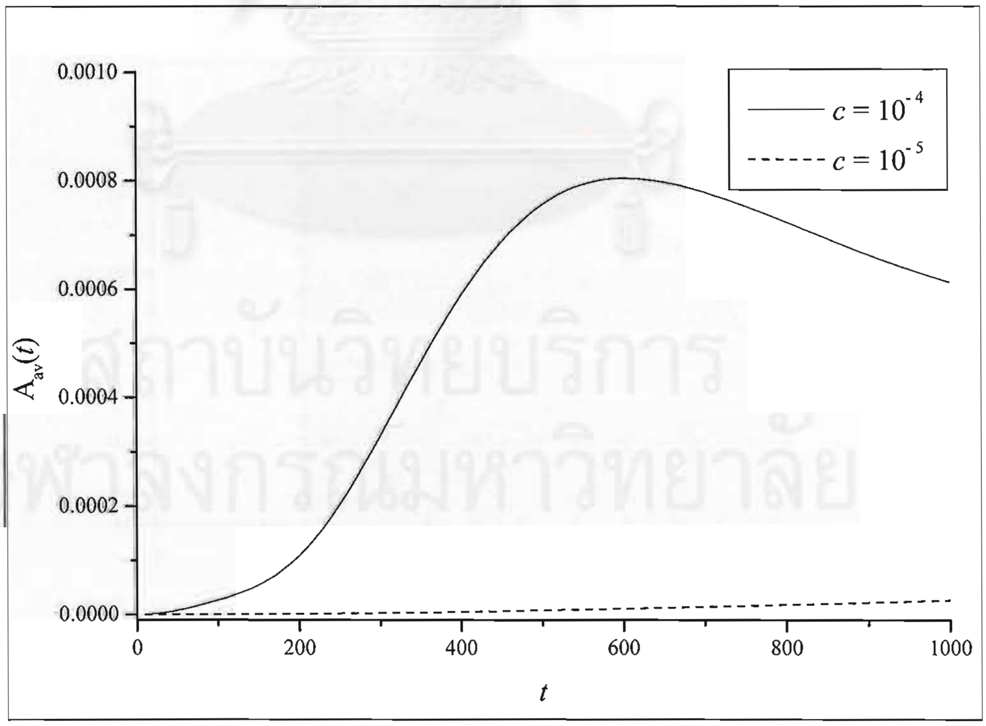

Figure 4.2.32: Average absolute errors of the LTDRM.

4.2.8 Example 13

As for the last example, we solve the vibrations of a membrane problem with a source term of the form

$$\nabla^2 u - \frac{1}{c^2}\frac{\partial^2 u}{\partial t^2} = z - 10u - \frac{\partial u}{\partial t} - 3\frac{\partial u}{\partial x} + \frac{\partial u}{\partial y} \quad \text{on } \Omega, \qquad \textbf{(4.2.30)}$$

where the domain Ω is shown in Figure 4.2.33 and the known function z is shown in Appendix C. The Neumann boundary conditions are imposed on Γ_1 and Γ_3. On Γ_2, the Dirichlet boundary condition is prescribed. The exact solution of this problem is

$$u(x,y,t) = \cos(x^2 + y^2)e^{-\sin(ct)}. \qquad \textbf{(4.2.31)}$$

To test the accuracy of FDDRM and LTDRM for this problem, 50 collocation points (as shown in Figure 4.2.33) are used. Average relative errors for $c = 10^{-5}$ and 10^{-6} (as illustrated in Figures 4.2.34 – 4.2.35) show that both methods give accurate results when $c \leq 1\times10^{-5}$.

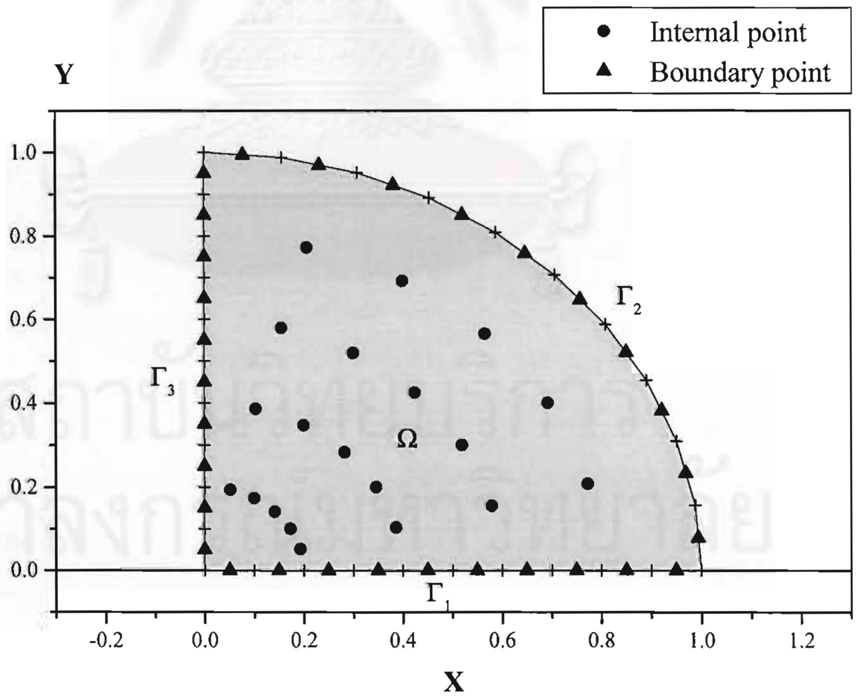

Figure 4.2.33: The domain Ω and all collocation points in Example 13.

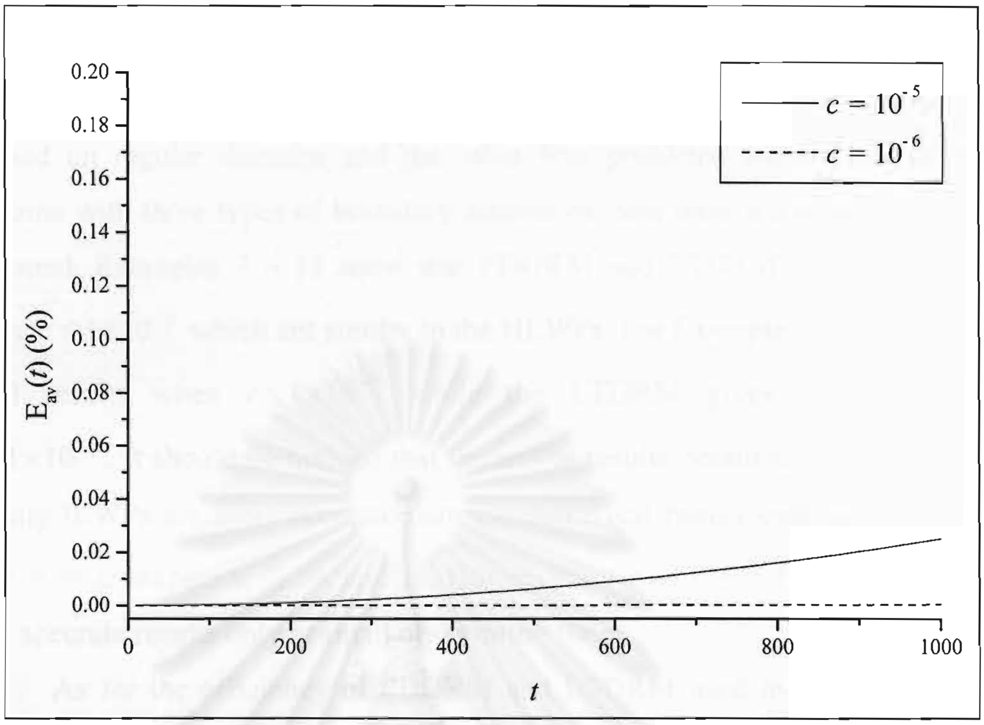

Figure 4.2.34: Average relative errors of the FDDRM.

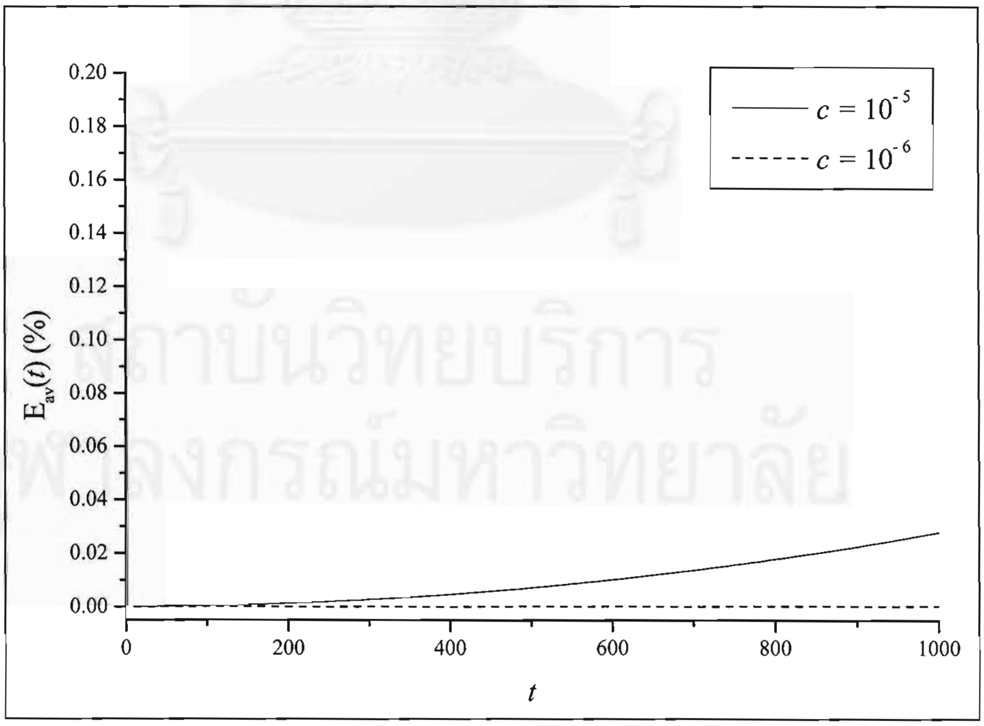

Figure 4.2.35: Average relative errors of the LTDRM.

4.2.9 Discussions for ILWPs

Eight ILWPs have been solved by using FDDRM and LTDRM. Four problems are defined on regular domains and the other four problems are defined on irregular domains with three types of boundary conditions, and their solutions are not easy to be found. Examples 7 – 13 show that FDDRM and LTDRM give accurate results when $c \leq 1\times10^{-5}$ which are similar to the HLWPs. For Example 6, the FDDRM gives good results when $c \leq 1\times10^{-5}$ while the LTDRM gives good results when $c \leq 1\times10^{-6}$. It should be noticed that numerical results obtained from FDDRM when solving ILWPs are more accurate than the numerical results obtained from LTDRM such as in Examples 6, 7, 10, and 11. However, for $c > 1\times10^{-5}$ FDDRM and LTDRM give accurate results only at small observation times.

As for the efficiency of FDDRM and LTDRM used in ILWPs, it should be noted that although many source terms or the function b are included in the governing equation of each problem, computer implementations of FDDRM and LTDRM are not more complicate which differ from LTBEM, FEM and FDM. Similar to HLWPs discussion, FDDRM is more time consuming when the solutions at a large observation time needs to be evaluated.

Chapter 5

Concluding Remarks

In this thesis, two numerical approaches called the Finite Difference Dual Reciprocity Method (FDDRM) and the Laplace Transform Dual Reciprocity Method (LTDRM) are proposed and applied to solve Linear Wave Equations (LWEs) in $\mathbf{R}^2$, including Homogeneous Linear Wave Equations (HLWEs) and Inhomogeneous Linear Wave Equations (ILWEs).

The highlights of these two methods are the transformation of an LWE into a Poisson equation using some finite difference techniques or some Laplace transform techniques, and utilization of the DRM to solve this transformed equation. With these proposed methods, time-free and boundary-only integral equations are obtained. Consequently, the dimension of the problem under consideration is virtually reduced by two. Since FDDRM uses some finite difference techniques, a solution at any specific time can be attained with a step-by-step calculation in the time domain. On the other hand, LTDRM needs a numerical inversion of the Laplace transform to retrieve a solution in the time domain.

Five examples of Homogeneous Linear Wave Problems (HLWPs) and eight examples of Inhomogeneous Linear Wave Problems (ILWPs) are presented and solved by these two methods. These problems are defined on regular domains or irregular domains with three types of boundary conditions prescribed for which their exact solutions are difficult to be found.

Numerical solutions obtained from these two methods show a very good agreement with the corresponding analytical solutions for small observation times as well as large observation times with the same accuracy when $c \leq 10^{-5}$. Unfortunately, when $c > 10^{-5}$ numerical solutions are often accurate only at small observation times. However, our numerical experiments show that if the exact solutions are polynomial functions of degree 2 or 1 of variable t, numerical solutions are very accurate for long time period even though $c > 10^{-5}$. In addition, it should be noted that numerical solutions obtained by FDDRM are more accurate than the ones obtained by LTDRM in ILWPs.

From the computational point of view, computer implementations of FDDRM and LTDRM are easier than existing methods such as FDM, FEM, BEM, and LTBEM.

From the efficiency point of view, since the numerical inversion of the Laplace transform called "Stehfest's algorithm" is utilized in this research with $N_p = 6$, only 6 systems of linear equations are solved in order to obtain a value of the unknown function at a large observation time. When comparing with FDDRM, LTDRM is faster and more efficient. As far as the data storage is concerned, 6 LTDRM solutions are required in the Laplace transformed space for a single time step. Such a disadvantage is however compensated by the fact that the LTDRM allows unlimited time step size with no increase in computer storage and execution time.

From all of those points of view and numerical results presented herein, we may conclude that FDDRM and LTDRM are powerful methods for solving Linear Wave Problems (LWPs) when the velocity of wave propagation denoted by c is less than or equal to 1×10^{-5}. LTDRM is better than FDDRM when the solutions at a large time are needed. However, the FDDRM is suggested for solving ILWPs. As for $c > 10^{-5}$, numerical solutions obtained by these two methods are often not accurate which is the limitation of FDDRM and LTDRM. Therefore, for the future works, FDDRM and LTDRM may be improved so that they can be used to solve LWPs for $c > 10^{-5}$. Moreover, it is possible to extend these methods to solve nonlinear wave equations.

References

1. Brebbia, C. A. **The boundary element method for engineering**. London: Pentech Press, 1979.

2. Brebbia, C. A. and Walker, S. **Boundary element techniques in engineering**. London: Butter worths, 1979.

3. Cruse, T. A. and Rizzo, F. J. *J. Math. Anal. Applic.* 22 (1968): 244.

4. Cruse, T. A. and Rizzo, F. J. *J. Math. Anal. Applic.* 22 (1968): 341.

5. Papoulis, A. Q. *Appl. Math.* 14 (1957): 4.

6. Manolis, O. D. and Beskos, D. E. *Int. J. Num. Meth. Eng.* 17 (1981): 573.

7. Cruse, T. A., Snow, D. W., and Wilson, R. B. Numerical solution in axis symmetric elasticity. *Comp. Struct.* 7 (1977): 445 – 451.

8. Tang, W. *Transforming Domain into Boundary Integrals in BEM – A Generalise Approach,* Lecture Notes in Engineering, Eds. C. A. Brebbia and S. A. Orszary, Berlin: Spronger – Verlag, 1988.

9. Nardini, D. and Brebbia, C. A. **A new approach for free vibration analysis using boundary elements in Boundary Element Method in Engineering**. Berlin: Springer – Verlag, 1982.

10. Nowak, A. J. The multiple reciprocity methods for solving transient heat conduction problems. *BEM X* (1988): 81 – 93.

11. Nowak, A. J. and Brebbia, C. A. The multiple reciprocity method – A new

approach for transforming BEM domain integral into the boundary. *Eng. Anal. Boundary Elements* 6 (1989): 164 – 167.

12. Ahmad, S. and Benerjee, P. K. Free vibration analysis by BEM using particular Integrals. *J. Eng. Mech.* 112 (1989): 682 – 695.

13. Atkinson, K. E. The numerical evaluation of particular solutions for Poisson's Equation. *IMA J. Num. Anal.* 5 (1985): 319 – 338.

14. Nardini, D. and Brebbia, C. A. **Boundary integral formulation of mass matrices for dynamic analysis**. Berlin: Springer – Verlag, 1985.

15. Partridge, P. W. and Brebbia, C. A. Computer implementation of the BEM dual reciprocity method for the solution of Poisson type equation. *Software for Engineering Workstations* 5 (1989): 199 – 206.

16. Partridge, P. W. and Wrobel, L. C. The dual reciprocity boundary element method for spontaneous ignition. *Int. J. Num. Meth. Eng.* 30 (1990): 953 – 963.

17. Partridge, P. W., Brebbia, C. A., and Wrobel, L. C. **The Dual Reciprocity Boundary Element Method**. UK: Computational Mechanics Publication and Elsevier Applied Science, 1992.

18. Brebbia, C. A., Telles, J. C. F. and Wrobel, L. C. **Boundary Element Techniques: Theory and Applications in Engineering**. Berlin: Springer – Verlag, 1984.

19. Stehfest, H. Algorithm 368: numerical inversion of Laplace transform. *Comm. ACM* 13 (1970): 47 – 49 and 624.

20. Moridis, G. J. and Reddel, D. L. The Laplace transform boundary element (LTBE) method for the solution of diffusion – type equation. *BEM XIII* (1991): 83 – 97.

21. Cheng, H. T. and Lin, J. Y. Hybrid Laplace transform technique for nonlinear transient thermal problems. *Int. J. Heat Mass Transfer* 34 (1991): 1301 – 1308.

22. Zhu, S. P., Satravaha, P., and Lu, X. P. Solving linear diffusion equations with the dual reciprocity method in Laplace space. *Engineering Analysis with Boundary Elements* 13 (1994): 1 – 10.

Appendices

Appendix A

Consider an ILWE in the form

$$\nabla^2 u(\bar{x},t) - \frac{1}{c^2}\frac{\partial^2 u}{\partial t^2}(\bar{x},t) = z(\bar{x},t), \quad \bar{x} \in \Omega,\, t > 0. \qquad \textbf{(A.1)}$$

After transforming this equation into Laplace space, we obtain that

$$\nabla^2 U(\bar{x},p) = \frac{1}{c^2}\left(p^2 U(\bar{x},p) - p u_0(\bar{x}) - v_0(\bar{x})\right) + Z(\bar{x},p). \qquad \textbf{(A.2)}$$

Approximating Z as described in Equation **(3.3.8)** gives the error $E(\bar{x},p)$ of the form

$$Z(\bar{x},p) = \frac{z(\bar{x},t)}{p} + E(\bar{x},p). \qquad \textbf{(A.3)}$$

Substituting this equation into Equation **(A.2)**, we get

$$\nabla^2 U(\bar{x},p) = \left(\frac{1}{c^2}\left(p^2 U(\bar{x},p) - p u_0(\bar{x}) - v_0(\bar{x})\right) + \frac{z(\bar{x},t)}{p}\right) + E(\bar{x},p). \qquad \textbf{(A.4)}$$

Approximating the RHS of the above equation without the error term with the interpolation functions $f_j,\ j = 1, 2, \ldots, N+L$ leads to

$$\nabla^2 U(\bar{x},p) = \sum_{j=1}^{N+L} \alpha_j f_j(\bar{x}) + E(\bar{x},p). \qquad \textbf{(A.5)}$$

By using the DRM technique with this equation, we can show that

$$U(\bar{\varsigma},p) = \Psi(\bar{\varsigma},p) + \frac{1}{c_{\bar{\varsigma}}} \int_{\Omega} E(\bar{x},p) u^*(\bar{x})\, d\Omega, \qquad \textbf{(A.6)}$$

where

$$\Psi(\bar{x},p) = \frac{1}{c_{\bar{\varsigma}}}\left(-\sum_{k=1}^{N} U_k(p) h_{\bar{\varsigma}k} + \sum_{k=1}^{N} Q_k(p) g_{\bar{\varsigma}k} + \sum_{j=1}^{N+L}\left(\alpha_j\left(c_{\bar{\varsigma}}\hat{u}_{\bar{\varsigma}j} + \sum_{k=1}^{N}\hat{u}_{jk} h_{\bar{\varsigma}k} - \sum_{k=1}^{N}\hat{q}_{jk} g_{\bar{\varsigma}k}\right)\right)\right) \qquad \textbf{(A.7)}$$

which is the approximate solution in the LTDRM procedure. Now, we have to show that this approximate solution $\Psi(\bar{x},p_\nu),\ \nu = 1, 2, \ldots, N_p$ does give the exact solution $u(\bar{\varsigma},t_i)$ in the time domain. By using Stehfest's algorithm, we have

$$u(\bar{\varsigma},t_i) = \frac{\ln 2}{t_i} \sum_{\nu=1}^{N_p} W_\nu\, U(\bar{\varsigma},p_\nu), \qquad \textbf{(A.8)}$$

where $p_\nu = \dfrac{\ln 2}{t_i}\,\nu$, $\nu = 1, 2, \ldots, N_p$. Substituting Equation **(A.6)** into Equation **(A.8)**, we get that

$$u(\varsigma, t_i) = \frac{\ln 2}{t_i} \sum_{\nu=1}^{N_p} W_\nu \, \Psi(\varsigma, p_\nu) + \frac{\ln 2}{t_i c_\varsigma} \int_\Omega \left(\sum_{\nu=1}^{N_p} W_\nu \, E(\bar{x}, p_\nu) \right) u^*(\bar{x}) \, d\Omega \,. \tag{A.9}$$

If we can show that

$$\sum_{\nu=1}^{N_p} W_\nu \, E(\bar{x}, p_\nu) = 0, \tag{A.10}$$

then this proof is complete. Our computational experiments show that

$$\sum_{\nu=1}^{N_p} \frac{W_\nu}{\nu} = 1 + \varepsilon_{N_p}, \tag{A.11}$$

for $N_p = 2, 4, \ldots, 16$ where $\left| \varepsilon_{N_p} \right| < 10^{-7}$. In fact, for $N_p = 2, 4, 6,$ and 8, $\left| \varepsilon_{N_p} \right| = 0$.

Hence

$$\begin{aligned}
\sum_{\nu=1}^{N_p} W_\nu \, E(\bar{x}, p_\nu) &= -\left(\sum_{\nu=1}^{N_p} W_\nu \frac{z(\bar{x}, t_i)}{p_\nu} \right) + \left(\sum_{\nu=1}^{N_p} W_\nu \, Z(\bar{x}, p_\nu) \right) \\
&= -\frac{t_i}{\ln 2} \, z(\bar{x}, t_i) \left(\sum_{\nu=1}^{N_p} \frac{W_\nu}{\nu} \right) + \left(\sum_{\nu=1}^{N_p} W_\nu \, Z(\bar{x}, p_\nu) \right) \\
&= 0,
\end{aligned}$$

and thus complete the proof.

Appendix B

Let $u(\bar{x},t)$ be the exact solution at a point $\bar{x}$ at time t and $u_{app}(\bar{x},t)$ be the approximate solution at a point $\bar{x}$ at time t which is obtained by a numerical method. An absolute error at a point $\bar{x}$ at time t denoted by $A(\bar{x},t)$ is defined as

$$A(\bar{x},t) = \left| \, u(\bar{x},t) - u_{app}(\bar{x},t) \, \right|, \tag{B.1}$$

if $u(\bar{x},t) \neq 0,$ a relative error at a point $\bar{x}$ at time t denoted by $E(\bar{x},t)$ is defined as

$$E(\bar{x},t) = \frac{A(\bar{x},t)}{\left| u(\bar{x},t) \right|} \times 100. \tag{B.2}$$

Let $\bar{x}_1, \bar{x}_2, \ldots, \bar{x}_{N_s}$ be points in the considered domain Ω which are called sample points. An average absolute error at time t denoted by $A_{av}(t)$ is defined as

$$A_{av}(t) = \frac{1}{N_s} \sum_{k=1}^{N_s} A(\bar{x}_k, t), \tag{B.3}$$

and an average relative error at time t denoted by $E_{av}(t)$ is defined as

$$E_{av}(t) = \frac{1}{N_s} \sum_{k=1}^{N_s} E(\bar{x}_k, t). \tag{B.4}$$

In this research, an average relative error at time t or $E_{av}(t)$ is used to measure the accuracy of numerical solutions obtained from FDDRM and LTDRM when $\left| u(\bar{x}_k, t) \right| > 10^{-4}$ where $\bar{x}_k$, $k = 1,2,\ldots, N_s$, are sample points. On the other hand, an average absolute error at time t or $A_{av}(t)$ is used when $\left| u(\bar{x}_k, t) \right| \leq 10^{-4}$.

Appendix C

From Example 8,

$$A_{nm} = \frac{16}{n^3 m^3 \pi^6}\left(1-(-1)^m-(-1)^n+(-1)^{m+n}\right), \tag{C.1}$$

$$B_{nm} = \frac{kA_{nm}}{2l_{nm}}, \tag{C.2}$$

$$l_{nm} = \frac{\sqrt{4c^2\lambda_{nm}-k}}{2}, \tag{C.3}$$

$$\lambda_{nm} = \pi^2(n^2+m^2). \tag{C.4}$$

From Example 10, the exact solution is

$$u(x,y,t) = \left(1-e^{\left(0.01-(x^2+y^2)\right)}\right)\sin(ct). \tag{C.5}$$

From Example 12,

$$\begin{aligned} z(x,y,t) = &-\frac{1}{2}\sin(ct)\big(4\cos(y)\sin(x)+(-14\cos(x)+\sin(x)-20c\sin(x))\sin(y)\big) \\ &-\frac{1}{2}\cos(ct)\big(4\cos(y)\sin(x)+(-14\cos(x)+\sin(x)+20c\sin(x))\sin(y)\big). \end{aligned} \tag{C.6}$$

From Example 13,

$$\begin{aligned} z(x,y,t) = &-e^{-\sin(ct)}\left(\cos(x^2+y^2)(-10+4x^2+4y^2+c\cos(ct)+\cos^2(ct)+\sin(ct)\right)+ \\ &2(2+3x-y)\sin(x^2+y^2). \end{aligned} \tag{C.7}$$

Curriculum Vitae

Sanae Rujivan was born in February 27, 1976. He received a bachelor degree in Mathematics from the Department of Mathematics, Faculty of Science, Chulalongkorn University in 1997.